Philipps Universität Marburg

Identification and characterization of M23 peptidase VcsP involved in cell separation in *Vibrio parahaemolyticus*

DISSERTATION

zur Erlangung des Doktorgrades

der Naturwissenschaften
(Dr. rer. nat.)

dem Fachbereich Biologie

der Philipps-Universität Marburg

vorgelegt von

JAN HEERING

aus Malchin

Marburg an der Lahn, 2019

Die Untersuchungen zur vorliegenden Arbeit wurden von September 2015 bis September 2019 am Max-Planck-Institut für terrestrische Mikrobiologie unter der Leitung von Dr. Simon Ringgaard durchgeführt.

Vom Fachbereich Biologie der Philipps-Universität Marburg als Dissertation angenommen am: ____ . ____ . _____

Erstgutachter: Dr. Simon Ringgaard

Zweitgutachter: Prof. Dr. Martin Thanbichler

Weitere Mitglieder der Prüfungskommission:

Prof. Dr. Michael Bölker

Prof. Dr. Lars-Oliver Essen

Tag der mündlichen Prüfung: ____ . ____ . _____

Die während der Promotien erzielten Erbebnisse wurden zum Teil in folgenden Originalpublikationen veröffentlicht:

Heering, J., Alvarado, A., Ringgaard, S. Induction of Cellular Differentiation and Single Cell Imaging of *Vibrio parahaemolyticus* Swimmer and Swarmer Cells. *J. Vis. Exp.* 2017*; e55842,* doi:10.3791/55842

Heering, J., Ringgaard, S. Differential localization of chemotactic signaling arrays during the lifecycle of *Vibrio parahaemolyticus*. Front. Microbiol. 2016; 7:1767, doi:10.3389/fmicb.2016.01767

Heering, J., Irazoki O., Brenzinger S., Cava F., Briegel S., Ringgaard S. Identification and characterization of M23 peptidase VcsP involved in cell separation in *Vibrio parahaemolyticus*. In preparation.

Abbreviations

GlcNAc	N-acetylglucosamine
MurNAc	N-acetylmuramic acid
Ala	Alanine
Glu	Glutamic acid
meso-DAP	*meso*-diaminopimelic acid
iGln	Isoglutamine
Lys	Lysine
IM	Inner membrane
OM	Outer membrane
PG	Peptidoglycan
UDP	Uridine diphosphate
TG	Trans-glycosylation
TP	Trans-peptidation
PBP	Penicillin binding protein
D-AA	D-amino acid
GTase	Glycosyltransferase
TPase	Trans-peptidases
CPase	Carboxypeptidase
EPase	Endopeptidase
µ-	Micro
OD	Optical density
aa	Amino acid
Amp	Ampicillin

Cm	Chloramphenicol
DNA	Deoxyribonucleic acid
FC	Fold change
sfGFP	Superfolder green fluorescent protein

List of figures

List of tables

Abstract

The peptidoglycan is an important structural element of the bacterial cell envelope and is involved in many cellular processes such as maintenance of cell shape, cell division as well as protection against extracellular stresses. Established model organisms like *Escherichia coli* or *Bacillus subtilis* have been studied extensively regarding peptidoglycan biosynthesis as well as degradation. The main goal of our research is to apply established knowledge and at the same time widen the understanding of peptidoglycan biogenesis in the human pathogen *Vibrio parahaemolyticus*. While the spatio-temporal organization of many synthetic and lytic enzymes is required during the bacterial cell cycle, this work focuses on the characterization of M23 peptidases, a class of enzymes responsible to reverse the trans-peptidation reaction that link the stem peptides of parallel glycan strands.

Here we show that the *V. parahaemolyticus* genome encodes for seven M23 peptidases, some of which are homologues to identified factors important for cell division and shape in other organisms. However, we also find three previously uncharacterized, paralogous M23 peptidases. Through series of experiments, we identify one particular protein, VcsP, to be important for cell separation through its conserved M23 peptidase domain. Upon its deletion, cells exhibit a chaining phenotype that compromises the cell envelope, increasing its sensitivity to Polymyxin type antibiotics. We distinctly show that VcsP is the most important out of three paralogues. Interestingly, the dimorphic lifestyle of *V. parahaemolyticus* is unaffected in the absence of VcsP and cells are able to differentiate from swimmer to swarmer cell type. We utilized several approaches to find interaction partners and affectors of VcsP, and so far we show that *vcsP* is co-transcribed with *vp0549*, which encodes for a PilZ domain protein that binds the second messenger c-di-GMP.

Together these findings have significantly increased our knowledge of M23 peptidases in *V. parahaemolyticus* and it will be interesting to find out more about VcsP and its effects in the future. We also raised additional questions in this study that we would like to address in future research.

Zusammenfassung

Das Peptidoglycan ist ein wichtiges Strukturelement der bakteriellen Zellhülle und ist an vielen zellulären Prozessen wie der Erhaltung der Zellform, der Zellteilung sowie dem Schutz vor extrazellulären Stressbedingungen beteiligt. Etablierte Modellorganismen wie *Escherichia coli* oder *Bacillus subtilis* wurden intensiv hinsichtlich der Peptidoglykanbiosynthese und dessen Abbaus untersucht. Das Hauptziel unserer Forschung ist es, fundiertes Wissen anzuwenden und gleichzeitig das Verständnis der Peptidoglycan-Biogenese im menschlichen Krankheitserreger *Vibrio parahaemolyticus* zu erweitern. Obwohl die räumlich-zeitliche Organisation vieler synthetischer und lytischer Enzyme während des bakteriellen Zellzyklus erforderlich ist, konzentriert sich diese Arbeit auf die Charakterisierung von M23-Peptidasen, einer Klasse von Enzymen, die für die Umkehrung der Transpeptidationsreaktion verantwortlich sind, welche die Stammpeptide paralleler Glykanstränge verbinden.

Wir zeigen, dass das Genom von *V. parahaemolyticus* für sieben M23-Peptidasen kodiert, von denen einige Homologe zu bereits identifizierten Faktoren sind, die für die Zellteilung und -form in anderen Organismen wichtig sind. Wir finden aber auch drei bisher nicht charakterisierte, paraloge M23-Peptidasen. In einer Reihe von Experimenten identifizieren wir ein bestimmtes Protein, VcsP, das für die Zelltrennung durch seine konservierte M23-Peptidasendomäne wichtig ist. Nach der Entfernung von *vcsP* zeigen die Zellen einen kettenbildenden Phänotyp, der die Zellhülle kompromittiert und ihre Empfindlichkeit gegenüber Antibiotika vom Polymyxin-Typ erhöht. Wir zeigen deutlich, dass VcsP der wichtigste von drei Paralogen ist. Interessanterweise ist der dimorphe Lebensstil von *V. parahaemolyticus* in Abwesenheit von VcsP unbeeinflusst und die Zellen sind in der Lage, sich von Schwimmer zu Schwärmerzelltyp zu differenzieren. Wir haben mehrere Ansätze genutzt, um Interaktionspartner und Affektoren von VcsP zu finden, und bisher haben wir gezeigt, dass *vcsP* mit *vp0549* co-transkribiert wird, welches für ein PilZ-Domänenprotein kodiert, das den sekundären Botenstoff c-di-GMP bindet.

Zusammen haben diese Ergebnisse unser Wissen über M23-Peptidasen im Organismus *V. parahaemolyticus* deutlich erweitert, und es wird interessant sein, mehr über VcsP und seine Auswirkungen in der Zukunft zu erfahren. In dieser Studie haben wir zusätzliche Fragen gestellt, die wir in der zukünftigen Forschung ansprechen möchten.

Table of contents

1 Introduction

1.1 Bacterial cell envelope

The bacterial cell envelope is the main line of defense against external threats and is usually comprised of an inner membrane (IM), an outer membrane (OM) in gram-negative bacteria and peptidoglycan (PG). The PG is a polysaccharide network which is cross-linked via peptide sidechains (Glauner *et al.*, 1988; Gan *et al.*, 2008; Vollmer and Bertsche, 2008) that forms a thin layer between the inner and outer membranes of gram-negative bacteria, and a thicker layer on the cell surface in gram-positive bacteria. One exception are L-forms or cell wall-deficient bacteria that can develop from both gram-negative and gram-positive bacteria and do not assemble a PG layer (Errington, 2013). The PG serves as a bacterial exoskeleton and promotes maintenance of the shape and size of bacterial cells (Lawler *et al.*, 2007; Sycuro *et al.*, 2010; Young, 2010). The presence of PG allows bacteria to remain viable in environments where the extracellular osmolarity is lower than the intracellular turgor pressure. The PG's importance for bacterial survival is also the reason why most commonly used antibiotics, including the beta lactams, cephalosporins and glycopeptides target the PG synthesis pathways (Schneider *et al.*, 2010).

1.2 Gram-negative organisms

The gram-negative bacterial cell envelope is comprised of three main layers: the inner membrane, the peptidoglycan cell wall, and the outer membrane. The two membrane layers form a cellular compartment - the periplasm (Mitchell, 1961).

1.2.1 The outer membrane

The OM is a lipid bilayer that is comprised of phospholipids on the inner leaflet and glycolipids on the outer leaflet. A particularly important component of the outer membrane are lipopolysaccharides (LPS) - lipid and a polysaccharide chains composed of O-antigen, lipid A and core (Kamio *et al.*, 1976). The LPS is the main molecule to trigger an immune system response and it is responsible for the endotoxic shock in humans and other organisms that can be infected by Gram-negative bacteria (Alexander *et al.*, 2001; Raetz *et al.*, 2002). In addition to being a protective layer

that provides resistance to some antibiotics, the OM also provides mechanical stiffness and strength to the bacterial cell in general. Contrary to the prevailing dogma that only the PG is responsible to carry the weight imposed onto the cell by the environment , it was proposed that the OM is the major load-bearing element of the cell envelope (Rojas *et al.*, 2018). Both lipopolysaccharides, especially the O-antigen and proteins like the Tol-Pal complex, contribute to the stiffness of the outer membrane. The deformation of the cell envelope in response to stretching, bending and other forces was severely increased when the OM was weakened either chemically or genetically (Rojas *et al.*, 2018).

The outer membrane harbors both lipoproteins and β-barrel proteins. *Escherichia coli* has around 85 predicted OM lipoproteins, compared to 118 of *Vibrio parahaemolyticus*, most of them with an unknown function (Sankaran *et al.*, 1994; Miyadai *et al.*, 2004; Babu *et al.*, 2006). Lipoproteins attach lipid moieties to an amino-terminal cysteine residue and are embedded in the inner leaflet of the OM, whereas β-barrel proteins are usually integral or transmembrane spanning proteins. Many outer membrane proteins (OMPs), including porins, OmpF, OmpC and LamB, allow the passive diffusion of small molecules such as mono- and disaccharides and amino acids into the periplasm (Cowan *et al.*, 1992; Schirmer *et al.*, 1995). The outer membrane protein OmpA can also function as a porin (Arora *et al.*, 2000) and in many pathogenic bacteria, OmpA proteins have important roles including bacterial adhesion, invasion, or intracellular survival as well as evasion of host defenses (Confer *et al.*, 2013). There are also large β-barrels OMPs that function as gated channels in the transport of large ligands such as Fe-chelates or vitamins such as vitamin B-12 (Nikaido, 2003).

1.2.2 The periplasmic space

Located between the outer and inner membrane is the periplasmic space, a cellular compartment that is densely packed with proteins (Mullineaux *et al.*, 2006). It allows Gram-negative bacteria to insulate and contain potentially harmful degradative enzymes such as RNAse I, which is involved in degradation of rRNA during periods of stress or non-growth (Beacham, 1979) or alkaline phosphatase (MacAlister *et al.*, 1972). Other proteins that inhabit this compartment include the periplasmic binding proteins, which function in sugar (He *et al.*, 2009) and amino acid transport and chemotaxis (Machuca *et al.*, 2017), and chaperone-like molecules that function in envelope biogenesis (Sklar, Wu, Kahne, *et al.*, 2007). The peptidoglycan sacculus, which determines the cells shape, is also be found in the periplasmic space, and it forms a single large polymer that is

constructed out of repeating units of the disaccharide N-acetyl glucosamine-N-actyl muramic acid, which are cross-linked by peptide side chains (stem peptide) (Figure 3) (Vollmer and Bertsche, 2008). (More on peptidoglycan in section 1.4)

1.2.3 The inner membrane

The IM is comprised out of a bilayer of phospholipids and it was shown that the phospholipid composition changes in order to adapt to environmental stress conditions (Rowlett *et al.*, 2017). *Vibrio* species for example possess unique machineries with the ability to take up a broad range of fatty acids from the environment when compared to other enteric bacteria and use them to build alternative lipids to integrate into the IM (Giles *et al.*, 2011). In addition, minor lipids can be found in the IM including poly-isoprenoid carriers (C55), which function in the translocation of activated sugar intermediates that are required for envelope biogenesis (Raetz *et al.*, 1990).

In contrast to protein complexes that reside in only one specific part of the cell envelope, there are some molecular machines that span the entire cell envelope. One example is the flagellar complex: The C-ring is located in the cytoplasm close to the IM and connects through the MS-ring to the motor proteins, which are located in the periplasm. Followed by the proximal and distal rod, that span the PG and connect to the OM, the L-ring bridges the OM and connects to the hook. Finally, the flagellar filament is assembled through this passage across IM, PG and OM, and is ultimately located outside the cell envelope (DePamphilis *et al.*, 1971; Macnab, 2003; Fitzgerald *et al.*, 2014). Similarly, the type III secretion system (Kubori, 1998), which is a needle like appendage and used to inject toxins into the cytoplasm of eukaryotic host cells, is a trans-envelope machinery as well. As a protection mechanism against a wide variety of toxic molecules such as antibiotics, bacterial cells also span efflux pumps across the entire cell envelope. These are responsible, in part, for much of the antibiotic resistance in pathogenic bacteria (Koronakis *et al.*, 2000, 2004; Murakami *et al.*, 2006; Symmons *et al.*, 2009).

1.2.4 Envelope Assembly

Although the IM, periplasm with the PG mesh and the OM are crowded with lipids, peptides and proteins, none of these components are synthetized at their final destination (Figure 1). Instead,

they are synthesized in the cytoplasm and afterwards translocated or flipped across the IM (Berg *et al.*, 2004; Mohammadi *et al.*, 2011; Leclercq *et al.*, 2017). Periplasmic components have to be released from the IM, peptidoglycan components have to be released, polymerized and integrated into the existing PG, and OM components must be transported across the entire periplasm. In addition, the lack of ATP outside the cytoplasm makes it even more difficult to perform these tasks (Okuda *et al.*, 2012).

Periplasmic proteins or outer membrane proteins (OMP) are initially synthetized in precursor form (Figure 1). At their amino terminus they have attached a signal sequence, which targets them for translocation from the cytoplasm (Natale *et al.*, 2008). This translocation reaction is catalyzed by the IM protein complex SecYEG (Berg *et al.*, 2004) and the essential ATPase SecA, together with the proton motive force, drives this translocation reaction (Zimmer *et al.*, 2008). Usually, periplasmic and OM proteins are translocated in post-translational fashion. In the case of the SecYEG translocation machinery, which is unable to handle folded proteins, proteins are secreted in their linearized form, from the amino to the carboxy terminus. This is achieved by the cytoplasmic SecB chaperone, which maintains these proteins in an unfolded form until they can be secreted (Randall *et al.*, 2002). During the secretion process, the signal sequence is removed by type I SPase (Carlos *et al.*, 2002). Other nonessential components of the Sec machinery like SecD, SecF, and YajC, have been implicated in facilitating the release of secreted proteins into the periplasm (Tsukazaki *et al.*, 2011) and were also shown to contribute to the regulation of adhesion in *Vibrio* species (Guo *et al.*, 2018).

During their transit through the periplasm, OMPs are protected by periplasmic chaperons (Figure 1): SurA (Behrens, 2001; Bitto *et al.*, 2003), Skp (Chen *et al.*, 1996; Walton *et al.*, 2009), and DegP (Krojer *et al.*, 2008; Shen *et al.*, 2009). These three proteins appear to function in parallel and redundant pathways for OMP assembly, where SurA functions in one pathway and DegP/Skp function in the other. Loss of either of these two pathways leaves the cells viable, but cells cannot tolerate loss of both, as mutants lacking SurA and Skp, or SurA and DegP display massive defect in OMP assembly (Rizzitello *et al.*, 2001). Although those two pathways are redundant, the major OMPs show preference for the SurA pathway (Sklar, Wu, Kahne, *et al.*, 2007). Structural insight also suggest that DegP is a chaperone or carrier for folded rather than unfolded OMPs (Krojer *et al.*, 2008).

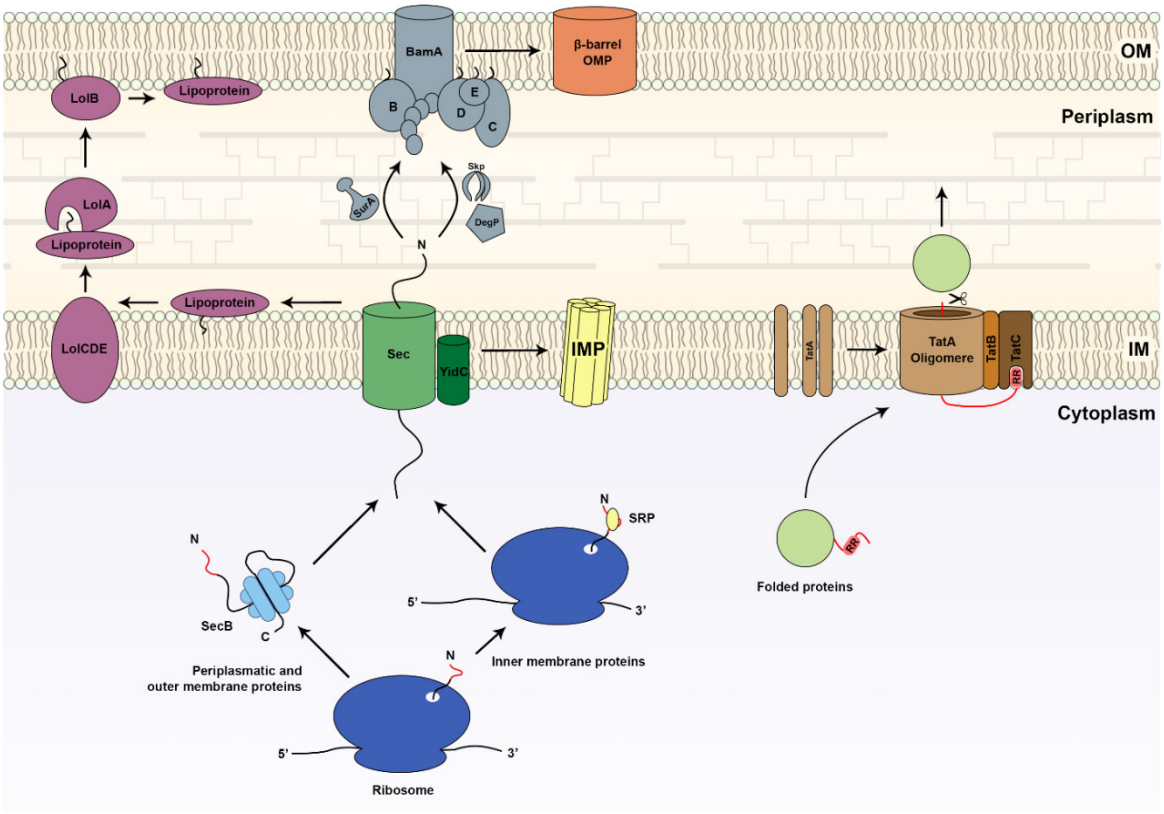

Figure 1: Cell envelope protein biogenesis and transport pathways

IM proteins are co-translationally synthetized and directed to Sec and inserted into the membrane, whereas periplasmic and OM proteins (OMPs) are post-translationally translocated. OM lipoproteins are lipidated at the outer leaflet of the IM and then transported to the OM by the Lol pathway. β-barrel OMPs transit the periplasm in unfolded states with the help of chaperones SurA, Skp and DegP and are then folded and inserted into the OM by the Bam complex. Proteins that were previously folded in the cytoplasm can be translocated to the periplasm by the Tat complex. BamA, -B, -C, -D, -E, β-barrel assembly machine components; DegP, periplasmic protease and putative chaperone; LolA, -B, -CDE, localization of lipoprotein machinery components; Sec, secretion machinery; SecB, cytoplasmic chaperone; Skp, periplasmic chaperone; SRP, signal recognition particle; SurA, periplasmic chaperone; TatA, -B, -C, twin-arginine export channel for folded proteins. Adapted from Hagan *et al.* (2011) and Palmer and Berks (2012).

The periplasmic chaperones deliver OMPs to an assembly site in the OM termed the Bam complex (Figure 1). This complex is composed of an essential large β-barrel protein, BamA, and four lipoproteins, BamBCDE (Wu *et al.*, 2005; Sklar, Wu, Gronenberg, *et al.*, 2007). BamA is highly conserved in Gram-negative bacteria and homologs of BamA have been discovered in both mitochondria and chloroplasts (Moslavac *et al.*, 2005), which are thought to be derived from Gram-negative bacteria. BamD is the only essential lipoprotein of the Bam complex (Malinverni *et al.*, 2006), and it is highly conserved in Gram-negative bacteria as well. One mechanism proposes that upon delivery of the OMP to the outer membrane together with its chaperon, the BAM complex would only function in the insertion of the protein into the membrane rather than in its folding

(Huber *et al.*, 2008). An alternative model proposes that the periplasmic chaperones deliver the OMPs to the periplasmic components of the BAM complex, and then both of them together fold the OMPs. Only when folded successfully, the OMPs would be guided into the outer membrane, possibly with the assistance of additional periplasmic factors (Gessmann *et al.*, 2014; Talmon *et al.*, 2016). However, the first model is more compelling, due to the observation that unfolded OMPs are degraded through DegP protease activity, whereas folded OMPs are not (Huber *et al.*, 2008; Krojer *et al.*, 2008). Additionally, a folded OMP could be observed in the center of the DegP cage crystal structure was observed (Krojer *et al.*, 2008). Furthermore, once loaded with its OMP cargo, DegP can interact directly with lipid and potentially help insert the protein into the membrane (Krojer *et al.*, 2008).

Precursor lipoproteins also have an amino-terminal signal sequence and they are translocated by the Sec machinery. However, in this case SPase II removes the signal sequence (Paetzel, 2019). After the removal of the signal sequence, an additional fatty acyl chain is linked to the N-terminal cysteine amino group (Sankaran *et al.*, 1994) and allows the final lipoprotein to be tethered to the outer leaflet of the IM. Although some lipoproteins remain in the IM through a single amino acid determinant (Yamaguchi *et al.*, 1988; Yokota *et al.*, 1999), most of them are designated for the outer membrane (Remans *et al.*, 2010). The Lol system, which transports lipoproteins to the OM (Figure 1) (Narita *et al.*, 2006) uses an ATP-dependent ABC transporter (LolCDE) that extracts the molecule from the IM (Narita *et al.*, 2002). The lipoprotein is passed to the soluble periplasmic carrier LolA. In turn, LolA shuttles the molecule to the lipoprotein LolB at the OM assembly site. In order to avoid translocation to the OM by the Lol system, IM lipoproteins have a “Lol avoidance” signal, most commonly an aspartate residue at position two of the mature lipoprotein (Yamaguchi *et al.*, 1988; Yokota *et al.*, 1999).

A second protein translocation system in the IM called Tat is able to translocate folded proteins using only a proton gradient as an energy source (Figure 1) (Berks *et al.*, 2003; Müller, 2005). *E. coli* uses the Tat system, amongst other things, for the translocation of secreted proteins (Voulhoux, 2001). *Vibrio* species use the Tat system for similar tasks, specifically the translocation of extracellular proteases (Sandkvist *et al.*, 1993; He *et al.*, 2011). Additionally, it was shown that the Tat system is also important for virulence and pathogenicity towards fish and squid (Dunn *et al.*, 2008; He *et al.*, 2011). Other bacteria that live in extreme environments, such as thermophiles, use the Tat system extensively (Rose *et al.*, 2002). One proposed explanation is that it is easier to fold proteins in the cytoplasm than in the periplasm due to the availability of major ATP-dependent

chaperones like GroEL and DnaK (Georgopoulos, 1992; Gething *et al.*, 1992). The Tat system is composed of three components: TatB and TatC target proteins that are marked for translocation by TatA. Activated TatBC will recruit TatA, which is present in the membrane mostly as monomers, to allow oligomerization (Oates *et al.*, 2005). The exact mechanism is not completely understood, but TatA might form a channel, which is used to transport the substrate (Gohlke *et al.*, 2005; Leake *et al.*, 2008). Alternatively, TatA might deform the membrane and in this way allow the re-orientation of the polar phospholipid head groups of the substrate (Figure 1) (Smith *et al.*, 2017).

The Sec machinery also handles IM proteins that are targeted for co-translational translocation by the signal recognition particle (SRP) and the SRP receptor FtsY (Figure 1) (Bernstein, 2000). Generally, IM proteins are very hydrophobic substrates that are prone to form aggregates (Yeagle, 2016) and therefor post-translational translocation of these proteins would be inefficient and perhaps dangerous for the cell. The prokaryotic SRP consists of a single protein Ffh (fifty four homolog) and an RNA Ffs (four point five S RNA) that together as a complex have GTPase activity (Schlünzen *et al.*, 2005).

A second IM translocase called YidC is responsible for inserting small IM proteins but has also been shown to play a role in the SecYEG-dependent insertion machinery for insertion of large proteins (Guo *et al.*, 2018). YidC family members can also be found in eukaryotic cell compartments like mitochondria and chloroplasts (Xie *et al.*, 2008).

The LPS together with the core polysaccharide as well as the O-antigen are both synthesized in the inner leaflet of the IM (Figure 2). The ABC transport protein MsbA is responsible to flip the LPS to the outer leaflet of the IM and the O-antigen is synthesized on a poly-isoprenoid carrier (C55) before it is flipped to the outer leaflet. Only afterwards, the O-antigen is ligated to the LPS core in the outer leaflet of the IM, a reaction catalyzed by WaaL (Raetz and Whitfield 2002). Several essential proteins are required to transport LPS to the cells surface and these proteins have been termed Lpt (lipopolysaccharide transport) (Sperandeo et al. 2007, Sperandeo et al. 2008, Braun and Silhavy 2002; Bos et al. 2004, Wu et al. 2006, Ruiz et al. 2008). LptD together with LptE forms a complex in the OM. This large complex connects with LptA, which resides in the periplasm. LptF and LptG sit in the IM and likely interact with the cytoplasmic protein LptB, a predicted ATPase, to form an ABC transporter. These three proteins, together with LptC, extract LPS from the IM and passes it to LptA. LptA in turn delivers the LPS to the OM assembly site, LptD and LptE (Figure 2). When any of the

seven components are removed, LPS accumulates in the outer leaflet of the IM and is unable to reach the OM (Sperandeo et al. 2008, Ruiz et al. 2008).

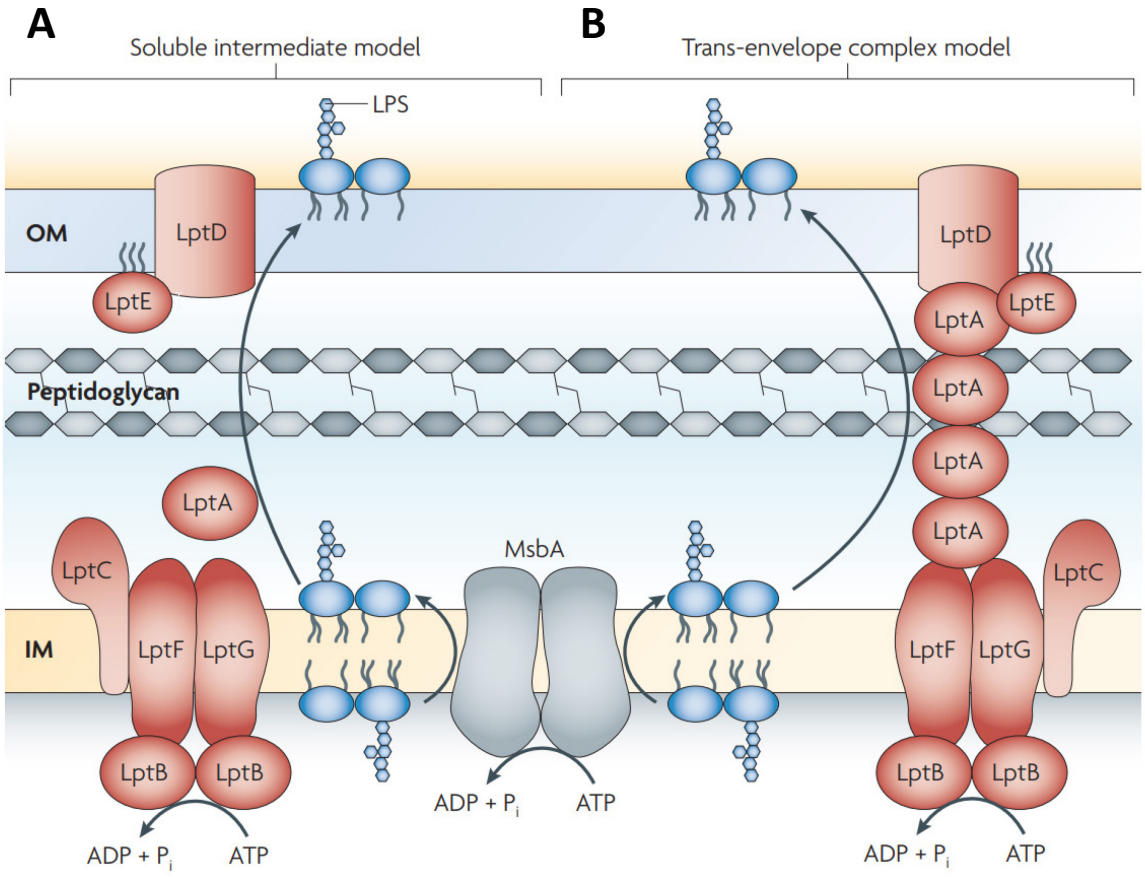

Figure 2: LPS transport pathway

The lipopolysaccharide core (LPS) molecules are flipped across the IM by the ABC transporter MsbA. If available, the O-antigen is translocated independently and then ligated to the LPS core by the WaaL ligase (step not shown). LptC then extracts the LPS from the IM complex (LptFGB). (A) In the soluble-intermediate model, LptA serves as a soluble chaperone that transports LPS to the LptDE assembly site on the OM. (B) In the trans-envelope complex model, the Lpt factors constitute a multiprotein complex that spans the entire cell envelope. Adapted from Ruiz *et al*. (2009).

1.3 Gram-positive organisms

The Gram-positive cell envelope differs in several key aspects from the Gram-negative one: most importantly, the outer membrane is absent. The outer membrane is responsible to protect Gram-negative organisms from unfavorable environmental conditions, e.g. toxic molecules. In addition, it also provides a stabilizing layer around the cell. Gram-positive bacteria are often living in harsh environments, they have to overcome the lack of an outer membrane, and the resulting increased turgor pressure applied on the plasma membrane. Thick layers of peptidoglycan surround Gram-

positive microorganisms and weaved into are long anionic polymers, called teichoic acids (Shockman *et al.*, 1983). There are different classes of these polymers, mainly the wall teichoic acids (WTA), which are covalently attached to peptidoglycan, and the lipoteichoic acids (LTA), which are anchored to the head groups of membrane lipids (Neuhaus *et al.*, 2003). All together, these polymers are the major contributors to envelope structure and function, as they contribute up to 60% of the Gram-positive cell wall (Ellwood *et al.*, 1968). Furthermore, although neither LTAs nor WTAs are essential, deleting either synthesis pathway produces organisms that have cell division and morphological defects. Additionally, trying to delete both pathways produces a synthetic lethal phenotype (Morath *et al.*, 2005; Oku *et al.*, 2009). In addition to the TAs, the Gram-positive cell surfaces expose many proteins, some of which are analogous to periplasmic proteins of Gram-negative organisms (Dramsi *et al.*, 2008). In order to retain extracellular proteins, Gram-positive organisms developed various strategies: some contain membrane-spanning helices, some are attached to lipid anchors inserted in the membrane and others are covalently attached to the peptidoglycan (Scott *et al.*, 2006) or some bind to teichoic acids (Fernández-Tornero *et al.*, 2001). The composition of surface exposed proteins varies highly depending on the environmental conditions as well as growth conditions (Pollack *et al.*, 1994).

Comparing the chemical structure of peptidoglycan in Gram-positive organisms to that in Gram-negatives reveals a broad range of similarities: it is composed of a disaccharide-peptide that form linear glycan strands through glycosidic linkages. These strands are cross-linked into a mesh through the stem-peptides that are attached to the disaccharide repeat. While Gram-negative peptidoglycan is only a few nanometers thick, resulting in only a few layers, the Gram-positive peptidoglycan is 30–100 nm thick and contains many layers (Yao *et al.*, 1999; Reith *et al.*, 2011).

Among Gram-positive organisms, the peptidoglycan structure can vary to different degrees, but the most noticeable difference is usually the peptide cross-links between glycan strands (Figure 3) (Vollmer and Bertsche, 2008). For example, *Staphylococcus aureus* incorporates a penta-glycine branch that extends from the third amino acid of one of the stem peptides. Three non-ribosomal peptidyl transferases FemA, FemB and FemX have been identified that assemble this penta-glycine (Ton-That *et al.*, 1998; Rohrer *et al.*, 2003) and although *S. aureus* can tolerate the loss of FemA or FemB, the deletion of FemX is lethal. FemX is responsible to attach the first glycine unit to the stem peptide (Hegde *et al.*, 2001; Hübscher *et al.*, 2007). Although many Gram-positive organisms contain branched stem peptides, *Bacillus subtilis* does not. In fact, the stem peptides and crosslinks in *B. subtilis* are identical in structure to those found in *E. coli* (Hayhurst *et al.*, 2008). The branched stem

peptides of *S. aureus* and other Gram-positive organisms have been shown to influence the degree of flexibility of the cell wall. Studies of intact and isolated Gram-positive cell walls and showed that while the glycan constituents and stem peptides were relatively rigid, the cross-bridging peptide linkages (especially the penta-glycine bridge of staphylococcal peptidoglycan) exhibited relatively large movements. It is hypothesized that this flexibility allows changes in the packing of the glycan strands in response to cell growth (Lapidot *et al.*, 1979a, 1979b). Additionally, the branched stem peptides also serve as an attachment site for covalently-associated proteins (Desvaux *et al.*, 2006). They have also been implicated in resistance to beta lactam antibiotics (Chambers, 2003) and it is speculated that the evolution of branched peptides in the peptidoglycan biosynthetic pathway may be an adaptation to avoid the effect of beta-lactam antibiotics (Rohrer *et al.*, 2003; Pratt, 2008; Sauvage *et al.*, 2008).

1.4 Peptidoglycan Biogenesis

Escherichia coli has been the most studied gram-negative organism regarding peptidoglycan (PG) biosynthesis; however, many of those insights can be transferred to other organisms. When compared to Gram-positive bacteria, Gram-negative bacteria have a relatively thin PG layer of only a few nanometer thickness and it is proposed to only be made out of a few parallel glycan strands (Matias *et al.*, 2003). The PG is a mesh-like structure responsible to give cells their distinctive shape. That shape is retained even when the PG sacculus is isolated (Yao *et al.*, 1999). The disaccharide-pentapeptide precursors (lipid II), which are the main building blocks of the final PG, are generated in the cytoplasm through several enzymatic reactions. After a precursor molecule is generated, it is flipped into the periplasm and cross-linked to an existing glycan strand.

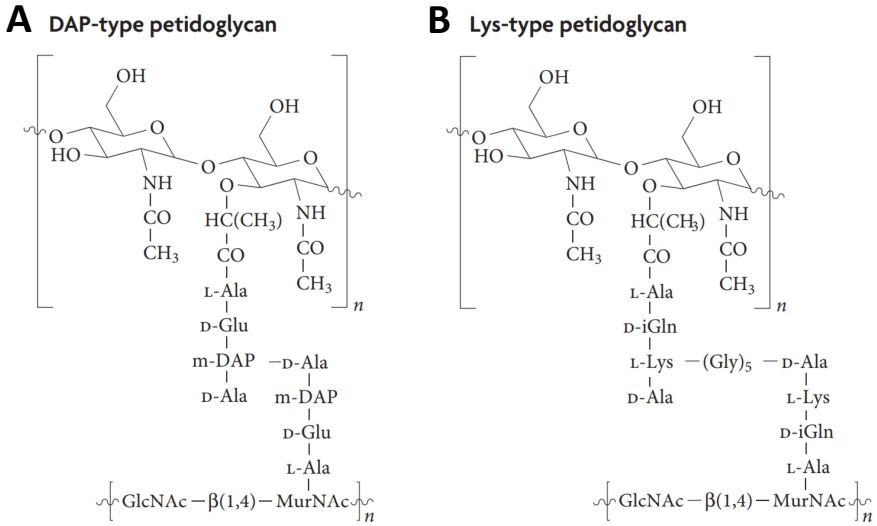

Figure 3: Peptidoglycan structure and function

Structures of (A) DAP-type peptidoglycan of Gram-negative bacteria with its characteristic *meso*-DAP at the third stem peptide position and (B) Lys-type peptidoglycan of Gram-positive bacteria with the characteristic L-Lys at the third stem peptide position and the additional interpeptide bridge. Areas marked with [ ] show the glycan strands, which are connected via β-1,4-glycosidic bonds and they are cross-linked by stem peptide side chains. Adapted from Royet and Dziarski (2007).

1.4.1 Structure and Synthesis

Peptidoglycan precursor generation and the integration into the PG mesh are decoupled through compartmentalization. The precursor molecules (lipid I and lipid II) are synthesized in the cytoplasm through a chain of enzymatic reactions (Figure 4) (Vollmer and Bertsche, 2008). In a first step, amino sugars are converted to GlcNAc and attached to uridine diphosphate (UDP) to produce UDP-GlcNAc. In a further step, MurA and MurB catalyze the reaction to transform UDP-GlcNAc into UDP-MurNAc. Afterwards, the stem peptide chain is generated by ATP-dependent ligases through the successive addition of L-alanine (MurC), D-glutamic acid (MurD), *meso*-DAP (MurE) and the dipeptide D-alanine–D-alanine (MurF, DdlA) (Figure 4). Although D-amino acids are rare building blocks in bacterial cells, they are very important for the PG and the racemases Alr, DadX and MurI are responsible to synthetize these D-amino acids from L-amino acid precursors (Vollmer and Bertsche, 2008). In order to transport the UDP-MurNAc subunit to the periplasm, it is attached to undecaprenyl-phosphate (C_{55}-P), an essential lipid (Manat *et al.*, 2015), by the enzyme MraY, generating the lipid I precursor. In an additional step, MurG catalyzes the transfer of UDP-GlnNAc onto lipid I, which leads to the generation of lipid II (Heijenoort, 2001). Lipid II is then flipped across the inner membrane. Different proteins have been proposed to act as flippases: FtsW and RodA, both membrane proteins of the SEDS family, have been suggested to flip lipid II precursor in *E.coli* (Ikeda *et al.*, 1989; Mohammadi *et al.*, 2011; Leclercq *et al.*, 2017). However, more recent work identifies FtsW and RodA as peptidoglycan GTases that function together with a bPBP partner and pair with the cell wall elongation and division machineries (Meeske *et al.*, 2016; Taguchi *et al.*, 2019). Additionally, compared to FtsW, RodA lacks a transmembrane channel, which would enable lipid II transport (Sjodt *et al.*, 2018). Furthermore, MurJ was also indicated to be required for lipid II transport as shown in *E. coli* as well as *B. subtilis* (Ruiz, 2008; Sham *et al.*, 2014; Meeske *et al.*, 2015; Leclercq *et al.*, 2017; Kumar *et al.*, 2019).

Once lipid II is facing the periplasm, the first step of PG biogenesis is the polymerization of disaccharide-pentapeptide precursors into existing glycan strands by trans-glycosylation (TG) (Typas *et al.*, 2012). Afterwards, the peptide residues of these new glycan strands are crosslinked (trans-peptidation (TP)) and integrated into the existing PG. Both TG and TP reactions are mediated by penicillin binding proteins (PBPs) which are anchored into the inner membrane (Sauvage *et al.*, 2008). *Vibrio* species possess the same PG synthetic enzymes as *E. coli* and although they seem to utilize similar processes for cell wall synthesis, elongation and maintenance, there are some

differences. The stem peptide is initially generated with a common structure of L-Ala–D-Glu–*meso*-DAP–D-Ala–D-Ala (Figure 4) (Vollmer and Bertsche, 2008), however isolated PG often only shows a small amount of penta-peptides, but rather tetra-, tri- or dipeptides. Many stem peptide-modifying enzymes are anchored in the IM facing the PG, which are able to reduce the length of the stem or modify its components to e.g. integrate alternative D-amino acids. Two adjacent stem peptides can be cross-linked in different positions although the majority are of the DD-type, which is the connection between D-Ala (position 4) of one peptide and *meso*-DAP (position 3) of the other peptide (Glauner *et al.*, 1988). That reaction is performed by DD-transpeptidases. Cross-links of the LD-type are less frequent. Here *meso*-DAP residues of two peptides are connected by LD-transpeptidases (Vollmer and Bertsche, 2008). The energy required for these reactions is gained by the cleavage of the D-Ala–D-Ala bond of the stem-peptide, which functions as an energy donor (Terrak *et al.*, 1999).

Although *V. cholerae* and *E. coli* seem to utilize similar processes for cell wall synthesis, elongation and maintenance, there is at least one major difference. When *V. cholerae* enters stationary phase, its periplasmic amino acid racemase BsrV synthetizes D-amino acids (D-AAs), especially D-Met and D-Leu in addition to D-Ala and D-Glu, which are then incorporated into PG (Glauner *et al.*, 1988; Lam *et al.*, 2009; Cava *et al.*, 2011; Kuru *et al.*, 2012). Mutants that do not produce or cannot incorporate D-AA into PG are hypersensitive to osmotic stress, indicating that D-AAs influence the strength of stationary phase PG. However, the precise role of D-AAs in stationary phase, and the means by which they modulate *V. cholerae* PG, remain to be identified. Although *V. cholerae* and *V. parahaemolyticus* are closely related and share most of the mechanisms and homologous enzymes mentioned above, little is known about cell wall synthesis, elongation and maintenance in *V. parahaemolyticus* specifically.

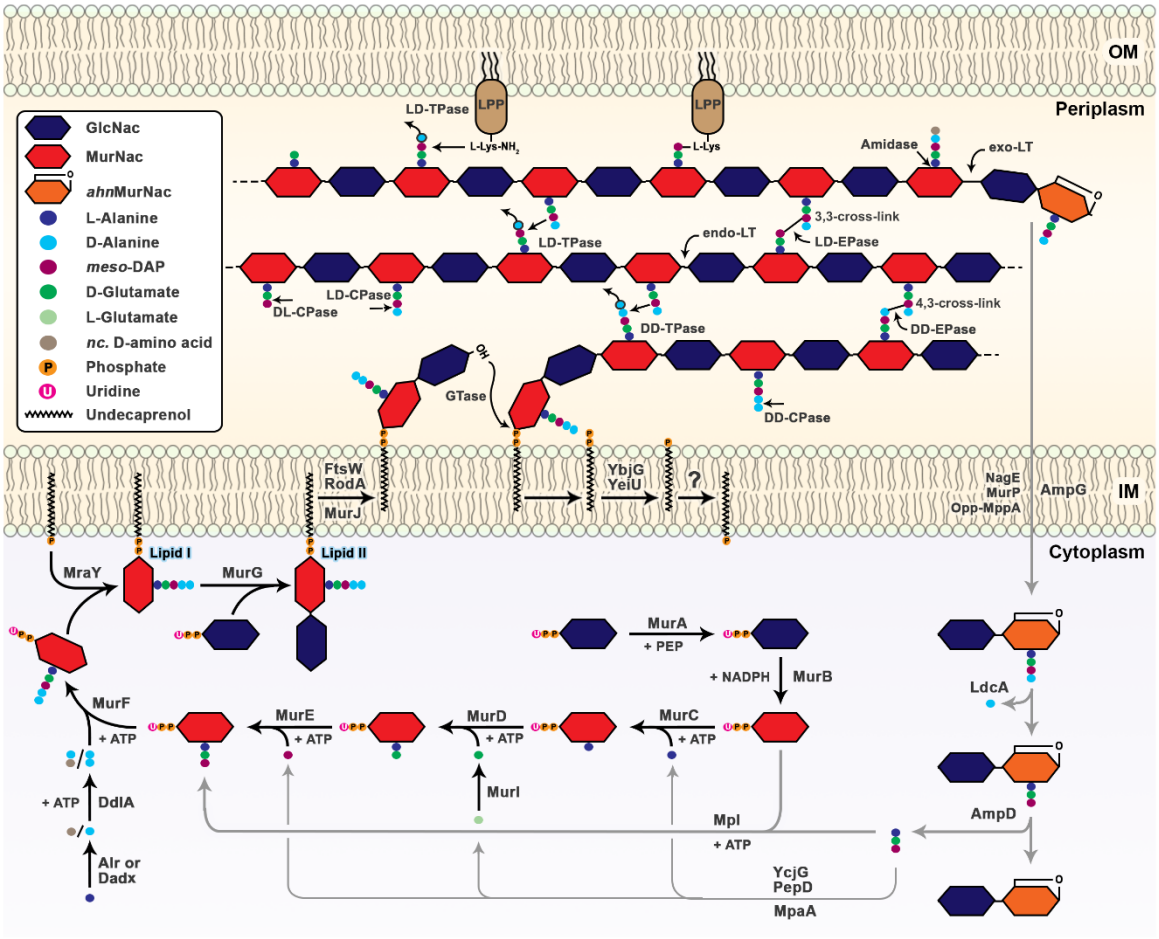

Figure 4: Peptidoglycan synthesis and recycling pathway

The lipid I and lipid II precursors are synthesized in the cytoplasm and linked to undecaprenol before being flipped into the periplasm by MurJ, possibly FtsW and RodA. Glycosyltransferases (GTase) catalyze the polymerization of the glycan strand, whilst trans-peptidases (TPase) cross-link the stem peptide by a 4,3-crosslink to the present PG mesh. LD-trans-peptidases catalyze the formation of 3,3-crosslinks between stem peptides or attach them to Lpp to anchor the PG layer to the OM. The terminal ends of stem peptides are clipped by DD-, LD-, and DL-carboxypeptidases (CPases), and cross-links between stem peptides are cleaved by DD- and LD-endopeptidases (EPases). Amidases remove the entire stem peptide from MurNAc. The glycan backbone is cleaved by exo- or endo-lytic transglycosylases (LTs), generating glycan-strand terminal 1,6-anhydro-N-acetylmuramic acid (*anh*MurNAc). One example of PG component recycling is the regeneration of released *anh*MurNAc-pentapeptide. *Anh*MurNAc-pentapeptide is transport into the cytoplasm and stem peptide is entirely reused, or the terminal amino acids are consecutively removed and fed back into the synthesis pathway. Abbreviations: Alr, Ala racemase; DadX, Ala racemase; DdlA, D-ala–D-ala ligase; GlcNAc: N-acetylglucosamine; MurNAc: N-acetylmuramic acid; *meso*-DAP: *meso*-diaminopimelic acid; MraY: UDP-MurNAc-pentapeptide phosphotransferase; MurA: UDP-GlcNAc enolpyruvyl transferase; MurB: UDP-MurNAc dehydrogenase; MurC: UDP-MurNAc–L-Ala ligase; MurD: UDP-MurNAc-L-Ala–D-Glu ligase; MurE: UDPMurNAc-L-Ala-D-Glu–meso-DAP ligase; MurF: UDP-MurNAc-tripeptide–D-alanyl-D-ala ligase; MurG: UDP-GlcNAc-undecaprenoyl-pyrophosphoryl-MurNAc-pentapeptide transferase; MurI: Glu racemase; YbjG, YeiU: undecaprenol-phosphate regeneration; AmpG, NagE, MurP, Opp-MppA: recycling transporter across IM; LdcA: carboxypeptidase; AmpD: amidase; YcjG: epimerase; PepD: dipeptidase; MpaA: amidase, MpI: ligase; NADPH: nicotinamide adenine di-nucleotide phosphate; PEP: phosphoenolpyruvate. Adapted from Typas *et al*. (2012).

1.4.2 Synthases

In order for cells to grow and divide, the PG sacculus needs to be extended. Responsible for those reactions are penicillin-binding proteins (PBPs), a group of proteins that are characterized by their ability to bind penicillin (Suginaka *et al.*, 1972). Although not all PBPs are PG synthases, many of them are involved in PG biogenesis. PG synthases can be classified into three types: bi-functional glycosyltransferases (GTase), trans-peptidases (TPase) (class A PBPs), monofunctional TPases (class B PBPs) and monofunctional GTases (Figure 4) (Vollmer and Bertsche, 2008). In *E. coli* mainly two PBPs are responsible for cell elongation and cell division, respectively: the bi-functional enzymes PBP1A and PBP1B (Figure 5), which are able to catalyze both, trans-glycosylation (TG) and trans-peptidation (TP) reactions. Those two enzymes belong to class A PBPs and although PBP1A and PBP1B perform similar tasks, they become essential in the absence of each other (Kato *et al.*, 1985; Yousif *et al.*, 1985). *In vivo* studies have shown that *E. coli* PBP1A and PBP1B activities are dependent on outer membrane lipoproteins LpoA and LpoB, respectively (Paradis-Bleau *et al.*, 2010; Typas *et al.*, 2010). It has been suggested that LpoA and LpoB activate the TP activity of their respective PBP partner-protein (Lupoli *et al.*, 2014), performing a regulatory role in PG synthesis, instead of a catalytic. Despite PBP1s localizing to the inner membrane and Lpo proteins localizing to the outer membrane, direct interaction of PBP1/Lpo pairs were observed. Additionally, the structure of LpoB revealed a long flexible stretch at the N-terminus that can reach through the periplasm and bind to PBP1B (Egan *et al.*, 2014). It has been hypothesized that the Lpo activator proteins allow for the detection of gaps in the PG network. At this site the PBP1/Lpo interaction can take place and in this way induce synthesis of new PG (Typas *et al.*, 2012). *E. coli* encodes for a third PBP1 protein: PBP1C acts as a GTase (Typas *et al.*, 2012), which is membrane-anchored and in combination with a bacterial α2-macroglobulin YfhM, forms the YfhM/PBP1c complex that functions in bacterial colonization, PG repair and periplasmic defense against host proteases, helping them in escaping the immune response (Budd *et al.*, 2004). There are two Class B PBPs or mono-functional TPases, which are well-characterized and widely conserved: PBP2 co-localizes with MreB and is essential for cell elongation (van der Ploeg *et al.*, 2013). PBP3 (FtsI) is part of the divisome and required for cell division (Spratt, 1975; de Pedro *et al.*, 1997; Weiss *et al.*, 1999; Typas *et al.*, 2012). According to some reports, the already mentioned SEDS family proteins FtsW and RodA, which might be involved in flipping lipid II to the outer leaflet of the IM, also possess GTase activity (Cho *et al.*, 2016; Meeske *et al.*, 2016). Another protein shown to have GTase activity is MtgA. MtgA localizes to the divisome and interacts with other cell division proteins (Derouaux *et al.*, 2008). *V. cholerae* also possesses PG

synthetic enzymes similar to *E. coli*, including homologues of the PBP activators LpoA and LpoB (Dörr *et al.*, 2014). It has been observed that *V. cholerae* lacking PBP1A or LpoA are more sensitive to a variety of cell wall stresses when compared to wildtype cells or those lacking PBP1B/LpoB. This suggests that in *V. cholerae* PBP1A plays the main role in PG synthesis (Dörr *et al.*, 2014).

1.4.3 Lytic enzymes

Not only PG synthetizing proteins play an important role but also enzymes that are able to cleave PG in various positions are critical for the survival and growth of bacteria. In general, bacteria encode for large variety of lytic enzymes that can target different components of the PG backbone. One class of enzymes, which cleave the β-1,4- glycosidic bonds between MurNAc and GlnNAc and thereby producing 1,6-anhydro-N-acetylmuramic acid (terminal ends), are named lytic trans-glycosylases (LTase) (Figure 4) (Höltje *et al.*, 1975). In *E.coli*, the majority of LTases are membrane-anchored, however also a soluble periplasmic LTase has been discovered (Romeis *et al.*, 1994; Höltje, 1998).

1.4.3.1. Endopeptidases

Another class of lytic enzymes are endopeptidases (EPases), which are able to cleave the peptide bonds that link the stem peptides of parallel glycan strands (Figure 4). Through this mechanism the trans-pepdidation is reversed, thus creating space in the PG layer where new glycan strands can be inserted (Höltje, 1998; Singh *et al.*, 2012; Dörr *et al.*, 2013). Endopeptidases can be categorized according to the type of cleavage site: LD-endopeptidases (cleavage between L- and D-amino acids/meso-DAP) and DD-endopeptidases (cleavage between D-amino acids) (Foster *et al.*, 2000). These endopeptidases possess the characteristic catalytic domain of M23/LytM metalloproteases with its conserved metal binding site motifs, HxxxD and HxH. These two motifs have been shown to coordinate binding of a zinc ion for catalytic activity (Rawlings *et al.*, 2008; Cohen *et al.*, 2009; Zastrow *et al.*, 2014) and *in vitro* experiments show that most M23 peptidases cleave glycyl-glycine bonds (lysostaphin) in the peptidoglycan of Gram-positive organisms (Spencer *et al.*, 2010). Interestingly, M23 peptidases are also present in bacteria that do not possess glycyl-glycine peptide linkages in their PG (Ragumani *et al.*, 2008), indicating that these enzymes perform other tasks. M23 metallopeptidases can be divided into two subfamilies: M23A and M23B. The M23A subfamily

contains beta-lytic endopeptidases that cleave glycine-bonds in the cell walls of Gram-positive bacteria (Li *et al.*, 1990) and are often secreted into the environment as a defense-mechanism against other bacteria (Spencer *et al.*, 2010). The M23B subfamily mostly contains proteins involved in peptidoglycan remodeling.

M23 peptidase domains can be found in combination with many other domains. Some M23 peptidases are secreted extracellularly and target other bacteria in the environment. These beta-lytic enzymes usually have the M23 domain located at the N-terminal region (after these enzymes have been processed and the pro-region was removed) or possess a centrally located catalytic M23 domain (Rawlings *et al.*, 2008; Spencer *et al.*, 2010). In contrast, M23 domains involved in PG remodeling of the host cell are often located C-terminally (Rawlings *et al.*, 2008). Many bacterial species encode multiple copies of M23 peptidases that perform a specific task under certain intra- or extracellular conditions and are often redundant (Firczuk *et al.*, 2007). For example, *V. cholerae* encodes two cell division M23 proteins: EnvC and NlpD, required for activation of a cell separation amidase during cell division and three cell elongation M23 proteins: ShyA, ShyB and ShyC (Dörr *et al.*, 2013).

Most well-studied bacteria complete the cell cycle by binary fission (Adams *et al.*, 2009). This process is usually divided into three steps: (I) the invagination of the inner membrane, PG and the outer membrane, (II) cell separation by the formation of independent cytoplasmic compartments and (III) maturation of new poles and final detachment of the old and new daughter cell (Adams *et al.*, 2009). In *E. coli*, the last process requires the regulated action of amidases, together with their M23 activators, to cleave the septal PG (Tidhar *et al.*, 2009; Uehara *et al.*, 2009; Möll *et al.*, 2014; Ercoli *et al.*, 2015). Examples of such amidase activating M23 peptidases are EnvC, NlpD in *E. coli* and SpoIIQ in *Bacillus subtilis*, which is involved in sporulation. Interestingly, these proteins do not display hydrolytic activity as they lack important Zn^{2+} coordinating residues (Meisner *et al.*, 2012; Peters *et al.*, 2013). Despite this catalytic deficiency, EnvC and NlpD play critical roles in activation of amidases, through protein interaction (Domínguez-Gil *et al.*, 2016). Most cell separation amidases have auto-inhibitory domains within their active sites, suggesting that amidase activity is blocked prior to cell division (Yang *et al.*, 2012). This was demonstrated with AmiB of *Bartonella henselae* (*B. henselae*), *E. coli* AmiC and Ami1 of *M. tuberculosis* (Yang *et al.*, 2012; Kumar *et al.*, 2013; Rocaboy *et al.*, 2013). Disrupting that regulation in *E. coli* by deleting *envC* and *nlpD* results in long chains of cells with distinct cytoplasmic compartments but connected layers of PG (Uehara *et al.*, 2009, 2010). An *E. coli* mutant lacking all cell separation amidases exhibits a similar phenotype (Heidrich *et al.*,

2001, 2002; Priyadarshini *et al.*, 2007). The activation of *E. coli* amidases seems to require direct interaction with EnvC and NlpD (Uehara *et al.*, 2009) and it is suggested that EnvC and NlpD activate their respective amidases through conformational changes that act on the auto-inhibitory domains in the amidase active sites (Yang *et al.*, 2012). In addition, *E. coli* encodes two more M23 peptidases: YebA, which was shown to be a D,D-endopeptidase and the uncharacterized YgeR (Singh *et al.*, 2012). Non-typeable[1] *Haemophilus influenzae* (NTHI) encodes for three M23 peptidases that are homologous to YebA, EnvC and NlpD of *E. coli* (Ercoli *et al.*, 2015). Interestingly, an *envC* NTHI mutant showed a drastic reduction of periplasmic protein abundance, suggesting that NTHI EnvC facilitates a gateway through cross-linked PG that maintains the surface protein content (Ercoli *et al.*, 2015). Deletion of NTHI *yebA* resulted in massive membrane blebbing, indicating that NTHI YebA could be directly involved in cell division (Ercoli et al., 2015). *Caulabacter crescentus* encodes a M23 peptidase involved in cell division called DipM, among seven genes that encode putative M23 peptidases (Möll *et al.*, 2010). Similarly to *C. crescentus* DipM, *S. elongatus* DipM facilitates cell division and localizes to mid-cell (Miyagishima *et al.*, 2014).

Both PG-synthesizing and PG-hydrolyzing enzymes are important for PG remodeling and ultimately also the cell shape (Cabeen *et al.*, 2005). In most bacterial species, cells elongate their cell body by incorporating new PG material along their lateral axis. *V. cholerae* for example, encodes for three elongation-specific M23 peptidases: sidewall hydrolase (*shy*) *A*, *B* and *C*. These peptidases have been shown to be non-essential for cell division but are strictly required for cell elongation. Time-lapse microscopy revealed that in a ShyAC deletion background, the depletion of an inducible copy of *shyA* leads to a 50% decrease in cell elongation rate (Dörr *et al.*, 2013). Previously it had only been shown that cell elongation is facilitated by NlpC/P60 endopeptidases such as *E. coli* Spr and YdhO and penicillin-binding proteins, however *V. cholerae* ShyABC is one of the first examples that also M23 peptidases are involved in that process (Singh *et al.*, 2012; Dörr *et al.*, 2013).

In addition to cell elongation, M23 peptidases have also been shown to facilitate cell shape as demonstrated in *H. pylori* (Bonis *et al.*, 2010; Sycuro *et al.*, 2010). M23 peptidases Csd (cell shape determinant) 1, 2 and 3 alter the PG crosslinking and in this way contribute to the generation of the helical shape of *H. pylori*. Deletion of all three *csd* genes leaves cells unable to develop the helical shape and produces cells with highly aberrant cell morphologies, additionally also affecting pathogenicity. Csd2 is the only protein of the three with a degenerate M23 domain and might not

[1] Lack of distinct capsular antigens

be directly involved in PG re-modelling (An *et al.*, 2016). However, the interaction between Csd1 and Csd2 might provide substrate specificity for Csd1, which is the catalytically active subunit of the Csd1 Csd2 heterodimer (An *et al.*, 2016).

Under nutrient limitation and other external stresses bacterial species such as *Bacillus* and *Clostridium* undergo differentiation which ultimately lead to the formation of highly resistant endospores (Galperin *et al.*, 2012; Higgins *et al.*, 2012; Paredes-Sabja *et al.*, 2014). Endospores consist of two PG layers: an inner cell wall, which will become the new PG layer of germinating cells and an outer spore-specific cortex. Compared to the inner cell wall, the PG of the spore cortex is only loosely cross-linked but is the major contributor to the spore's resistance to external stresses like heat. The M23 peptidase LytH of *B. subtilis* has been shown to be a sporulation-specific component in the cortex structure formation (Horsburgh *et al.*, 2003). Spores of the *lytH* deletion mutant are less resistant to heat, and analysis of the spore cortex PG content revealed the loss of muropeptides containing single L-alanine side chains (Horsburgh *et al.*, 2003). This suggests that the LytH is an LD-M23 peptidase involved in the production of the single L-alanine side chains in the spore cortex. SpoIIQ harbors a degenerate M23 domain and it is important for localizing a number of proteins involved in spore maturation during endospore formation (Meisner *et al.*, 2011). Meisner *et al.* demonstrated that SpoIIQ interacts with SpoIIIAH through its degenerate M23 domain. In return, SpoIIIAH enables the recruitment of several other proteins to the mother cell forespore channel (Meisner *et al.*, 2011; Crawshaw *et al.*, 2014) and ultimately leads to progression in spore formation. Deleting *spoIIQ* results in a non-sporulating strain (Meisner *et al.*, 2011). The introduction of point mutations in the M23 domain of SpoIIQ impairs its localization to the forespore septal membrane by disrupting the interaction with SpoIID and SpoIIP, which are important to anchor SpoIIQ in the septal membrane (Rodrigues *et al.*, 2013).

1.4.3.2. Carboxypeptidases

Another class of PG lytic enzymes are the carboxypeptidases (CPases), which remove the terminal amino acid (usually D-alanine) from the stem peptides (Figure 4) (Vollmer, Joris, *et al.*, 2008). These types of enzymes can also be categorized according to the type of cleavage site: LD-carboxypeptidases (cleavage between L- and D-amino acids/meso-DAP) and DD-carboxypeptidases (cleavage between D-amino acids). *E. coli* encodes for at least four CPases (Vollmer and Bertsche, 2008). Depending on the environmental conditions, the cells might utilize a different set of CPases,

as it was shown that the activity of PBP6B was increased at acidic pH (Peters *et al.*, 2016). PBP5 (DacA) localizes to the lateral cell wall and the division site and its deletion results in a cell-population with increased occurrence of branched cells (Potluri *et al.*, 2012). In *V. cholerae*, the PBP5 homologue has been attributed to its halo-tolerance (Möll *et al.*, 2015) and its deletion displays slow growth, aberrant morphology and altered peptidoglycan structure. Upon deletion of DacB in *V. parahaemolyticus*, the cells exhibit morphological defects with the formation of aberrantly shaped cells (Hung *et al.*, 2013).

1.4.3.3. Amidases

Amidases are responsible to cleave the bond between the glycan strand and the stem peptide (Figure 4) (Vollmer, Joris, *et al.*, 2008). In *E. co*li, five amidases (AmiA, AmiB, AmiC, AmiD and AmpD) have been identified and characterized (Jacobs *et al.*, 1995; Heidrich *et al.*, 2001; Bernhardt *et al.*, 2003; Uehara *et al.*, 2007). AmiA, AmiB and AmiC are soluble periplasmic proteins and have an Ami_3 domain located at the C-terminus (Heidrich *et al.*, 2001; Korndörfer *et al.*, 2006). While AmiC is required for cell separation and localizes to the division site of *E. coli*, AmiA shows a diffuse distribution (Bernhardt *et al.*, 2003). AmiD is a lipoprotein that is anchored to the outer membrane and it does not participate in cell separation (Uehara *et al.*, 2007). However, in contrast to the other four amidases, AmiD is able to cleave intact peptidoglycan (PG) as well as soluble fragments that contain N-acetylmuramic acid regardless of the presence of an anhydro form or not (Kerff *et al.*, 2010). AmpD is a cytoplasmic enzyme that can act as a negative regulator of β-lactamase expression (Jacobs *et al.*, 1995). In addition, it specifically cleaves the *anh*MurNAc-L-alanine bond of PG in order to recycle cell wall components (Uehara *et al.*, 2007). As described in section 1.4.3.1, the activity of the amidases can be influenced by endopeptidases of M23 zinc-metallopeptidases family (Firczuk *et al.*, 2007). These M23 endopeptidases activate amidases of *E. coli*, however they possess no catalytic activity (Uehara *et al.*, 2009). NlpD and EnvC localize earlier to the divisome than the amidases and require the activity of PBP3 (Peters *et al.*, 2011). Controlling amidase activity through M23/LytM activation is a wide spread mechanism of regulation. In *Pseudomonas aeruginosa*, the amidase AmiB and the three LytM proteins have been shown to play an important role in cell separation, envelope integrity and antibiotic resistance (Scheurwater *et al.*, 2007; Yakhnina *et al.*, 2015). Although M23 domain protein NlpD of *Neisseria gonorrhoeae* has intrinsic hydrolytic activity and binds PG, it also potentiates the activity of AmiC (Stohl *et al.*, 2016). Also in the cyanobacterium *Anabaena sp. PCC 7120*, a M23/LytM protein has been suggested to control the activity of an AmiC-

type cell wall hydrolase (AmiC1) (Bornikoel *et al.*, 2018). In this organism, AmiC1 is required in creating nanopores in the septal wall to generate cell-cell junctions that facilitate the communication of adjacent cells(Berendt *et al.*, 2012).

1.4.4 Peptidoglycan recycling

The turnover and recycling process of peptidoglycan components is very important for bacterial cells and it is estimated that roughly 50% of the PG is broken down and reused each generation (Park *et al.*, 2008). Periplasmic hydrolases and endopeptidases break the PG backbone, releasing anhydro-muropeptides, which are mainly transported into the cytoplasm by AmpG (Figure 4) (Jacobs *et al.*, 1994). Released anhydro-muropeptides can follow different pathways in which its building blocks are released and converted. The stem peptide can be cleaved off by the membrane-associated amidase AmiD (Uehara *et al.*, 2007) or by the cytoplasmic amidase AmpD (Jacobs *et al.*, 1995). In addition, the stem peptide can be processed by LD-carboxypeptidase LdcA, which releases free D-Ala and the tripeptide (Jacobs *et al.*, 1995). The tripeptide can either be incorporated directly by MpI to produce UDP-MurNAc-tripeptide (Mengin-Lecreulx *et al.*, 1996), or it can be broken down into individual amino acids by amidase MpaA (Uehara *et al.*, 2003), epimerase YcjG and dipeptidase PepD (Schroeder *et al.*, 1994). The genes encoding for AmpG (transporter), AmpD (amidase), LdcA (carboxypeptidase) and Mpl (ligase) are well conserved in a wide variety of proteobacteria, showing how important that mechanism is (Park *et al.*, 2008). Interestingly, some pathogenic bacteria like *H. pylori* and *Borrelia burgdorferi* lack AmpG and enzymes to cleave PG degradation products (Park *et al.*, 2008). Here, compounds that are cleaved from PG by lytic transglycosylases are likely to be released into their surroundings or injected into the cytoplasm of the host. It was shown that *H. pylori* injects Dap-containing material into the host cytoplasm via a bacterial type IV secretion system (Viala *et al.*, 2004). In a similar fashion it has been shown for *Bordetella pertussis* that it secretes large amounts of the intact anhydro-disaccharide-tetrapeptide into the environment (Cookson *et al.*, 1989).

1.5 Cell elongation and division

Bacterial cell growth can be divided into two distinct phases: cell elongation and division (Figure 5). During both phases it is important that PG biogenesis is tightly regulated in order to ensure the propagation of viable cells and the maintenance of morphological features (Typas *et al.*, 2012). The multi-enzyme complexes that facilitate this regulation are the elongasome and the divisome. The elongasome is responsible to synthetize and insert new PG along the lateral axis of the cell (Figure 5A). The divisome on the other hand generates the PG that is required during cell-pole maturation and the final separation of the daughter cell (Figure 5B) (Matteï *et al.*, 2010). MreB, an actin homologue, is an important cytoskeletal element in most rod-shaped bacteria and required for recruiting and guiding of the elongasome (Figure 5A) (Jones *et al.*, 2001; Daniel *et al.*, 2003). MreB is highly dynamic and moves along the short axis of cells, presumably together with the elongasome during peptidoglycan assembly. It was shown that MreB forms short nanofilaments, which are oriented perpendicularly to the long axis and that these fibers have a curvature preference, localizing to cylindrical regions and avoiding the poles (Bratton *et al.*, 2018). The MreB nanofibers are tethered to the inner leaflet of the inner membrane through the interaction with the integral IM protein RodZ as well as MreC and MreD (de Pedro *et al.*, 2001; Alyahya *et al.*, 2009; Bendezú *et al.*, 2009; Dominguez-Escobar *et al.*, 2011). In addition, these elongasome proteins interact with the PG synthases PBP1A, which is regulated by its OM associated partner protein LpoA, and PBP2 (Dörr *et al.*, 2014; Jean *et al.*, 2014). During cell division, the divisome is formed (Figure 5B). The tubulin homologue FtsZ facilitates the recruitment of PG synthases as well as hydrolases and additional factors required for cell division (Typas *et al.*, 2012). At first, ZipA and FtsA, which stabilize the Z ring, localize together with ZapA and FtsEX (Haney *et al.*, 2001; Corbin *et al.*, 2007; Arends *et al.*, 2009). Only at a later time point, the essential proteins FtsK, FtsQBL, FtsW, FtsN and FtsI (PBP3) are recruited to produce the mature divisome (Weiss *et al.*, 1999; Aaron *et al.*, 2007). FtsA and FtsN interaction has been shown to be important for septal PG synthesis and constriction (Weiss, 2015). PBP1B and its activator partner protein LpoB localize to the division site at a later stage together with amidases and their regulatory degenerate M23 peptidases EnvC and NlpD (Uehara *et al.*, 2009; Paradis-Bleau *et al.*, 2010; Dörr *et al.*, 2014). Here, in order to insert new material, the old PG mesh needs to be briefly disconnected, partially through the action of lytic transglycosylases and carboxypeptidases (Romeis *et al.*, 1994; Vollmer *et al.*, 1999). Finally, the envelope-spanning Tol-Pal complex, which is responsible for the invagination, is recruited to the divisome and the cell division takes place (Gerding *et al.*, 2007; Typas *et al.*, 2010). However, afterwards the disassembly of the

divisome is crucial. In *E. coli* it has been shown that this process involves at least five steps (Söderström *et al.*, 2016) and it begins with FtsZ leaving the former division site and ends with the disassembly of FtsN, hence following a first-in, first-out mechanism (Söderström *et al.*, 2016).

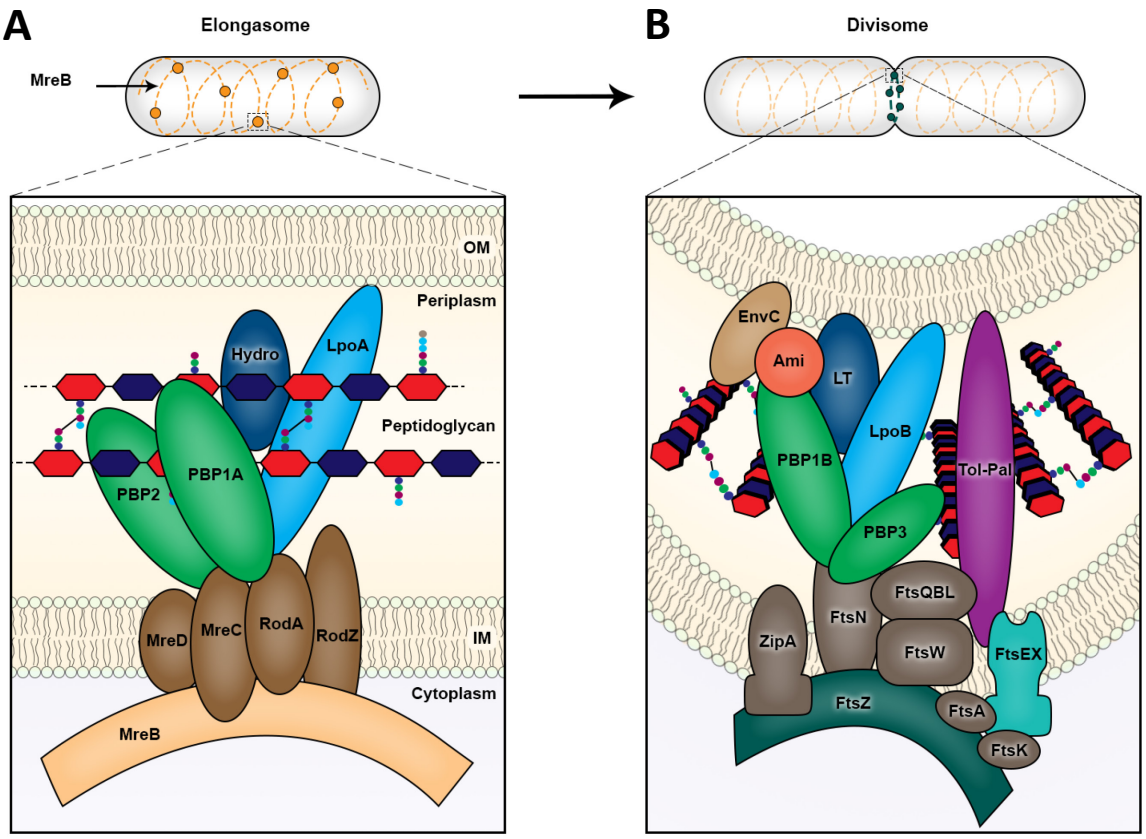

Figure 5: Elongasome and divisome complexes

Different multi-protein complexed are required during cell envelope elongation and cell division. (A) MreB and associated membrane proteins (MreCD, RodAZ) control and position the peptidoglycan synthases PBP1A and PBP2, as well as still-unknown hydrolases (Hydro) during the lateral elongation of the cell envelope. (B) After previous arrival of early divisome components (FtsA, ZipA, ZapA, FtsEX, FtsK), the mature cell division complex is formed out of essential, inner membrane-localized cell division proteins. In addition, the peptidoglycan synthases PBP1B and PBP3, and amidase enzymes (Ami) with their activators (EnvC), lytic transglycosylases (LT), as well as proteins of the Tol–Pal complex, which are important for constriction of the outer membrane, altogether are important components of the divisome. Activity of the PBPs is regulated in part by outer membrane-anchored lipoproteins such as LpoA and LpoB. Adapted from Typas *et al*. (2012)

1.6 Model organism *Vibrio parahaemolyticus*

In this work *V. parahaemolyticus* was used as a model organism to study peptidoglycan remodeling by M23 peptidases and their influence on cell morphology.

V. parahaemolyticus is a rod-shaped gram-negative bacterium and belongs to the class of the γ-proteobacteria. It was first discovered in 1950 as a causative agent of a large, food borne disease outbreak in Japan (Fujino *et al.*, 1953). Just like its close relative *V. cholerae*, *V. parahaemolyticus* can colonize hosts like salmon, shrimps and crabs (Vasconcelos *et al.*, 1975) and causes seafood-borne gastroenteritis when consumed with raw or undercooked seafood (Daniels *et al.*, 2000; Newton *et al.*, 2012; Zarei *et al.*, 2012). Additionally, there is plenty of evidence involving *V. parahaemolyticus* in extra-intestinal infections, including infections of the ear, eye, blood, and wounds (Daniels *et al.*, 2000).

Environmental conditions often change and lead bacteria to develop various strategies to respond accordingly. In many cases, bacteria are able to transform into specialized cell-types. This differentiation can involve major changes in the cell cycle, cell morphology, or the spatiotemporal organization of cells. Differentiation between a planktonic swimmer cell and a swarmer cell that is specialized for movement over solid surfaces or in viscous environments is a distinct type of differentiation utilized by many bacteria, including species such as *Serratia* (Alberti *et al.*, 1990), *Aeromonas* (Kirov *et al.*, 2002), *Salmonella* (Harshey *et al.*, 1994), *Proteus* (Rather, 2005), and *Vibrio* (McCarter, 2004). In its natural marine habitat, *V. parahaemolyticus* usually occurs as short, swimming cells with a single polar flagellum (from here on referred to as swimmers). Upon environmental queues, it is able to differentiate into long, swarming cells (from here on referred to as swarmers). These cells can be up to 20 times longer than swimming cells and produce a large number of lateral flagella (McCarter, 2004). During the differentiation process, some cellular components like chemotaxis clusters have been shown to be repositioned along the lateral cell axis where the secondary motility system is formed (Heering *et al.*, 2016). The differentiation process also requires extensive regulation of cell envelope elongation, as cell division has to be delayed in order for the cells to increase in length. Swarmer cells might therefor utilize alternative sets of synthetic and lytic enzymes involved in PG remodeling to accomplish this and possibly evolved additional mechanisms, when compared to close relative *V. cholerae*, which does not swarm or differentiate. The swarmer cell type, although not observed yet in the environment, can be

generated under certain laboratory conditions (Heering *et al.*, 2017) and allows us to study this morphotype.

Although *V. cholerae* and *V. parahaemolyticus* are closely related and share most of the mechanisms and homologous enzymes required for cell wall biogenesis, little is known about cell wall synthesis, elongation and maintenance in *V. parahaemolyticus,* specifically. The worldwide persistence and increase of gastroenteritis cases caused by *V. parahaemolyticus* emphasizes the need for a better understanding of those processes, especially how this bacterium maintains cell viability throughout its cell cycle and as focused in the study: cell wall biogenesis.

1.7 Aim of Study

The peptidoglycan is important for structural maintenance and osmotic protection of the bacterial cell. Beta-lactam antibiotics, such as penicillin, inhibit peptidoglycan biogenesis through their action on penicillin binding proteins and in this way can cause cell death. In recent years, there have been increasing amounts of multi drug-resistant bacterial infections, which makes it very important to identify new anti-microbial targets. M23 peptidases were shown to be involved in peptidoglycan and membrane maintenance, but also other important cellular processes including cell division, sporulation and cell shape maintenance. As such, they are of general interest in microbial research and an ideal target for new drug development. In the human pathogen *V. parahaemolyticus* little is known about M23 peptidases and their role in cell division and cell shape, however some of the homologues proteins of that family have been studied in the close relative *V. cholera*. The aim of this study is to verify or find new functions of M23 peptidases in the dimorphic organism *V. parahaemolyticus* and to further elucidate their roles of in that organism and to further increase our general understanding for the role of this class of proteins.

2 Results

Other Gram-negative bacteria and close relatives of *V. parahaemolyticus* have been studied extensively regarding peptidoglycan remodeling. *V. parahaemolyticus* also possesses a large variety of synthetic and lytic enzymes, involved in remodeling of peptidoglycan as described in other organisms. Some of these enzymes are required for growth, cell division and cell shape maintenance. Lytic enzymes cleave the existing glycan strands and peptide side chains in order to provide the necessary space to insert new material (Vollmer and Bertsche, 2008). This study focuses on M23 peptidases, a class of enzymes shown to be important to cleave the peptide bond of stem peptides, which are interconnecting glycan strands. Members of this protein class have been indicated in many important cellular processes (see section 1.4.3.1).

2.1 *V. parahaemolyticus* encodes seven M23 peptidase domain proteins

We performed homology search using BlastP (Kegg2 database) on a conserved M23 domain and found that *V. parahaemolyticus* encodes for seven proteins that contain a predicted M23 peptidase domain (Figure 6A). VP0548, VPA1649 and VP1385 have an N-terminal cytoplasmic domain, followed by a transmembrane domain, which indicates that they are likely inserted into the inner membrane with the C-terminal region located in the periplasm. VP0548, VPA1649 and VP2834 are predicted to possess coiled-coil domains, which have been shown to be involved in protein-protein interactions (Truebestein *et al.*, 2016). Both VP2471 and VPA0517 have a putative PG binding domain (OapA domain) (Weiser *et al.*, 1995; Dörr *et al.*, 2013). These two proteins are homologues to the previously characterized peptidases important for cell elongation in *Vibrio cholerae*, ShyC and ShyA, respectively (Dörr *et al.*, 2013). VP2554 and VP2834 are homologous to NlpD and EnvC, respectively. Those proteins have been shown to be activators of amidase activity in many different bacteria, including *E. coli* and *V. cholerae* (Uehara *et al.*, 2010; Möll *et al.*, 2014). In addition, VP2554 also possess a LysM domain, which has been shown to bind to peptidoglycan (Buist *et al.*, 2008).

Multiple sequence alignment of the M23 domains of the seven proteins shows that only NlpD and EnvC homologues have degenerate zinc ion binding motifs and lack the important residues (HxxxD, HxH), as it has previously been shown in other organisms (Figure 6B) (Uehara *et al.*, 2010; Möll *et al.*, 2014). VP0548, VPA1649, VP1385, VP2471 (ShyC) and VPA0517 (ShyA) all have the conserved

amino acid motif, which is important for catalytic activity by coordinating a zinc ion (Rawlings *et al.*, 2008; Cohen *et al.*, 2009; Zastrow *et al.*, 2014).

Here we show that although some M23 peptidases are homologues to previously identified factors important for cell division and shape in other organisms, *V. parahaemolyticus* encodes for uncharacterized M23 peptidases as well. Importantly, homology is also not always in an indicator of conserved function, as *V. parahaemolyticus* might have evolved and adapted alternative or additional activity for those homologues enzymes.

In this study, we specifically focus on VP0548, which from now on will be designated as VcsP (*vibrio* cell separation peptidase).

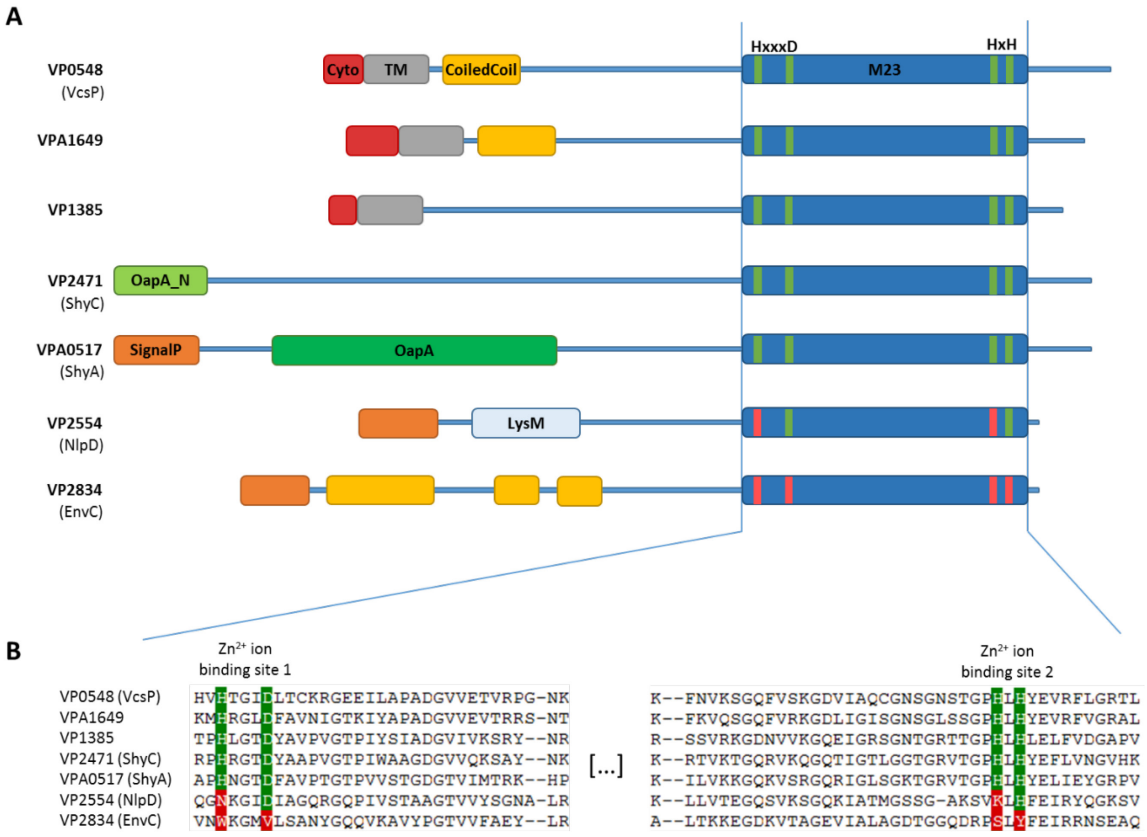

Figure 6: Protein domains and alignment of M23 peptidases encoded in *V. parahaemolyticus*

(A) SMART and PFAM databases were used to identify protein domains. Abbreviations: Cyto: cytoplasmic domain; TM: transmembrane domain; OapA_N: N-terminal region of the OapA domain; OapA: Opacity-associated protein A LysM-like domain; SignalP: signal peptide; LysM: lysin motif containing domain; M23: M23 peptidase domain. (B) ClustalOmega was used to produce the multiple sequence alignment of *V. parahaemolyticus* M23 peptidase domains.

2.2 Phylogenetic analysis of VcsP in comparison to ShyA and NlpD

After identifying seven M23 peptidases encoded in *V. parahaemolyticus*, sequence homology as well as phenotypic analysis (section 2.3) suggest that the proteins ShyA, ShyC, NlpD as well as EnvC are conserved in *V. parahaemolyticus*. To analyze how VcsP and its paralogues (VP1385, VPA1649) are distinct to these previously described proteins, we performed a phylogenetic analysis. Here we compared the phylogenetic relation of the 200 closest BLAST (KEGG2 database) hits of VcsP, ShyA and NlpD (total 600 sequences). In addition we also analyzed the conservation of the zinc ion binding motifs (HxxxD, HxH) (Figure 7, ring #3); the conservation of the genomic neighborhood (Figure 7, ring #2) and displayed the strains classification (Figure 7, ring #1).

From Figure 7, the 200 BLAST hits of each protein VcsP, ShyA and NlpD formed distinct clades and clustered together and thus showing VcsP likely is distinct from other previously characterized *Vibrio* M23 peptidases. Interestingly, VcsP appeared to be more closely related to ShyA as compared to NlpD. From the first ring of the phylogenetic tree, ShyA and NlpD were found to be highly conserved in the class of γ-proteobacteria and that VcsP related proteins, in addition to γ-proteobacteria, were found in ε-proteobacteria. Part of this class is *H. pylori* that encodes for Csd1, a protein which has been shown to be important for *H. pylori*'s distinct cell shape and mutants of this protein produce aberrantly shaped cells (Sycuro *et al.*, 2010; An *et al.*, 2016).

In order to determine if protein homology also corresponds to a conserved genetic neighborhood within the respective organism, we scored the – 5000 bp and + 5000 bp region of the corresponding gene with a nucleoid identity matrix (Figure 7, ring #2). All the +/- 5000 bp regions were compared to the corresponding *V. parahaemolyticus* input of *vcsP*, *shyA* and *nlpD*. That means that the genetic neighborhood of *V. parahaemolyticus vcsP* will have a 100 % identity score to itself, and a lesser score towards other organisms. The same applies to *shyA* and *nlpD*. Additionally, as the scoring is based on nucleotides (A, T, G, C), there is a 25 % chance that the occurrence of any of the four nucleotides is random, thus giving a minimal identity score of 25 %. The performed identity scoring showed that NlpD's genetic neighborhood is conserved in a wide variety of γ-proteobacteria, as the identity score is at least 50 % for the majority of the analyzed sequences. Organisms more closely related to *V. parahaemolyticus* showed an increasing identity scoring. This shows that the method we used to compare conservation is valid, as it has indeed been shown that *nlpD* is part of an operon with global regulator *rpoS* in *E. coli*, *V. cholerae* and other γ-proteobacteria (Lange *et al.*, 1994; Yildiz *et al.*, 1998). The identity scoring of the *vcsP* and *shyA* neighborhood on the other hand showed,

that in the majority of organisms the genetic neighborhood is not conserved and only closely related organisms have increased identity. This suggests, that both *vcsP* and *shyA* are probably not part of an operon or a highly conserved genetic neighborhood and rather isolated in terms of functional groups. Interestingly, while both *vcsP* and *shyA* show a high score (70 %) with other swarming *Vibrio* species such as *V. alginolyticus* and *V. harveyi*, only *shyA* shows an increased score of 50 % to *V. cholerae*. On the other hand, *vcsP* score to *V. cholerae* barely passes the 25 % minimum. Due to this genetic neighborhood conservation and the phylogenetic clustering, we propose VcsP to be part of a distinct class of M23 peptidases that is conserved in close relatives of *V. parahaemolyticus* (green colored clade).

Interestingly, VcsP (green triangle) paralogue VPA1649 (magenta triangle) was also found in the BLAST results; however VPA1649 separates earlier before the VcsP clade and is likely unrelated to VcsP and its function in *V. parahaemolyticus*. This is in agreement with results from the morphological effects of M23 peptidase deletion mutants (section 2.3 and 2.7).

We also evaluated the conservation of the distinct zinc ion binding motifs (HxxxD, HxH) and found that NlpD, as expected, has degenerate binding motifs throughout the BLAST results (Rocaboy *et al.*, 2013; Möll *et al.*, 2014). ShyA and VcsP on the other hand possess the conserved motifs, which have been shown to be required for catalytic activity (Bochtler *et al.*, 2004) and ShyA has been shown to be active *in vitro* (Dörr *et al.*, 2013).

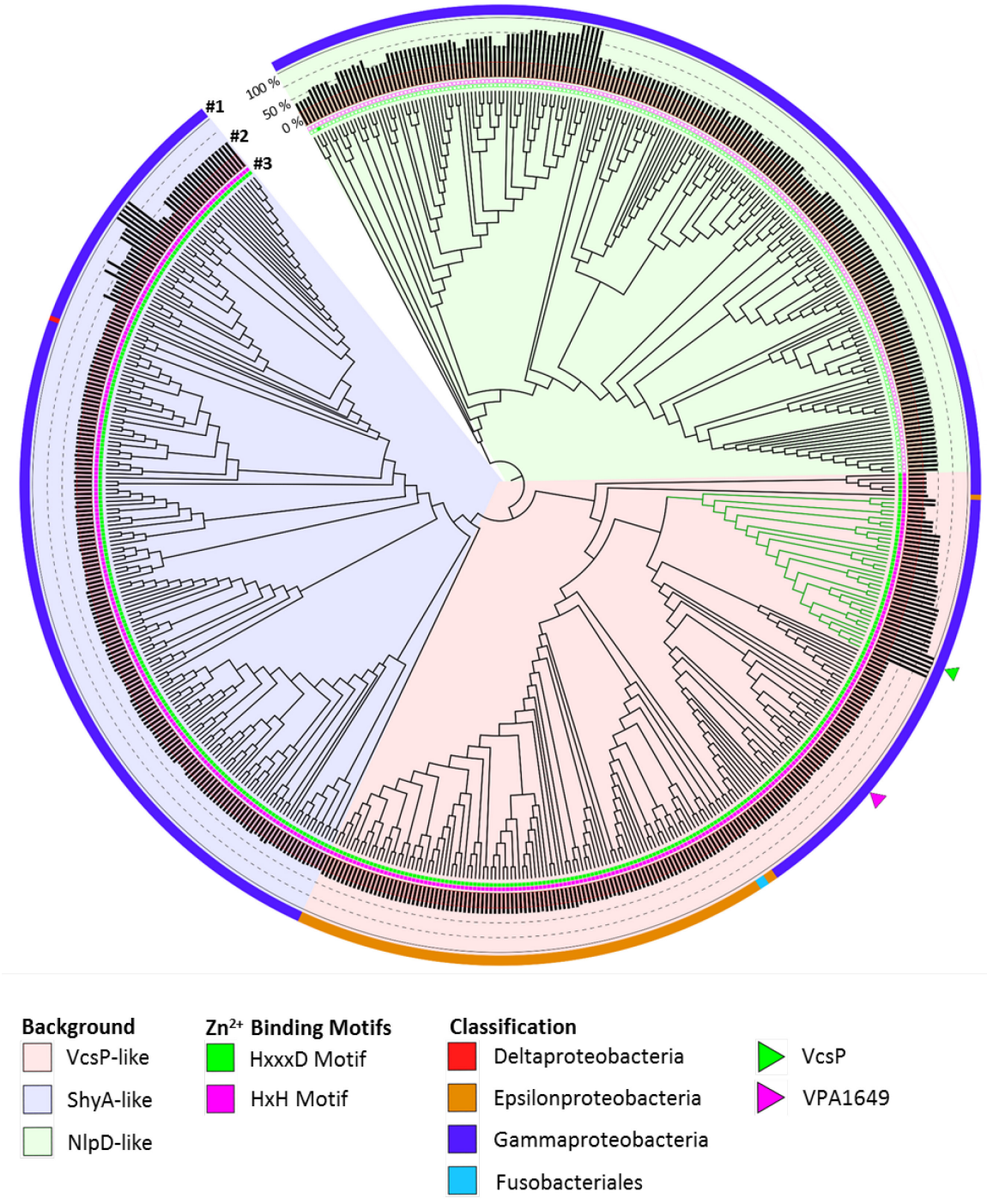

Figure 7: Phylogenetic tree depicting the relation of VcsP, ShyA and NlpD

Phylogenetic tree displaying 200 results of each VcsP, ShyA and NlpD proteins. Results were obtained from KEGG2 BlastP search with an E-value threshold of 10.0 and Clustal Omega Multiple Sequence Alignment was used to generate the alignment as well as the phylogenetic tree. The iTol software was used to visualize and customize the phylogenetic tree. The colored bar in ring #1 indicates the strains classification: red δ-proteobacteria, orange ε-proteobacteria, blue γ-proteobacteria and light blue Fusobacteriales. The black bars in ring #2 represents the +- 5000 bp genetic neighborhood identity score in percent. Minimal score is 25 % due to the one in four chance of a random occurrence of either A, T, G or C. Ring #3 displays the conservation of the zinc ion binding motifs HxxxD (green box) and HxH (magenta box). The green arrow indicates the position of VcsP and the magenta arrow indicates the position of VPA1649.

2.3 VcsP is required for cell separation

In-frame deletion mutants of the seven M23 peptidases were generated in order to determine their effects on cell morphology and the respective deletion strains were analyzed using phase contrast light microscopy (Figure 8). The deletion of *shyA*, as well as the double deletion of *nlpD* and *envC* showed characteristic phenotypes (Figure 8A), as they have been described previously in *V. cholerae* (Dörr *et al.*, 2013; Möll *et al.*, 2014). The s*hyA* deletion produced an increased amount of slightly elongated cells when compared to wildtype (Figure 8BC). The *nlpD envC* double mutant produced a cell chaining phenotype of the entire population, likely through the loss of amidase activation. Strains deleted for *vp1385*, *vpa1649* and *shyC* displayed no significant morphological phenotype when compared to wildtype cells. Interestingly, the deletion of *vcsP* resulted in a cell population, which formed elongated and chaining cells that were unable to separate.

The importance of VcsP becomes even more evident, when analyzing and quantifying the different cell types present in a population of the deletion mutant (Figure 8B). While in wildtype, under the same growth conditions, only less than 2 % of the population were elongated or chaining cells, the deletion of *vcsP* produced a population where almost 25 % of cells were elongated or chaining. Additionally, this is underlined by the cell length distribution of the entire population (Figure 8C). While wildtype cells were 2 µm long on average and never exceeded 5 µm cell length, Δ*vcsP* showed a much broader distribution. Cells were commonly longer than 5 µm and up to 14 µm long, with an average of 2.9 µm (Figure 8C).

In order to take a closer look at the chaining cells, we performed transmission electron microscopy (TEM) of wildtype and *vcsP* mutant cells in collaboration with Dr. Brenzinger and Prof. Briegel (Leiden, NL) (Figure 9). Wildtype cells formed a distinct and symmetric constriction in the center of the cell (Figure 9A) and no chaining cells were observed during TEM imaging. The *vcsP* mutant on the other hand formed chains of cells, with constrictions that were stretched to various degrees and presented membrane blebbing (Figure 9B, black and white arrows). In most cases, the cytoplasm of the dividing cells appeared to be separated while the outer membrane stays connected.

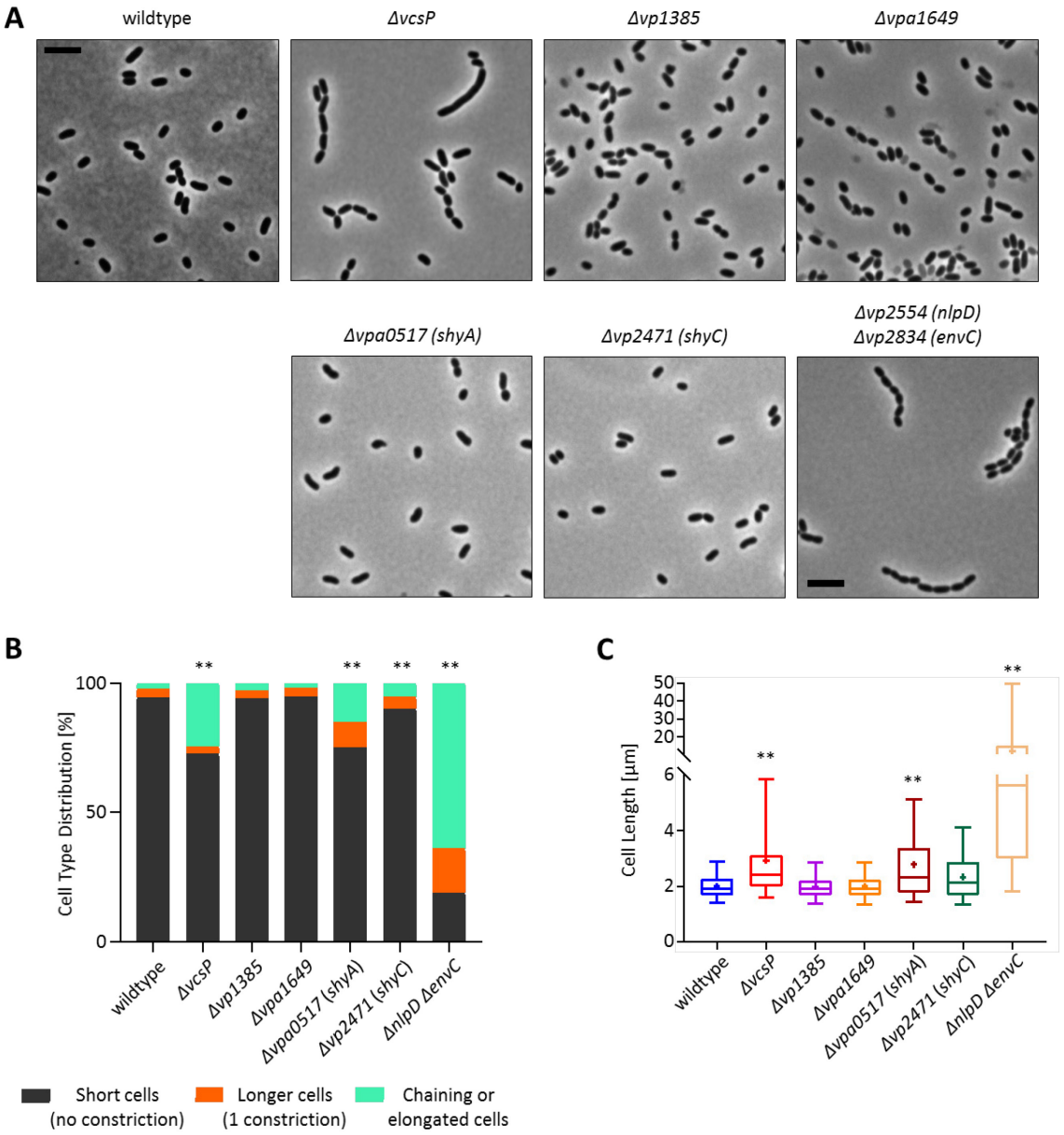

Figure 8: Single cell morphology and analysis of wildtype and M23 peptidase mutants

(A) Representative phase contrast microscopy images of wildtype and mutant cells of indicated strains. Cells were grown until an OD_{600} of 1.5 in LB medium, shaking and at 37 °C. Scale bar: 5 µm. (B) Cells were categorized into three types. 1: Cells with no visible constriction, that are within the 98th percentile of wildtype cell lengths; 2: Cells with one visible constriction, that are within the 98th percentile of wildtype cell lengths; 3: Cells with two and more visible constrictions or a cell length, outside the 98th percentile of wildtype cell lengths. Asterisks indicate a p-value of < 0.0001 (t-test) compared to chaining or elongated cells of wildtype. (C) Distribution of cell lengths in populations of wildtype and M23 peptidase mutants shown as a box plot. The box shows the 2nd and 3rd quartile of the values. The small plus symbol marks the mean value. The line in the box (50% of values) depicts the median. The whiskers mark the 5th and 95th percentile. Asterisks indicate a p-value of < 0.0001 (t-test) compared to wildtype. Quantifications are based on 2400 cells for the wildtype; 1000 cells for Δ*vcsP*, Δ*vp1385* and Δ*vpa1649*; 300 cells for Δ*shyA* and Δ*shyC*; 100 cells for Δ*nlpD* Δ*envC* double mutant.

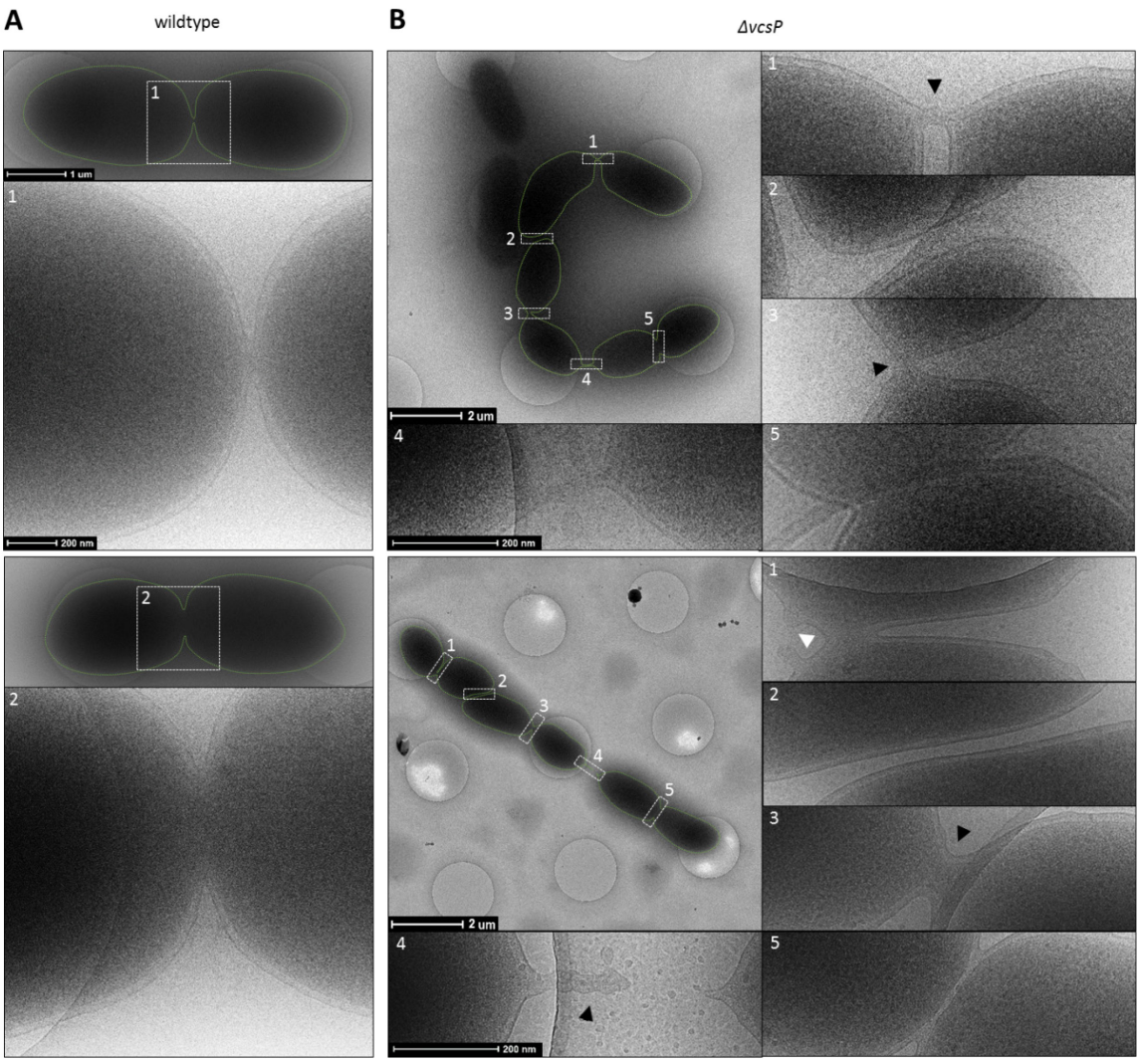

Figure 9: Transmission electron microscopy of wildtype and *vcsP* mutant

(A) Two wildtype *V. parahaemolyticus* cells at low and high magnifications. Scale bars indicated on the top cell also apply to the bottom one. (B) Two Δ*vcsP* mutant cells that display a chaining phenotype with magnifications of the constriction sites. The constriction sites display various stages of cell separation. *V. parahaemolyticus* strains were grown in LB to an OD_{600} of 0.5 and further prepared for imaging. Transmission electron microscopy images were recorded at an acceleration voltage set to 120kV and different magnifications. Black arrows indicate stretched constriction sites, white arrow indicates membrane blebbing.

In order to investigate if the chaining phenotype is due to a FtsZ defect, we performed fluorescent microscopy and localized YFP-FtsZ in both wildtype and Δ*vcsP* mutant strains (Figure 10). We observed that YFP-FtsZ localized to mid-cell in constricting wildtype cells as it had been shown previously (Figure 10A) (Galli *et al.*, 2017; Muraleedharan *et al.*, 2018). Additionally, YFP-FtsZ also localized to constriction sites in chaining and elongated Δ*vcsP* mutant cells, indicating that FtsZ ring formation still occurs at the correct cellular location (Figure 10B). We also observed that the FtsZ

ring was disassembled at some advanced constriction sites, suggesting that the chaining phenotype in this mutant is not the result of an arrested divisome complex or the inability to disassemble the FtsZ ring.

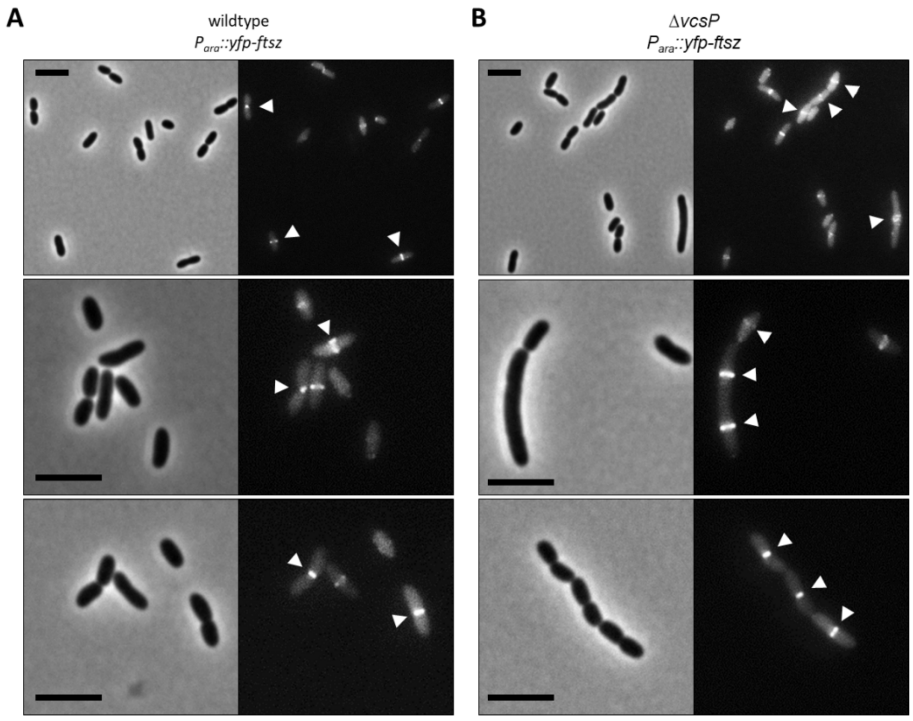

Figure 10: YFP-FtsZ localization in wildtyle and Δ*vcsP*

(A) Representative phase contrast and fluorescence microscopy images of wildtype and (B) Δ*vcsP* mutant, ectopically expressing an inducible YFP-FtsZ fusion protein. Cells were grown until an OD_{600} of 0.15 in LB medium and induced with 2 % L-arabinose and further incubated for 2 h shaking and at 37 °C. Scale bar: 5 µm. White arrows indicate the formation of a FtsZ ring.

2.4 Amino acid substitution of the M23 domain phenocopies Δ*vcsP*

M23 peptidases possess characteristic catalytic M23 domains with conserved metal binding site motifs, HxxxD and HxH. These two motifs have been shown to coordinate the binding of a zinc ion in the protein structure and are important for catalytic activity (Rawlings *et al.*, 2008; Cohen *et al.*, 2009; Zastrow *et al.*, 2014). In order to determine, if this binding motif is also important for VcsP and its function, we replaced the native *vcsP* locus with the gene *vcsP H175A*, which encodes for a VcsP protein variant, VcsP H175A, in which we have introduced an amino acid substitution, HxxxD to AxxxD. The resulting strain was subsequently analyzed for altered cell morphology (Figure 11).

Interestingly, the *vcsP H175A* mutant produced cells with the same phenotype as the *vcsP* deletion mutant (Figure 11A). Chaining or elongated cells were observed in 23 % of the population, which is similar to the *vcsP* deletion mutant (25 %) and significantly different when compared to in wildtype (2 %) (Figure 11B). The deletion mutant of *vcsP* and the *vcsP H175A* mutant on the other hand showed no significant difference compared to each other when looking at the cell length distribution (Figure 11C). Transmission electron microscopy also revealed that the *vcsP H175A* mutant forms stretched constrictions and exhibits membrane blebbing (Figure 11D), which is also the case in the *vcsP* deletion mutant. Membrane blebbing or stretched constriction sites had not been observed in wildtype cells.

These results show that the conservation of the zinc ion binding motif is important for VcsP and required for its function as the *vcsP H175A* mutant has a phenotype identical to that of a *vcsP* deletion mutant.

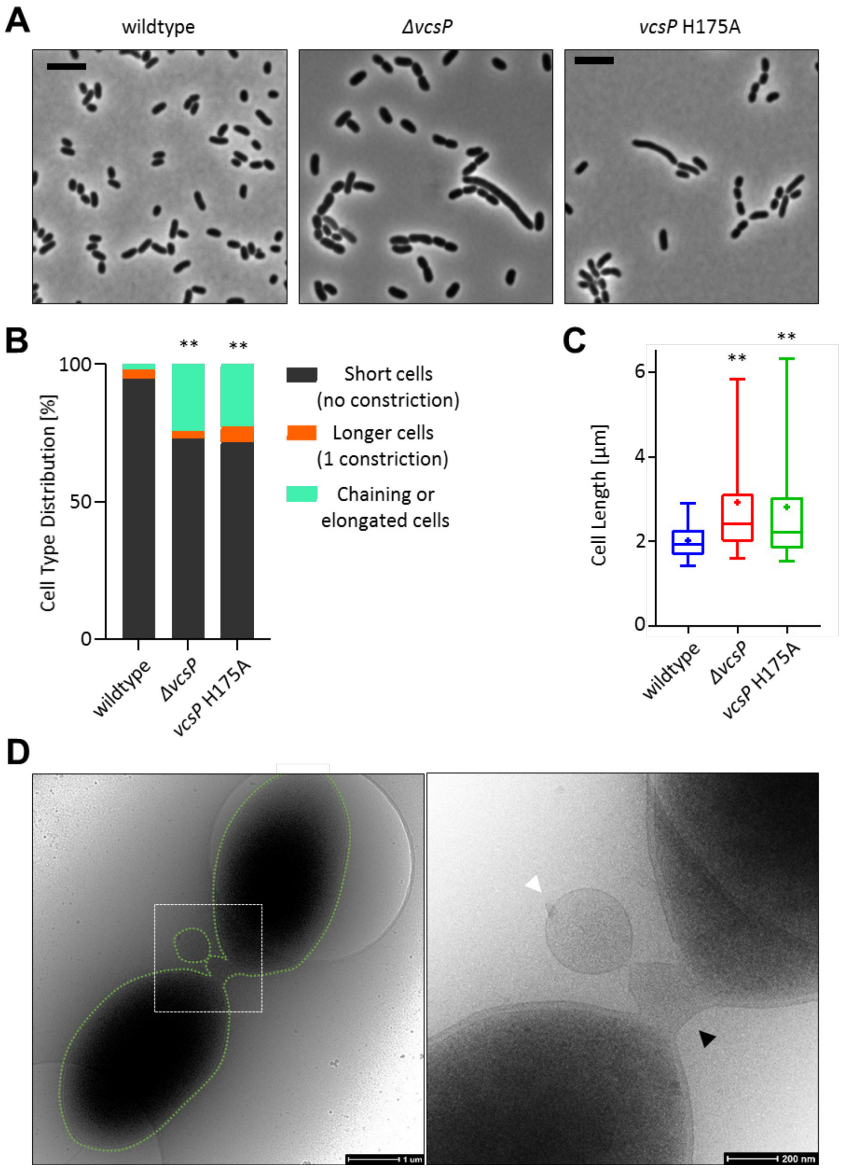

Figure 11: Single cell morphology and analysis of wildtype and *vcsP* mutants

(A) Representative phase contrast microscopy images of wildtype and mutant cells of indicated strains. Cells were grown until an OD_{600} of 1.5 in LB medium, shaking and at 37 °C. Scale bar: 5 µm. (B) Cells were categorized into three types as described in Figure 8. Asterisks indicate a p-value of < 0.0001 (t-test) compared to chaining or elongated cells of wildtype. (C) Distribution of cell lengths in populations of wildtype and M23 peptidase mutants shown as a box plot. The box shows the 2nd and 3rd quartile of the values. The small plus symbol marks the mean value. The line in the box (50% of values) depicts the median. The whiskers mark the 5th and 95th percentile. Asterisks indicate a p-value of < 0.0001 (t-test) compared to wildtype. Quantifications are based on 2400 cells for the wildtype; 1000 cells for Δ*vcsP* and 1000 cells for the *vcsP* H175A variant. (D) Representative image of a *V. parahaemolyticus vcsP H175A* mutant cell at low and high magnifications. The cell displays a separation phenotype and the constriction site is stretches and blebbing. The strain was grown in LB to an OD_{600} of 0.5 and further prepared for imaging. Transmission electron microscopy images were recorded at an acceleration voltage set to 120kV and different magnifications. Black arrow indicate stretched constriction site, white arrow indicates membrane blebbing.

2.5 Lack of VcsP has no effect on growth, swimming or swarming motility

In order to find out what other cellular processes might be affected by the lack of *vcsP*, we tested swarming and swimming motility as well as growth in rich and minimal medium and compared it to wildtype. The swarming assays were performed as previously described by incubating the cells overnight at 24 °C on special swarming agar (Heering *et al.*, 2016, 2017). The next day, swarm colony diameters were measured and normalized to the diameter of wildtype swarm colonies. The swimming abilities of the mutant strains and wildtype cells were assayed on 0.3 % agar plates. This low density LB agar permits the cells to expand the colony by swimming motility through the rotation of the polar flagellum.

We observed that the deletion mutant of *vcsP* as well as *vscP H175A* mutant showed no significant differences in swarming or swimming motility when compared to each other or the wildtype strain (Figure 12AB). During the swarming assays, we used the Δ*lafA* mutant strain as a control. *LafA* encodes for the major lateral flagella subunit, which has been previously shown to be required for motility over solid surfaces in swarming *V. parahaemolyticus* (Heering *et al.*, 2016, 2017). In the swimming assay, we used a Δ*cheW* mutant strain as a control. This strain has been previously shown to be impaired in directed movement through a semisolid or liquid environment due to a decrease of chemotactic behavior (Ringgaard *et al.*, 2014).

We also assayed the growth behavior of Δ*vcsP* as well as *vcsP H175A* mutant and observed that neither of the two mutants showed significant difference to wildtype or between each other (Figure 12F). All microscopy and growth experiments were performed in rich LB medium. In order to find out, if minimal medium, which usually decreases the growth rate, has an effect on Δ*vcsP* or *vcsP H175A* mutants, we checked growth in marine minimal medium, with glucose as a carbon source (Figure 12CDF). While the minimal medium showed the desired effect of a decreased growth rate, no significant difference between wildtype and mutant strains were observed (Figure 12F). Additionally, in minimal medium Δ*vcsP* also produced cells with a chaining or elongation phenotype when compared to wildtype (Figure 12C). Analyzing the cell populations grown in minimal medium in more detail revealed that almost 14 % of the Δ*vcsP* population were of the chaining or elongated cell type when compared to less than 2 % in wildtype (Figure 12D). The cell length distribution also highlights the significant differences between wildtype and Δ*vcsP* mutant grown in minimal medium (Figure 12E).

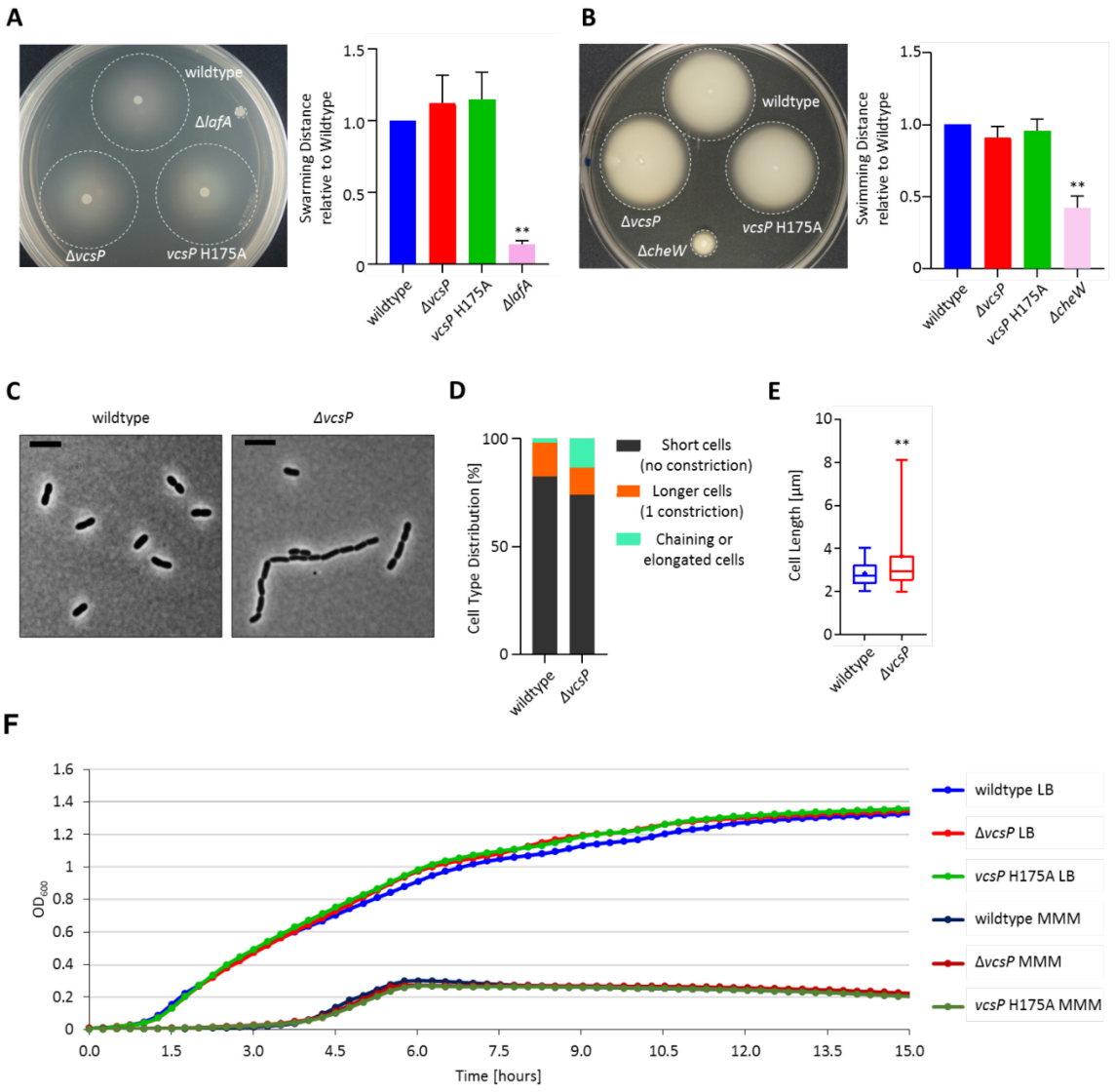

Figure 12: Motility and growth assays of wildtype and *vcsP* mutant strains

(A) Representative image of a swarming assay plate and graph displaying the relative swarming distance of mutant strains compared to wildtype. Quantification is based on three replicates with 10 plates each. (B) Representative image of a swimming assay plate and graph displaying the relative swimming distance of mutant strains compared to wildtype. Quantification is based 12 plates. (C) Representative phase contrast microscopy images of wildtype and mutant cells. Cells were grown until an OD_{600} of 1.5 in marine minimal medium (MMM), shaking and at 37 °C. Scale bar: 5 µm. (D) Cells were categorized into three types as described in Figure 8. Asterisks indicate a p-value of < 0.0001 (t-test) compared to chaining or elongated cells of wildtype. (E) Distribution of cell lengths in populations of wildtype and M23 peptidase mutants shown as a box plot. The box shows the 2nd and 3rd quartile of the values. The small plus symbol marks the mean value. The line in the box (50% of values) depicts the median. The whiskers mark the 5th and 95th percentile. Asterisks indicate a p-value of < 0.0001 (t-test) compared to wildtype. Quantifications are based on 300 cells for the wildtype and 600 cells for Δ*vcsP*. (F) Growth curve measurement at OD_{600} showing the increase in cell density over time of wildtype and mutant strains grown in LB or MMM at 37 °C shaking over the course of 15 h. (G) Evaluation of competitiveness of WT^{lac+}/WT^{lac-} and $WT^{lac+}/\Delta vcsP^{lac-}$ in a time-course experiment with 5 replicates. A competitive index of 1 indicates that the two strains are proliferating equally.

We did not observe any difference between mutant and wildtype when they were grown separately. To test their competiveness between each other, we inoculated liquid medium with a 1:1 ratio of wildtype cells, which are *lacZ+* and form blue colonies on LB agar supplemented with X-gal, and Δ*vcsP* cells, which are *lacZ-* and form white colonies. Afterwards we determined CFU/ml of the two strains tested and calculated the competitive index (Figure 13). As a control experiment, we used wildtype^{lac+} competing against wildtype^{lac-}. We found that although wildtype^{lac+} produced slightly more CFUs over time than wildtype^{lac-}(WT-), their competitive index stayed close to 1 even after 24 hours of incubation, indicating that they are proliferating similarly and that the *lacZ+* genotype has no negative influence. However, when we evaluated wildtype^{lac+} (WT+) and Δ*vcsP*$^{lac-}$(Δ*vcsP*-) in a competition assay, already after 4 hours there was a more than 10-fold difference between the WT+/WT- and WT+/Δ*vcsP*- experiments (Figure 13). After 24 hours, that difference exceeded 100-fold, indicating that in a competitive environment the *vcsP* deletion mutant is at a big disadvantage.

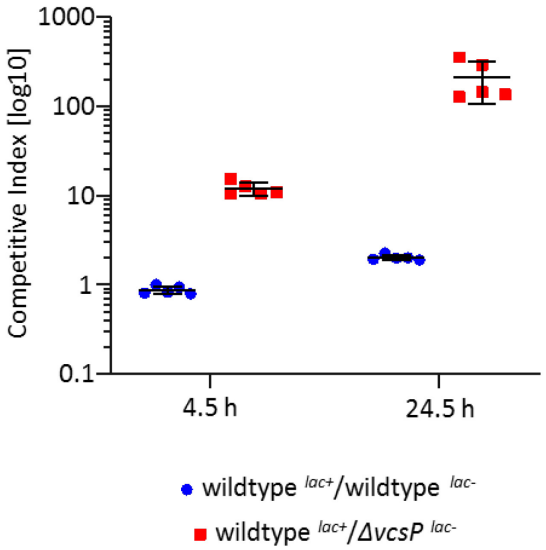

Figure 13: Competition assay between wildtype and Δ*vcsP*

Results of competition assays between WT and Δ*vcsP* strains. Blue circles indicate 5 experimental replicates of WT+/WT- competition after 4.5 h and 24.5 h. Red squares indicate 5 experimental replicates of WT+/Δ*vcsP*- competition after 4.5 h and 24.5 h. The black bar represents the mean and the whikskers represent the standard deviation.

Together these results show that the lack of *vcsP* has no influence on motility when compared to wildtype *V. parahaemolyticus*. Furthermore, both the Δ*vcsP* as well as *vcsP H175A* mutant behave in the same way in terms of motility and cell-density increase, underlining that disrupting the conserved M23 domain motif HxxxD, through either deletion or amino acid substitution is

responsible for the morphological phenotype. However, in a competitive environment with wildtype cells, the *vcsP* deletion mutant is rapidly outcompeted in its ability to form colonies.

2.6 VcsP-sfGFP primarily localizes to the pole and complements Δ*vcsP* defect

In order to show that the observed phenotype is not a result of polar effects in the mutant strain and to investigate if VcsP shows distinct localization inside the cell, we ectopically expressed an inducible VcsP-sfGFP fusion construct in a wildtype and Δ*vcsP* strain. It is important to note that the cells were grown for two hours after inducing the expression, and subsequently diluted for another two hours to an OD_{600} of 0.5. Only afterwards, the cells were imaged.

VcsP-sfGFP localized into distinct clusters in both wildtype and the *vcsP* deletion mutant and additionally was able to complement the deletion phenotype (Figure 14). Analyzing cell type (Figure 14B) and length distribution (Figure 14C) in wildtype and mutant cells ectopically expressing VcsP-sfGFP showed that there is no significant difference between the two strains in this experimental setup. While the deletion background had a slightly increased (but not significant) amount of chaining or elongated cells (3.5 %) compared to the wildtype (2 %), the cell length distribution emphasizes that this fluorescent fusion appeared to be functional and that both wildtype and mutant cell lengths were very similar, with only a few outlier cells. Additionally, these results also indicate that the overexpression of VcsP in wildtype has no negative impact on cell length or cell separation.

We observed that a subset of cells formed fluorescent VcsP-sfGFP clusters in both wildtype and deletion background and we analyzed the occurrence of fluorescent signals and its distribution within cells in more details (Figure 14D). In the wildtype background, we observed the formation of a fluorescent VcsP-sfGFP cluster in about 21 % of the population. The formation of more than one cluster almost never occurred and the majority of cells did not show any cluster formation. In the absence of the native *vcsP* gene, ectopically expressed VcsP-sfGFP formed a cluster in 9.3 % of the population. Otherwise, only diffuse signal could be observed in the deletion background. Out of those two populations (wildtype 21 %; Δ*vcsP* 9.3%) the majority of foci localized close to the cell pole but sometimes were also placed in the sub-polar region or close to mid cell, regardless of the cell length (Figure 14D).

Together these results suggest that VcsP-sfGFP is a functional fusion, able to complement the *vcsP* deletion phenotype and that VcsP-sfGFP can form clusters along the cell length, but predominantly close to the cell poles.

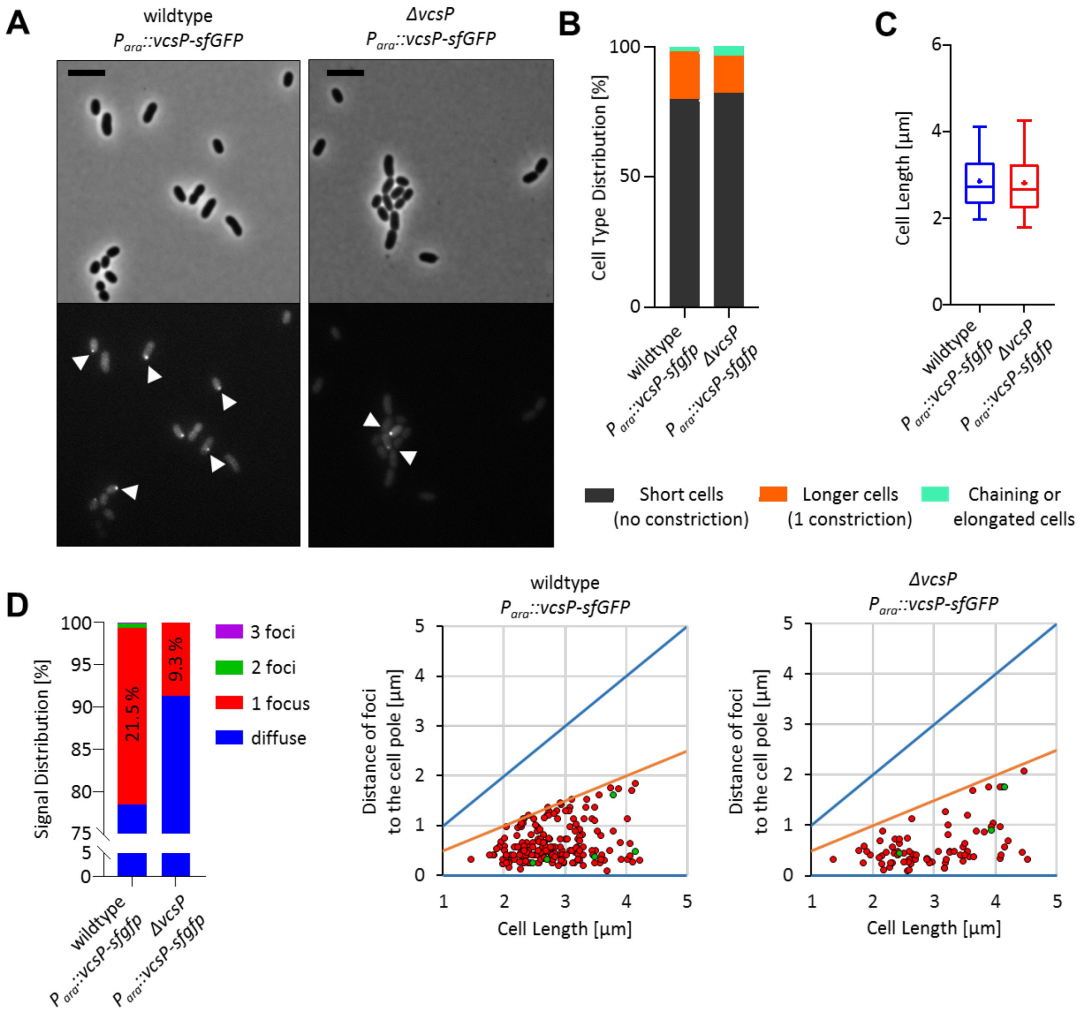

Figure 14: Localization of VcsP-sfGFP and complementation in a *ΔvcsP* background

(A) Representative phase contrast and fluorescence microscopy images of wildtype and Δ*vcsP* mutant, ectopically expressing an inducible VcsP-sfGFP fusion protein. Cells were grown until an OD_{600} of 0.15 in LB medium and induced with 2 % L-arabinose and further incubated for 4 h shaking and at 37 °C and constantly diluted to OD_{600} of 0.5. Scale bar: 5 µm. (B) Cells were categorized into three types as described in Figure 8. (C) Distribution of cell lengths in populations of wildtype and mutant shown as a box plot. The box shows the 2nd and 3rd quartile of the values. The small plus symbol marks the mean value. The line in the box (50% of values) depicts the median. The whiskers mark the 5th and 95th percentile. Asterisks indicate a p-value of < 0.0001 (t-test) compared to wildtype. Quantifications are based on 1200 cells for the wildtype and 1200 cells for Δ*vcsP*. (D) Signal distribution of wildtype and mutant cells. Fluorescent clusters were aligned to one pole.

2.7 Δ*vcsP* produces a unique phenotype compared to its paralogues

We showed that *V. parahaemolyticus* encodes for seven M23 peptidases and that except for previously characterized members of that protein family, which have been shown to produce morphological phenotypes upon deletion (*shyA*, *nlpD* and *envC*), Δ*vcsP* was the only other single deletion strain affected in cell morphology. Deletions of *vp1385* or *vpa1649* did not show a significantly different cell morphology when compared to wildtype (section 2.3).

In order to find out, if VcsP fulfills a unique role within the cell compared to its paralogues, we performed epistasis experiments, creating double and triple deletion mutants of *vcsP*, *vp1385* and *vpa1649* in all combinations (Figure 15). The Δ*vp1385* Δ*vpa1649* double mutant showed no morphological difference when compared to wildtype (Figure 15A) and this deletion strain showed a very similar cell type distribution where 3 % of the population formed elongated or chaining cells compared to 2 % in wildtype (Figure 15B). This is underlined by the cell length distribution, which showed no significant difference when compared to wildtype (Figure 15C). Interestingly, upon the deletion of *vcsP* in any combination with *vp1385* and/or *vpa1649*, the cells exhibited the same morphological phenotype as a single deletion of *vcsP* or the *vcsP H175A* mutant (Figure 15A). In addition, the cell type distribution in Δ*vcsP* Δ*vp1385,* Δ*vcsP* Δ*vpa1649* double mutants as well as the Δ*vcsP* Δ*vp1385* Δ*vpa1649* triple mutant (21 %, 22 % and 25 % of chaining cells, respectively) was very similar to that of a Δ*vcsP* single deletion strain (24 %; section 2.3) (Figure 15B). While these three strains showed a significantly different cell length distribution compared to wildtype, they were not significantly different between each other, emphasizing the importance of VcsP, but not VP1385 or VPA1649.

After previously showing that VcsP is required for cell separation in *V. parahaemolyticus*, the epistasis experiment delivers additional evidence that its function is unique when compared to VP1385 and VPA1649. We did not observe additive effects in double or triple deletion mutants of *vcsP*, *vp1385* or *vpa1649*, but rather exhibit the same phenotypes as the single *vcsP* deletion mutant.

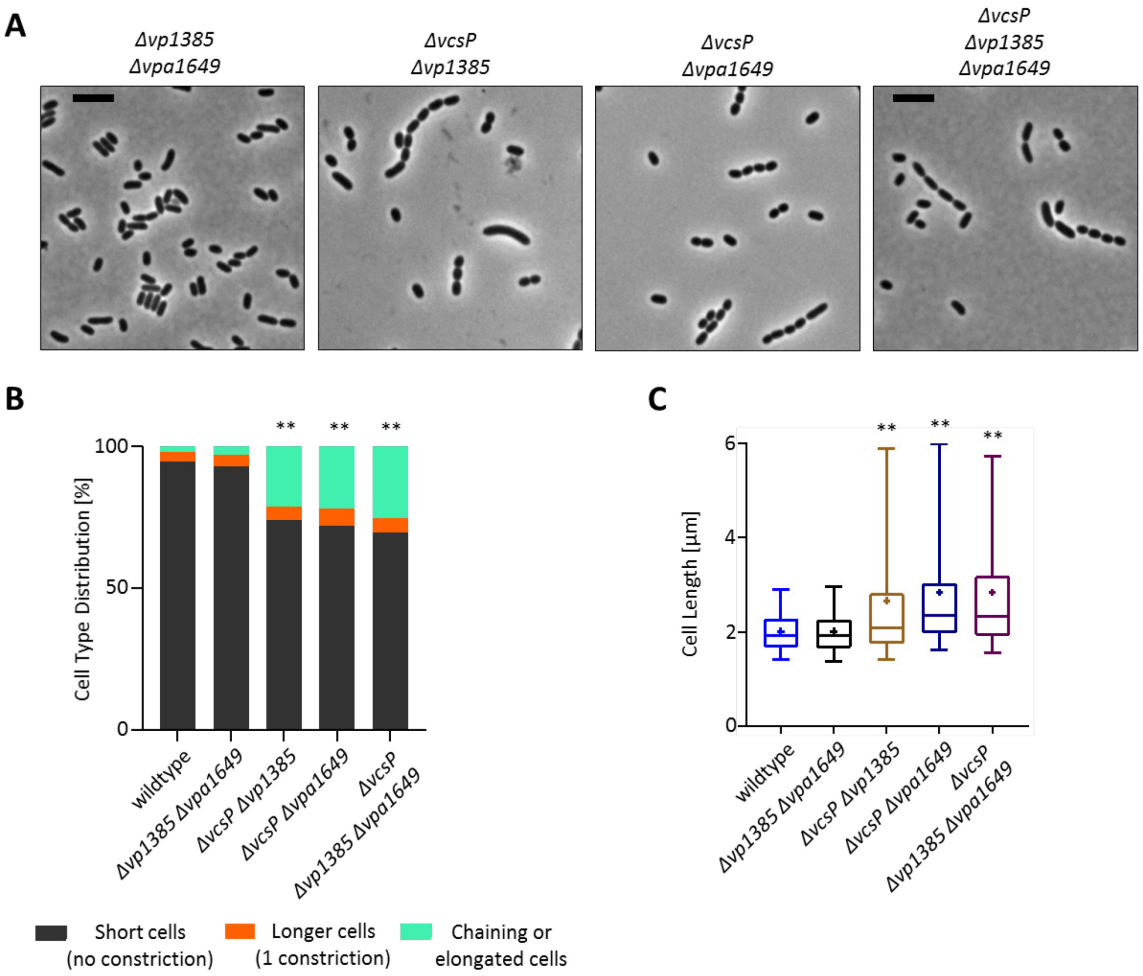

Figure 15: Epistasis experiment of *vcsP* and its paralogues

(A) Representative phase contrast microscopy images of wildtype and mutant cells of indicated strains. Cells were grown until an OD_{600} of 1.5 in LB medium, shaking and at 37 °C. Scale bar: 5 µm. (B) Cells were categorized into three types as described in Figure 8. (C) Distribution of cell lengths in populations of wildtype and M23 peptidase mutants shown as a box plot. The box shows the 2nd and 3rd quartile of the values. The small plus symbol marks the mean value. The line in the box (50% of values) depicts the median. The whiskers mark the 5th and 95th percentile. Asterisks indicate a p-value of < 0.0001 (t-test) compared to wildtype. Quantifications are based on 2400 cells for the wildtype and 1000 cells for each of the deletion mutants.

2.8 Δ*vcsP* shows increased sensitivity to Polymyxin antibiotics

To get a better understanding of what influence VcsP has on cell wall integrity, we tested effects of different antibiotics on wildtype, *ΔvcsP, vcsP H175A*, *Δvp1385*, *Δvpa1649,* *Δvp1385 Δvpa1649* double and *ΔvcsP Δvp1385 Δvpa1649* triple mutant cells. Dilution series were plated onto plates only containing LB agar and LB agar supplemented with different concentrations of Streptomycin, Penicillin G, Polymyxin B or Polymyxin E. Streptomycin binds to the 30s subunit of the ribosome and

through this action blocks global protein synthesis inside the cell (Luzzatto *et al.*, 1968). In this experiment, Streptomycin served as a control as it should affect wildtype and mutant strains similarly and has no specific influence on the bacterial cell wall. Penicillin G is a beta-lactam antibiotic and binds "penicillin binding proteins" (PBPs) (Lapage, 1945). Through its action on the PBPs, cell wall synthesis is inhibited thereby shutting down cellular growth. Penicillin G binds to most PBPs with similar specificity (Cho *et al.*, 2014). Polymyxin antibiotics are cyclic non-ribosomal polypeptides (NRPs) (Arnold *et al.*, 2007) that are able to integrate into the outer membrane of most gram-negative bacteria. Through this integration, the stability of the lipid-layer is compromised resulting in cell lysis.

Figure 16A shows the effect of the different antibiotics on the tested strains and Figure 16B quantifies these effects as CFU/ml [log10]. We previously showed that *vcsP* mutants increase cell-density in liquid growth similarly to wildtype (section 2.5). The same is the case when spotted as dilution series on LB agar. In addition, none of the other mutants showed any significant difference to wildtype on LB agar (Figure 16AB). We also observed that wildtype and mutant strains are similarly sensitive to the addition of 20 µg/ml Streptomycin (Figure 16AB). When supplementing increasing concentrations of Penicillin G to the agar plates, we observed that the *ΔvcsP* and *vcsPH175A* mutants are more resistant to this beta-lactam antibiotic compared to wildtype. Interestingly, also the double and triple deletion mutants were more resistant to Penicillin G (Figure 16AB). However, this increased resistance seems to be dose dependent, because at a concentration of 200 µg/ml Penicillin G, the strains displayed a very similar sensitivity compared to wildtype (data not shown). All tested strains, including wildtype displayed varying degrees of sensitivity to 5 or 20 µg/ml Polymyxin B and E (Figure 16AB). However, *ΔvcsP, vcsP H175A*, Δ*vp1385* Δ*vpa1649* double and Δ*vcsP* Δ*vp1385* Δ*vpa1649* triple mutants showed hypersensitivity to both of the Polymyxin antibiotics when compared to wildtype with a concentration dependent increase in sensitivity.

Together, these results suggest that the *ΔvcsP* and *vcsP H175A* mutants are compromised in their outer membrane because of the strong sensitivity to Polymyxin antibiotics. In addition, the Δ*vp1385* Δ*vpa1649* double mutant shows similar but weaker tendencies, suggesting some involvement in cell wall biogenesis, even though these strains did not show a significant morphological phenotype. This is additionally supported by the results of the Δ*vcsP* Δ*vp1385* Δ*vpa1649* triple deletion mutant, which is the most sensitive to Polymyxin antibiotics out of the all strains tested. Csd1 of *H. pylori*, which is involved in cell shape maintenance and closely related to VcsP (section 2.2), upon deletion shows no increased sensitivity to Polymyxin B compared to wildtype cells, indicating that this is not

a typical phenotype of endopeptidase deletion mutants. Interestingly, the same mutants that were more sensitive to Polymyxin antibiotics also showed an increase in Penicillin G resistance when compared to wildtype.

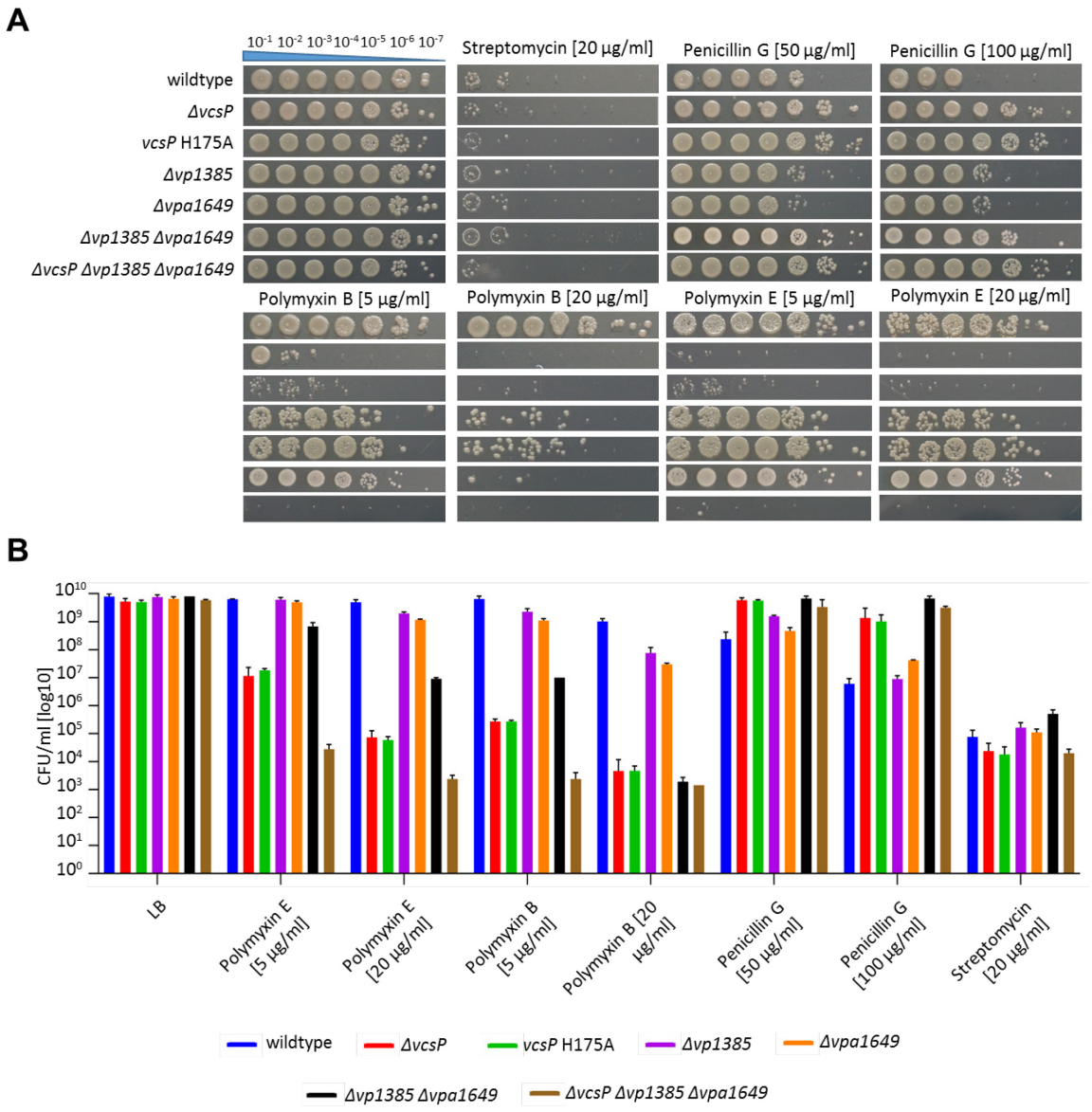

Figure 16: Effects of different antibiotics on wildtype and M23 peptidase mutants

(A) Wildtype and M23 peptidase mutant cultures plated in a serial dilution from 10^{-1} to 10^{-7} on LB agar and LB agar supplemented with 20 µg/ml Streptomycin, 5 and 20 µg/ml Penicillin G, 5 and 20 µg/ml Polymyxin B and 5 and 20 µg/ml Polymyxin E. (B) Bar graph depicting CFU/ml [log10] of wildtype and M23 peptidase mutants challenged with increasing concentrations of different antibiotics (as in A). Error bars indicate the standard deviation of experimental replicates.

2.9 Δ*vcsP* is affected in PG composition

The peptidoglycan is composed of sugars cross-linked by short stem peptides. The amino acids comprising the stem peptide can vary by species but are generally attached to muramic acid in the order L-alanine, D-glutamic acid, *meso*-diaminopimelic acid, D-alanine, D-alanine. Cross-linking occurs through the free amine of the third amino acid linking either the third or the fourth amino acid of another stem peptide. Generally, M23 peptidases are involved in breaking the cross-linkage between stem peptides and can show certain preference for either L,D or D,D peptide bonds (Foster *et al.*, 2000).

In order to find out, how VcsP might act on the peptidoglycan layer and what kind of reaction it is able to catalyze, we analyzed the peptidoglycan composition of wildtype and different M23 mutant strains in collaboration with Dr. Irazoki and Prof. Cava (Umeå, SWE) (Figure 17). The analysis was performed in three independent experiments. The PG was isolated from cells of an OD_{600} of 1.5 and digested using muramidase. Afterwards the muropeptides were analyzed using an UPLC.

Both *ΔvcsP* and *vcsP H175A* mutants showed increased amounts of total peptidoglycan content when compared to wildtype (Figure 17A), which is mainly attributed to increased amounts of dimers and trimers (D43, D34, D44, D45, $D44^{Anh}$, T344,$T444^{Anh}$; Table 13 and Table 14) at the expense of monomers (less M3, $M4^{G}$ and M4) (Figure 17BC). Consequently, both mutants had increased amounts of cross-linkages, which are mainly of the D,D kind, indicating that in the mutant backgrounds there is less endopeptidase activity. The deletion of *vpa1649* displayed a general profile similar to that of wildtype and did not show any enzymatic activity on the PG, including endopeptidase activity, under the tested conditions (Figure 17DE). Upon the deletion of *vp1385,* we observed increased amounts of dimers and trimers (D43, $D44^{Anh}$, T344; Table 15) at the expense of monomers (less M3, M4). In this mutant background, there was less endopeptidase activity and an accumulation of dimers in general, resulting in an increase of cross-linkages compared to wildtype. VP1385 appears to be an endopeptidase with specificity to muropeptide D43, as the lack of increased amounts of other dimers suggests (e.g., there is no increase in D44). The peptidoglycan profile of *Δvp1385* was similar to that of the *ΔvcsP* mutant. As the single deletion of *vpa1649* showed no changes in endopeptidase activity, the double mutant of *Δvpa1649* and *Δvp1385* presented a similar profile compared to the *Δvp1385* mutant. We found increased amounts of dimers and trimers (D43, $D44^{Anh}$, T344, $T444^{Anh}$) at the expense of monomers (less M3, M4, $M4^{G}$) and as a result increased amounts of cross-linkages of both L,D- and D,D- types. The *ΔvcsP Δvpa1649 Δvp1385* triple

deletion mutant had increased amounts of dimers and trimers (D43, D44^{Anh}, T344, T444) at the expense of monomers (less M3, M4, M4^{G}) and in this mutant background there was even less endopeptidase activity than in the single mutants. The triple mutant presented an accumulation of dimers in general with a significant increase of the total cross-linkage of both L,D- and D,D- types.

Together these results indicate that VcsP is an active D,D endopeptidase. Extinguishing its activity, either through the deletion of *vcsP* or altering the M23 domain through a H175A amino acid substitution, generates a very similar peptidoglycan profile. Interestingly, VP1385 also appears to be an active peptidase, which has an accumulative effect on endopeptidase activity together with VcsP.

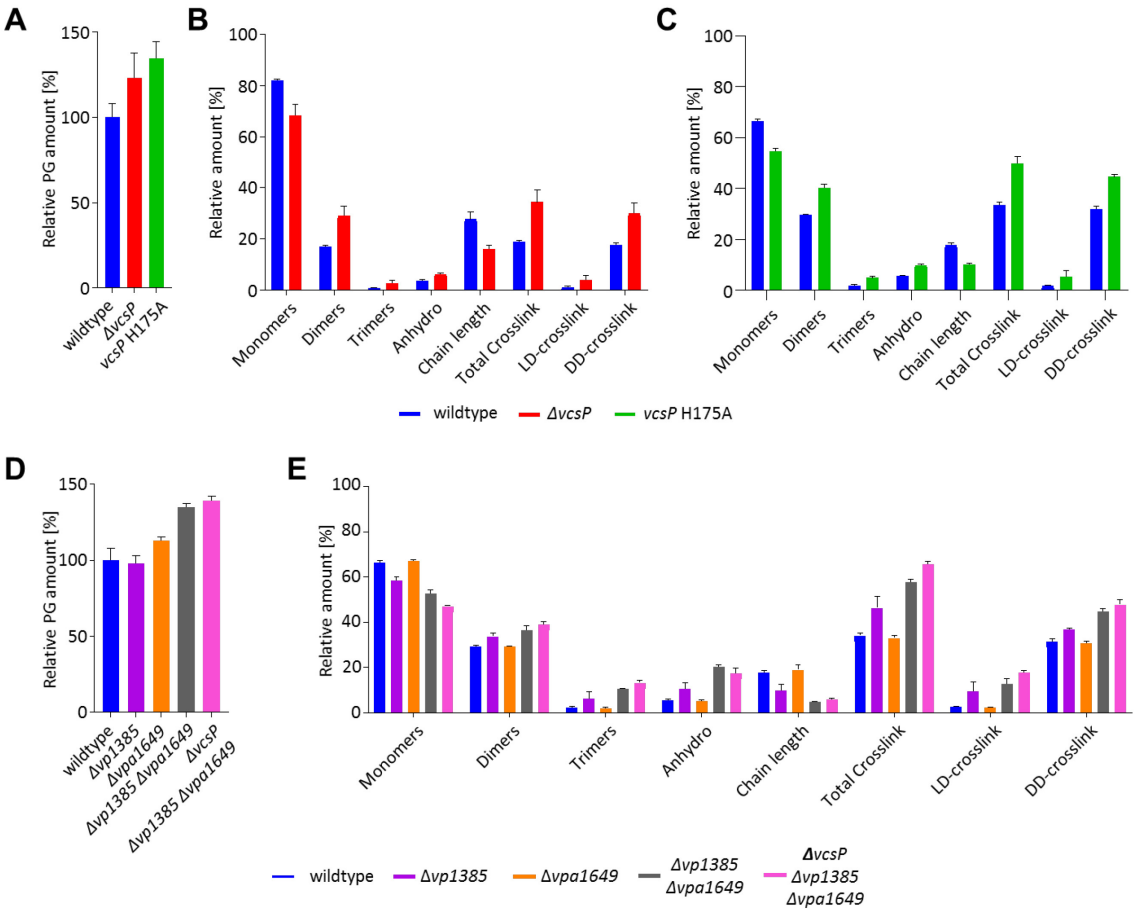

Figure 17: Peptidoglycan composition of wildtype and M23 peptidase mutants

(A/D) Bar graphs displaying the relative total amounts of peptidoglycan present in the indicated strains. (B/C/E) Bar graphs displaying the relative amounts of peptidoglycan subunits (monomers, dimers, trimers), relative amounts of terminal glycan strands (anhydro), relative chain length, relative total cross-linkages and relative LD- / DD-crosslinkages. PG was analyzed of strains grown in LB medium to an OD_{600} of 1.5, which were boiled in SDS for several hours and afterwards further prepared for the analysis.

2.10 VcsP protein purification

Until this point, the majority of experiments have been *in vivo* characterization of *vcsP* mutants and their effect on cell separation. In order to test VcsP activity *in vitro* and correlate that with peptidoglycan composition analysis, we started to purify different VcsP variants. All purification efforts use affinity purification to either Ni-NTA for His tagged proteins or amylose for MalE tagged proteins.

It has been previously shown that the entire protein is often not required to observe *in vitro* peptidase activity (Dörr *et al.*, 2013) and to increase yields during purification it is advisable to remove any transmembrane helices present from the protein structure. We started with the purification of His-tagged truncated variants (1-44aa removed) of both wildtype and H175A amino acid substitution (Figure 18). While the production of both variants could be induced using the pET vector system (IPTG -/+), the majority of the protein was located in inclusion bodies (data not shown) and only very small amounts could be retained in the soluble fraction during the elution process. This can be observed in both the stained protein SDS-PAGE gel as well as the accompanying immunoblot analysis. Due to the little amount of soluble VcsP protein, the Ni-NTA beads bind many proteins unspecifically, as shown by the additional bands of the SDS-PAGE gel.

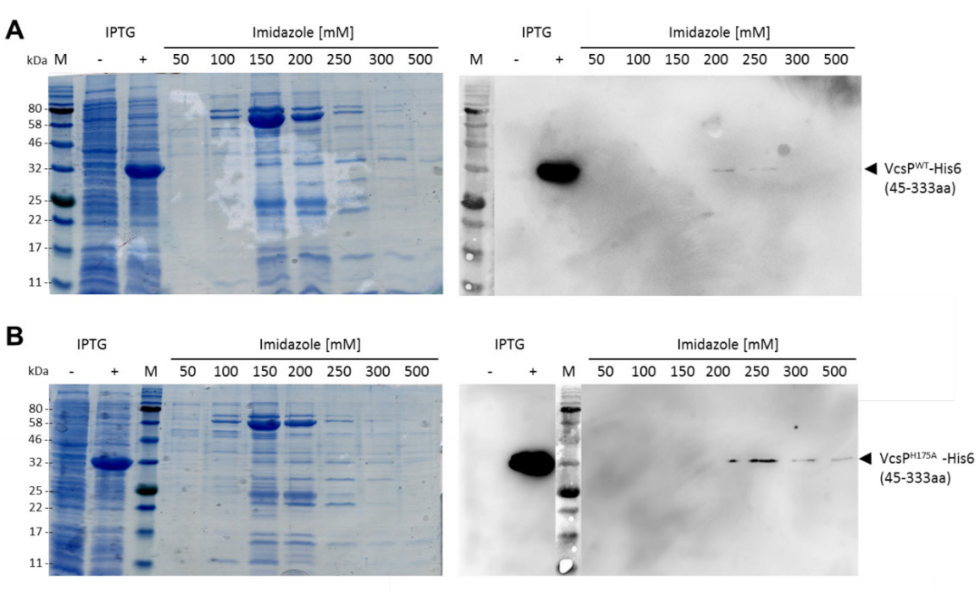

Figure 18: Purification of truncated variants of VcsP-His6

(A) On the left: SDS-PAGE gel showing the induction of the WT variant and elution fractions. On the right: Immunoblot analysis using anti-polyHis-HRP antibodies. (B) On the left: SDS-PAGE gel showing the induction of the H175A variant and elution fractions. On the right: Immunoblot analysis using anti-polyHis-HRP antibodies. Expected protein size for both variants of 33.8 kDa.

In order to improve the purification process and increase the amounts of soluble protein, we only expressed the isolated M23 domain of VcsP using the pET vector system (Figure 19). Using this protein variant, we were able to decrease the amount of background protein eluted in each fraction and also increased the amount of soluble protein. We used a concentration spinning column to pool several elution fractions in order to increase the protein concentration, however during this process the entire amount of purified protein precipitated, indicating that it is unstable under those conditions.

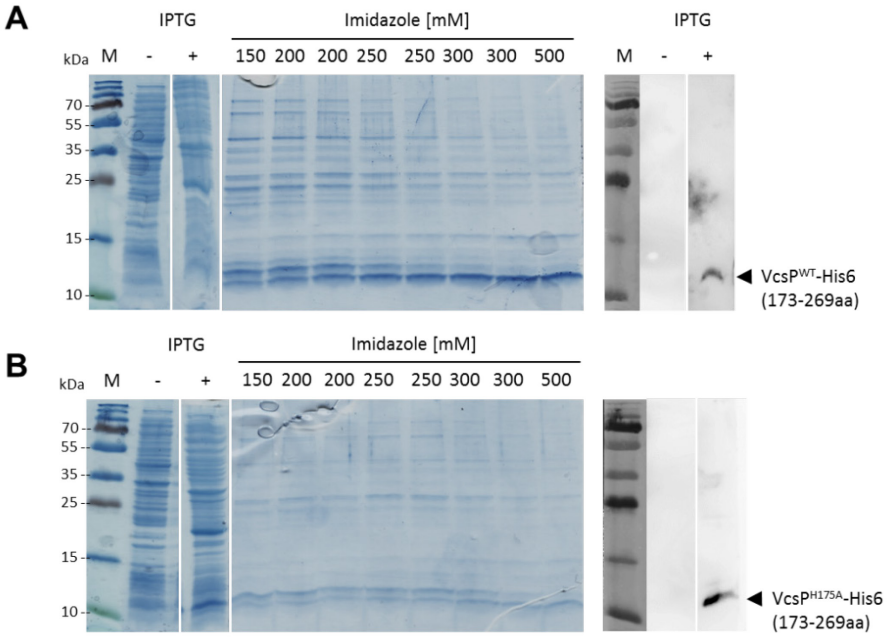

Figure 19: Purification of M23 domain variants of VcsP

(A) On the left: SDS-PAGE gel showing the induction of the WT variant and elution fractions. On the right: Immunoblot analysis using anti-polyHis-HRP antibodies. (B) On the left: SDS-PAGE gel showing the induction of the H175A variant and elution fractions. On the right: Immunoblot analysis using anti-polyHis-HRP antibodies. Expected protein size for both variants of 11.8 kDa.

In a different attempt to increase the amount of soluble protein, we fused the M23 domain of VcsP to the C-terminus of maltose binding protein MalE. This approach has been used to increase yield and protein solubility of membrane associated proteins (Eliseev *et al.*, 2004; Korepanova *et al.*, 2007; Saraswat *et al.*, 2013). Using this approach, we were able to purify MalE-VcsP (M23) in high amounts from the soluble fraction with very little secondary protein contamination. In an additional step, the linker region between MalE and the fused protein was cleaved with the site specific (Ile-Glu/Asp-Gly-Arg) protease „Factor Xa“ (Figure 20). While we did observe the cleavage of the fusion

protein, the majority of it stays uncleaved, even after over night incubation with „Factor Xa“. In an effort to purify different variants of VcsP, we were so far able to increase yield and solubility.

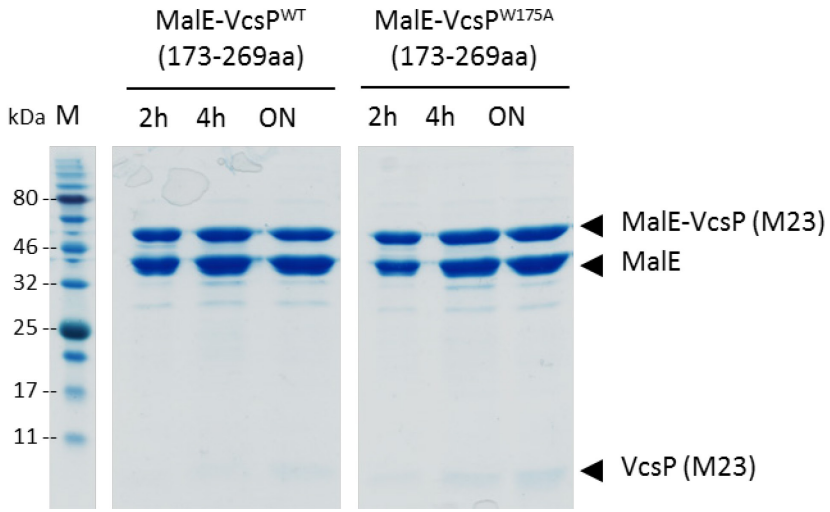

Figure 20: Factor Xa digestion of MalE-VcsP (M23) variants.

SDS-PAGE gel showing the cleavage over time of MalE-VcsP (M23) WT variant on the left and H175A variant rigth. Expected protein sizes: MalE-VcsP (M23) is 53.5 kDa, MalE 42 kDa and VcsP M23 domain 11 kDa.

2.11 Searching for VcsP interaction partners

2.11.1 PilZ domain protein VP0549

VcsP (*vp0548*) is located on the first chromosome of *V. parahaemolyticus* and next to *vp0549*, a gene encoding for a PilZ domain protein (Figure 21AB). PilZ domains have been shown to bind cyclic dimeric guanosine monophosphate (c-di-GMP) and usually function via protein-protein interactions (Ryjenkov *et al.*, 2006). C-di-GMP is a second messenger and widely found in bacteria (Hengge, 2009). It is responsible for a great variety of cellular and molecular responses. In *Caulobacter crescentus* the global c-di-GMP level controls its asymmetric lifecycle progression (Abel *et al.*, 2013) and in *V. cholerae* VieA, a two-component response regulator, modulates cellular c-di-GMP levels that influence exopolysaccharide (EPS) production and biofilm formation (Tischler *et al.*, 2004). In *Myxococcus xanthus* c-di-GMP regulates type-IV pilus-dependent motility through EPS accumulation and *pilA* transcription (Skotnicka *et al.*, 2015). In addition, it was recently shown that a minimal threshold of c-di-GMP is essential for fruiting body formation and sporulation in *M. xanthus* and that the active di-guanylate cyclase DmxB is responsible for increased c-di-GMP levels

during starvation (Skotnicka *et al.*, 2016). In *V. parahaemolyticus* low levels of c-di-GMP are required for swarmer differentiation and a swarming specific quorum sensing machinery has been shown to modulate c-di-GMP levels *in vivo* (Kim *et al.*, 2007; Trimble *et al.*, 2011). In *E. coli* and other enterobacteria, c-di-GMP controls motility through binding to the PilZ domain protein YcgR that in turn controls flagellar motor direction and speed through protein-protein interaction (Ryan *et al.*, 2006). In *Klebsiella pneumoniae* the PilZ domain containing protein MrkH has been shown to function as a transcriptional activator of the *mrkA* promoter that controls fimbriae production important for cell-surface contact and virulence (Yang *et al.*, 2013). In *V. cholerae*, five PilZ domain proteins have been identified and upon deletion of a subset of them, changes in biofilm formation, motility, and colonization of the small intestine in an animal model of infection were observed (Pratt *et al.*, 2007). *Vp0546* and *vp0547* are found next to *vcsP* and encode for an aldolase and dehydrogenase respectively, enzymes found in many cellular processes e.g glycolysis. In the other direction, *vp0550* encodes for a small open reading frame (ORF) with no conserved amino acid sequences, predicted protein structure or domains. *Vp0551* encodes for an ATP-depended ABC transporter and is part of the EttA superfamily, proteins involved in gating ribosomes entry into the translation elongation cycle (Boël *et al.*, 2014). There seems to be no indication that either the up- or downstream encoding genes of *vcsP/vp0549* form a functional unit or are involved a common process.

VP0549 consists of a single PilZ domain with conserved RxxxR and D/NxSxxG motifs (Figure 21B). These motifs have been shown to permit binding of the second messenger c-di-GMP and contribute to the formation of homodimers (Schäper *et al.*, 2017). VcsP is a 333 amino acid protein (Figure 21C) and consists of an N-terminal cytoplasmic domain, followed by a trans-membrane domain and a coiled-coil domain. Close to the C-terminal region locates a M23 peptidase domain. Cytoplasmic domains often infer signal specificity but have also been shown to influence ligand binding and regulate kinase activity in taxis receptors (Falke *et al.*, 2000). Transmembrane domains are a common architectural feature of M23 peptidases involved in PG remodeling and usually anchor the protein to the inner membrane (Ercoli *et al.*, 2015). Coiled coil domains are often non-sequence conserved structural features that create physical distance between proteins involved in many cellular processes and are conserved throughout all three kingdoms of life (Truebestein *et al.*, 2016).

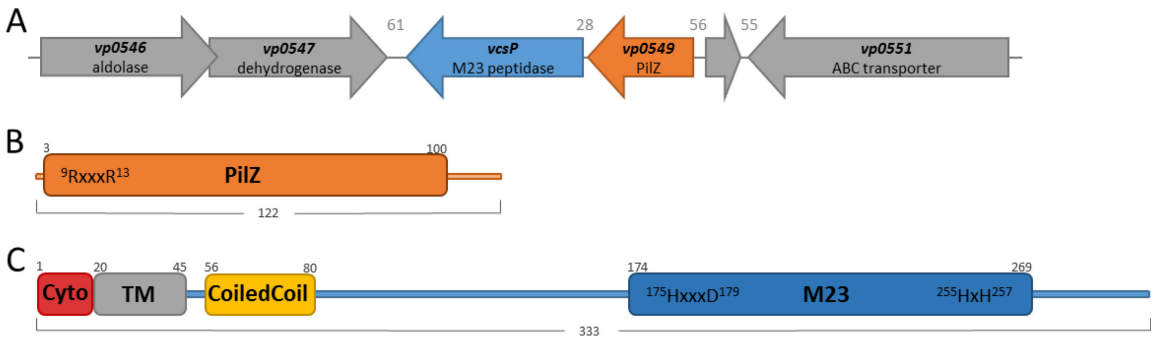

Figure 21: Genomic neighborhood and protein composition

(A) The genomic flanking region in front of *vcsP/vp0549* encodes for an aldolase and a dehydrogenase (*vp0546/vp0547* respectively). The subsequent genes encode for a small ORF (*vp0550*) and an ABC transporter of the EttA superfamily (*vp0551*). The numbers indicate the number of nucleotides between start and/or stop codons of the neighboring gene. (B) Protein composition of the PilZ domain protein VP0549. (C) Protein composition of the M23 endopeptidase VcsP.

2.11.1.1. *vcsP* is part of an operon with *vp0549*

There are 28 nucleotides between the stop and start codon of *vp0549* and *vcsP*, respectively (Figure 21A). In order to find out if both genes are transcribed together and part of an operon, we performed operon mapping on this genomic region. We chose primers that amplify 300 bp fragments of the indicated regions (Figure 22A). Region 3 is located in the center of *vcsP*; region 2 is in-between *vcsP* and *vp0549* and region 1 amplifies the center of *vp0549*. As a positive control, we used genomic DNA (gDNA) of *V. parahaemolyticus* and as a negative control we used RNA, which was used to produce the cDNA. Figure 22B shows that all three regions can be amplified using genomic DNA and that no PCR products can be amplified when using RNA as a template, which are both expected results. Interestingly, all three regions could be amplified using cDNA as a template, which indicates that *vp0549* and *vcsP* are indeed transcribed together.

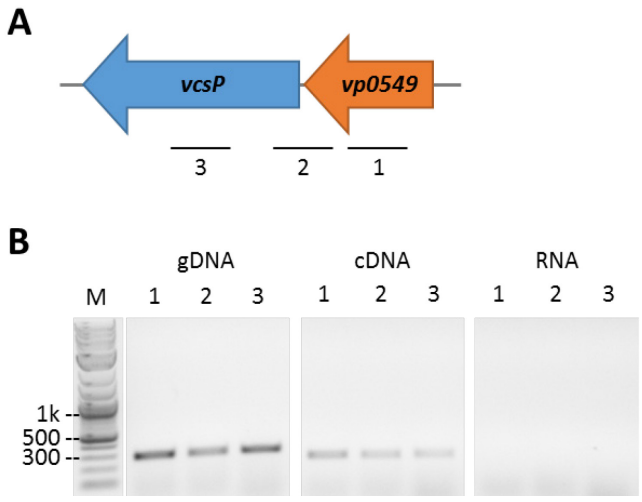

Figure 22: Operon mapping of *vcsP* and *vp0549* locus

(A) Schematic representation of the *vcsP* and *vp0549* locus. The locations of the primer pairs used in the operon mapping are indicated (1-3) and each primer pair amplifies 300 bp. (B) Agarose gel of PCR products showing *vcsP* and *vp0549* co-transcribed (cDNA). No PCR products were amplified in the negative-control lanes (RNA), and genomic DNA (gDNA) was used as a positive control. Marker and lanes were put together from the same gel.

2.11.1.2. VcsP and VP0549 self-interact

To find out whether the two proteins interact with each other, "bacterial adenylate cyclase-based two hybrid" (BACTH, bacterial-two-hybrid) assays were performed (Karimova *et al.*, 1998). Both the full-length protein and a truncated variant of VcsP (amino acids 1-45 removed) and full-length VP0549 were tested.

Based on the formation of blue colonies in the BACTH assay, both VP0549 and VcsP showed self-interaction (Figure 23). An interaction between VcsP variants and VP0549 was not observed in this assay. Although a negative result in BACTH is not a definitive answer to whether VP0549 and VcsP interact with each other, it does give an indication that they might not interact. Additionally, PilZ domain proteins, and VP0549 in particular, are likely only present in the cytoplasm, whereas M23 peptidase VcsP is likely an integral inner membrane protein, with the majority of the protein located in the periplasm. That only leaves the short cytoplasmic domain of VcsP to be available for direct interaction with VP0549. To give a more conclusive prediction another method such as co-immunoprecipitation (Co-IP) could be used to test for interaction between VcsP and VP0549.

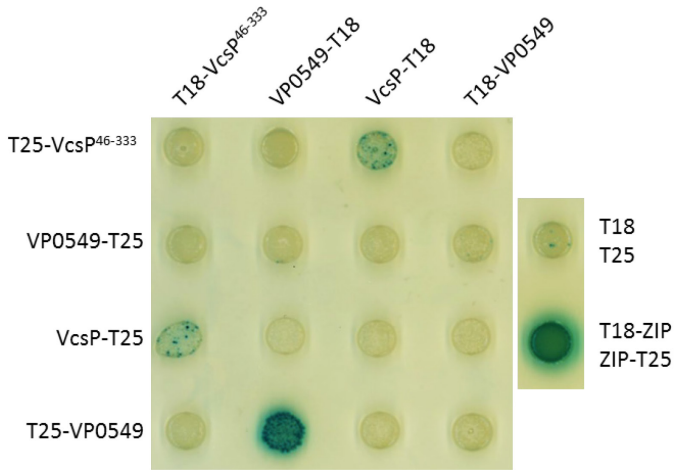

Figure 23: BACTH assay on VcsP and VP0549

Bacterial-two-hybrid assay of C-/N- terminal T18/T25 fusion-proteins. “46-333” indicates the truncated VcsP variant. Incubated 16 h at 30 °C and afterwards 24 h at RT. “T18/T25” served as the negative control, “T18-ZIP/ZIP-T25” served as the positive control.

2.11.1.3. VP0549 has no effect on cell separation

In order to find out, if VcsP and VP0549 are involved in the same cellular process although they do not seem to interact directly with each other in BACTH, we created an in-frame deletion mutant of *vp0549* and analyzed its morphology (Figure 24).

Under the tested conditions, we did not observe a morphological phenotype of the Δ*vp0549* mutant (Figure 24A) when compared to wildtype. When looking at the cell type distribution, we see that the Δ*vp0549* mutant population does not show any chaining or elongated cells. However, we observed that the occurrence of cells with a single constriction is reduced at 0.2 % when compared to 2 % in wildtype (Figure 24B). Although the mutant population has less cells that are currently dividing, we saw no significant difference in the overall cell length distribution when compared to wildtype (Figure 24C). Together these results suggest that VP0549 is not involved in cell separation in contrast to VcsP (section 2.3).

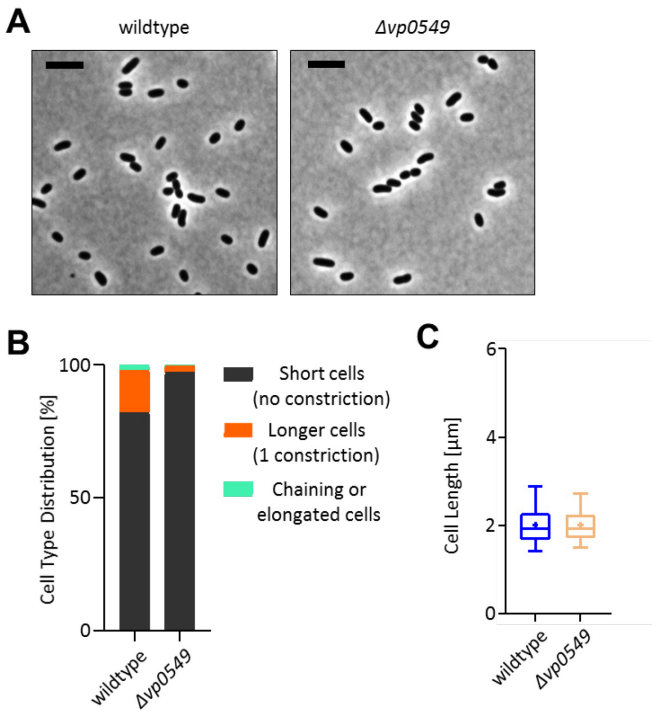

Figure 24: Single cell morphology and analysis of wildtype and Δ*vp0549* deletion strain

(A) Representative phase contrast microscopy images of wildtype and mutant cells. Cells were grown until an OD_{600} of 1.5 in LB medium, shaking and at 37 °C. Scale bar: 5 µm. (B) Cells were categorized into three types as described in Figure 8. (C) Distribution of cell lengths in populations of wildtype and Δ*vp0549* deletion mutant. The black line depicts the mean value and the whiskers mark the standard deviation. Asterisks indicate a p-value of < 0.0001 (t-test) compared to wildtype. Quantifications are based on 2400 cells for the wildtype and 620 cells for the deletion mutant.

2.11.1.4. VP0549 binds c-di-GMP *in vitro*

PilZ domain proteins have been shown to bind c-di-GMP (Pratt *et al.*, 2007) and to find out if VP0549 is cable of that as well, we purified His6-VP0549 through affinity purification. First, we performed a DRaCALA assay with the purified protein in collaboration with Dr. Dorota Skotnicka (MPI Marburg, GER). In this assay, the protein of interest is incubated with [^{32}P] radio-labeled c-di-GMP and subsequently spotted onto a nitro-cellulose membrane. As the spot dries on the membrane, the protein is immobilized in the center of the spot, whereas the residual liquid will still diffuse a few millimeters off the center before it also dries. Depending on whether the protein can bind the radio-labeled c-di-GMP or not, exposing the membrane will show the majority of radio-signal immobilized in the center of the spot or diffusely spread out throughout the whole spot, respectively.

VP0549^{WT} was able to bind c-di-GMP and behaved like the positive control DmxB^{WT} (Skotnicka *et al.*, 2016) that was incubated and exposed on the same membrane (Figure 25A). As the DRaCALA assay only provides a binary result, binding or no binding, we also performed an alternative binding assay based on bio-layer interferometry (BLI) in collaboration with Dr. Magdalena Polatynska and Dr. Dorota Skotnicka (MPI Marburg, GER). In this assay, a streptavidin coated tip is incubated first with biotinylated c-di-GMP and afterwards with the protein of interest. While measuring the reflection of white light, some wavelengths show constructive or destructive interference. If the protein of interest binds c-di-GMP in this setup, binding-specific shifts in the interference pattern can be measured and quantified. In addition to wildtype VP0549^{WT}, we also tested the VP0549^{R9D} variant. This variant has been reported for other PilZ domain proteins to diminish c-di-GMP binding (Ryjenkov *et al.*, 2006). The BLI results showed that over time, increasing amounts of VP0549^{WT} molecules bind to c-di-GMP (Figure 25). At 300 seconds, the biosensor was washed with disassociation buffer, showing the release of VP0549^{WT} molecules. Compared to the wildtype protein, VP0549^{R9D} showed very little response to the biosensor, indicating that it is indeed impaired in c-di-GMP binding. The “base” line showed the response of the sensor in the absence of c-di-GMP and presence of VP0549^{WT}, indicating that there is no unspecific binding of the WT protein to the tip. The BLI experiment confirms the previous DRaCALA results.

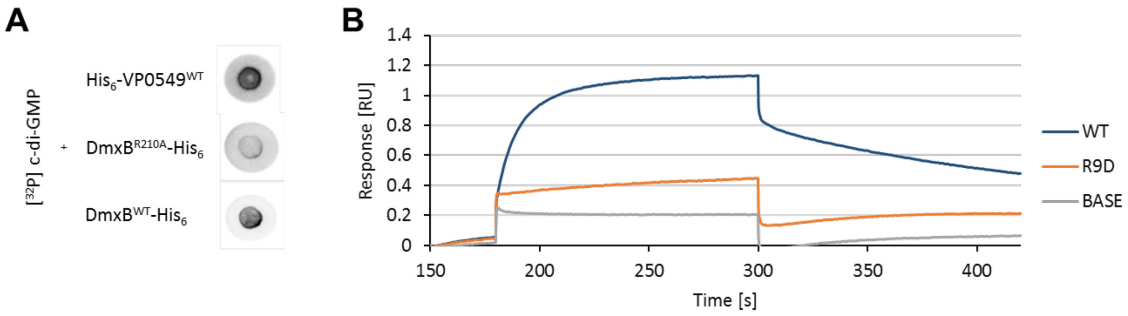

Figure 25: *In vitro* c-di-GMP binding assays

(A) DRaCALA assay showing that VP0549^{WT} is able to bind radio-labeled c-di-GMP, compared to positive and negative controls DmxB^{WT} and DmxB^{R210A}, respectively. (B) BLItz assay showing that VP0549^{WT} specifically binds c-di-GMP and that VP0549^{R9D} is impaired in c-di-GMP binding.

2.11.2 Co-Immunoprecipitation

To find interaction partners of VcsP, we used a C-terminally FLAG tagged variant of VcsP to perform a pulldown experiment. As a control, we used C-terminally FLAG tagged sfGFP.

We grew quadruplicate samples of wildtype cells ectopically expressing VcsP-FLAG or sfGFP-FLAG. Protein expression was induced at an OD_{600} of 0.3 and the cells were harvested after two hours of incubation. Afterwards, the samples were incubated in lysis buffer and sonicated 6 times for 20 seconds at 100 % power. Than we incubated the cells with 0.5 % NP40 (detergent) and repeated the previous sonication step. After spinning down the cell debris, we incubated the supernatant with anti-FLAG magnetic beads. During this step, soluble VcsP-FLAG protein (or sfGFP-FLAG for the control experiments) bound to the anti-FLAG antibody attached to the beads. In this step, proteins that were associated to VcsP could be co-purified with VcsP. Afterwards, we isolated the beads in magnetic sample holders, perform several washing steps to remove any residual detergent, and later added trypsin protease to digest the proteins bound to the magnetic beads. After incubating the samples with trypsin overnight, the peptide mix was further purified and prepared for mass-spectrometric analysis in collaboration with Dr. Timo Glatter (MPI Marburg, GER).

The mass-spectrometric analysis identified and annotated peptides of more than 1000 different *V. parahaemolyticus* proteins. To find significantly enriched proteins in the bait experiment, the data was further analyzed and the results are shown in Figure 26. The volcano blot compares the $\log_2$ fold change to the $-\log_{10}$ p-values with a significance cutoff of $-\log_{10}(2)$. Red squares indicate proteins significantly enriched in the control experiment and the blue squares indicate significantly enriched proteins in the bait experiment. VcsP peptides were exclusively found in the bait samples and sfGFP peptides were exclusively found in the control experiment. This indicates that the anti-FLAG magnetic beads functioned reliably as well as that no cross-contamination occurred during sample preparation. Looking at the blue squares in more detail, we found Pnp, Eno, Rne and RhlB, all part of the RNA degradosome (Carpousis, 2007). DnaJ, which has been shown to interact with DnaK and GrpE to form a cellular chaperone to prevent the aggregation of stress-denatured proteins and disaggregating proteins (Schröder *et al.*, 1993), was significantly enriched as well. In addition, also GroL chaperonins, which prevent misfolding and promote the refolding and proper assembly of unfolded polypeptides generated under stress conditions (Langer *et al.*, 1992), were found in the bait samples.

Interestingly, we found some proteins involved in cell wall biogenesis: Ffh, which is part of signal recognition particle (SRP) and involved in targeting and insertion of nascent membrane proteins into the inner membrane (Phillips *et al.*, 1992; Schlünzen *et al.*, 2005). Another protein that was significantly enriched is HflC, which is part of the HflCK complex responsible in inhibiting the SecY-degrading activity of FtsH and possibly helping quality control of integral membrane proteins (Saikawa *et al.*, 2004). BamA of the Bam complex was significantly enriched (BamBCD were also present in the bait samples, however do not exceed the $\log_2(2)$ cutoff) which is responsible for inserting proteins into the outer membrane (Knowles *et al.*, 2009; Hussain *et al.*, 2018). We also found SecD significantly enriched (SecABGY were also present in the bait samples, however do not exceed the $\log_2(2)$ cutoff), which is part of the Sec translocation machinery responsible to translocate unfolded proteins across the inner membrane (Tsukazaki *et al.*, 2011; Guo *et al.*, 2018).

Together these results suggest that overproduction and accumulation of VcsP-FLAG can cause stress response, despite not causing a morphological phenotype. The significantly enriched proteins were all involved in membrane associated protein biogenesis and translocation. Although those results indicate that VcsP-FLAG is translocated to the inner membrane, maybe with the help of SRP and the Sec machinery, none of the enriched proteins is directly involved in peptidoglycan remodeling.

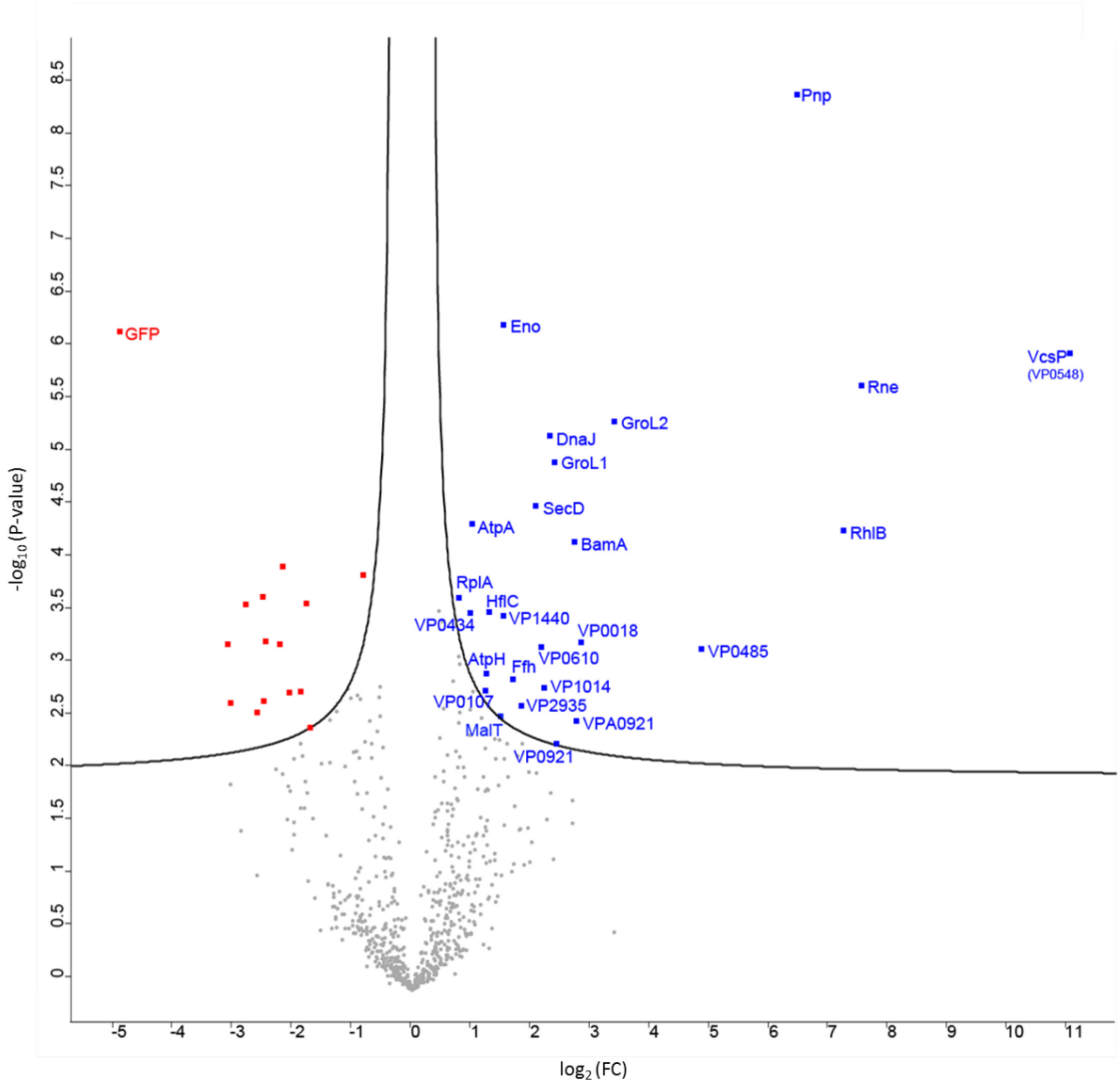

Figure 26: Overview of significantly enriched targets in a VcsP Co-IP experiment

Volcano plots of significantly enriched proteins from a Co-IP experiment analysis of wildtype cells ectopically expressing VcsP-FLAG or sfGFP-FLAG protein variants. While the X-axis represents fold change (sfGFP-FLAG VS. VcsP-FLAG) of the individual hits, the Y-axis represents the statistical significance of the corresponding targets. The two curves (black) depict the set threshold (dictated by these parameters: FDR=0.01, S0=0.2). All the points (red squares) to the left of the leftmost curve indicate significantly less abundant targets, whereas those to the right of the rightmost curve indicate significantly enriched hits of VcsP-FLAG.

3 Discussion

Cellular growth and division are inherently important for the proliferation of bacterial cells and these processes require highly coordinated enzymatic activity in order to remodel the peptidoglycan mesh. During growth as well as division, the current PG polymer needs to be disconnected in order to insert new building blocks and separate mother and daughter cells. In addition to peptidoglycan synthetizing proteins, many different lytic enzymes are involved in that process, including M23 peptidases. M23 peptidases can be divided into two subfamilies: M23A and M23B. The M23A subfamily contains beta-lytic endopeptidases that cleave glycine-bonds in the cell walls of Gram-positive bacteria (Li *et al.*, 1990) and can be used as a defense-mechanism against other bacteria (Spencer *et al.*, 2010). The M23B subfamily mostly contains proteins involved in peptidoglycan remodeling and specifically those proteins are the focus of this work. While this type of enzyme has been extensively studied in *E. coli*, little is known about its role in the pathogenic γ-proteobacterium *V. parahaemolyticus*. We showed that out of seven M23 domain-containing proteins, four are homologues to previously characterized proteins that can also be found in *E. coli* and *V. cholerae.* One of the remaining uncharacterized proteins was particularly important for cell separation in *V. parahaemolyticus* and in this work, we focused on detailed characterization of this particular protein, which we renamed VcsP for "*Vibrio* cell separation peptidase".

3.1 M23 endopeptidases of *Vibrio parahaemolyticus*

M23 endopeptidases are lytic enzymes, which are able to cleave the peptide bonds that link the stem peptides of parallel glycan strands. This reaction reverses the trans-pepdidation, thus creating space in the PG layer where new glycan strands can be inserted (Höltje, 1998; Singh *et al.*, 2012; Dörr *et al.*, 2013). These enzymes can be categorized into L,D-endopeptidases (cleavage between L- and D-amino acids/*meso*-DAP) and D,D-endopeptidases (cleavage between D-amino acids) according to the type of cleavage site (Foster *et al.*, 2000). As the name suggests, M23 endopeptidases possess the characteristic catalytic domain of M23 metalloproteases with conserved metal binding site motifs, HxxxD and HxH. These two motifs have been shown to coordinate binding of a zinc ion and are required for catalytic activity (Rawlings *et al.*, 2008; Cohen *et al.*, 2009; Zastrow *et al.*, 2014).

We performed homology search on a conserved M23 domain using BlastP and found that *V. parahaemolyticus* encodes for seven proteins that contain a predicted M23 peptidase domain. We found that four of these proteins are homologous to previously characterized proteins. Specifically, VP2554 and VP2834 are homologous to NlpD and EnvC, proteins shown to be activators of amidase activity in many different bacteria, including *E. coli* and *V. cholerae* (Uehara *et al.*, 2010; Möll *et al.*, 2014). Their M23 domains have degenerate zinc ion binding motifs, as it is also the case for its homologues in other bacteria. Upon the deletion of *nlpD* and *envC* in *V. parahaemolyticus*, the cells exhibited a chaining phenotype, similar to the deletion of those genes in other organisms (Uehara *et al.*, 2010). VP2471 and VPA0517 are homologues to the previously characterized peptidases important for cell elongation in *V. cholerae*, ShyC and ShyA respectively (Dörr *et al.*, 2013) and upon their deletion in *V. parahaemolyticus* we observed aberrantly shaped cells, a similar phenotype as the ones described. Finding these proteins conserved in *V. parahaemolyticus* suggests that they fulfill an important function in proteobacteria in general. In case of NlpD and EnvC, their regulation of amidase activity represents an evolved mechanism, which was passed on from a common ancestor without much alteration. ShyA and ShyC on the other hand are less wide spread, however can also be found in a large variety of bacterial organisms, indicating their conserved function. Additionally to the proteins homologous in other bacteria, in *V. parahaemolyticus* we found VP0548 (VcsP), VP1385 and VPA1649. These three proteins are very similar to each other in their domain composition, having a N-terminal cytoplasmic domain, follow by a trans-membrane domain and in the case of VcsP and VPA1649 having a coiled coil domain, with all three having a C-terminal M23 peptidase domain. Due to their similarity in overall domain composition, VcsP, VP1385 and VPA1649 can be considered paralogues.

To find out in more details, what sets apart VcsP from the other two groups of M23 endopeptidases present in *V. parahaemolyticus*, namely NlpD with a degenerate M23 domain involved in amidase activation and ShyA as an elongation specific D,D-endopeptidase, we generated a phylogenetic tree of VcsP, NlpD and ShyA homologues. We showed that VcsP of *V. parahaemolyticus* forms a distinct clade with closely related organisms and that these organisms have a conserved genetic neighborhood, unlike homologues found in e.g. *V. cholerae*. We also identified that distantly related protein Csd1 of *H. pylori* can be found in the group of VcsP homologues, however functionally this protein has been shown to give *H. pylori* its distinct shape (Sycuro *et al.*, 2010; An *et al.*, 2016) and the morphological phenotype of its inactivation is different compared to Δ*vcsP* (discussed in the following section). Additionally our analysis reflected that *nlpD* is part of a conserved genomic

neighborhood, as it has been shown to be part of an operon with global regulator *rpoS* in *E. coli*, *V. cholerae* and other γ-proteobacteria (Lange *et al.*, 1994; Yildiz *et al.*, 1998). Interestingly, while *vcsP* and *shyA* of *V. parahaemolyticus* showed a high conservation of genomic neighborhood to close relatives like *V. alginolyticus* and *V. harveyi* as expected, the conservation of genomic neighborhood in *V. cholerae* was very different. This is another indication that VcsP of *V. parahaemolyticus* and its homologue in *V. cholerae* (VC0843) do not share the same cellular function. This is additionally supported by findings, which map *vc0843* as part of the *V. cholerae* pathogenicity island involved in intestinal colonization (Zhu *et al.*, 2002; Jude, 2008) and that the *V. parahaemolyticus* pathogenicity islands map to locations that do not include *vcsP* (*vp0548*) (Makino *et al.*, 2003; Chao *et al.*, 2010).

Together these findings show that although *V. parahaemolyticus* encodes for several conserved and well-studied M23 peptidases, additionally also harbors so-far uncharacterized ones. Especially VcsP showed a distinct presence in *V. parahaemolyticus* and closely related organisms, which seems to be unrelated to homologues proteins from organisms like *V. cholerae* or *H. pylori*.

3.2 VcsP is an endopeptidase and affects cell separation

After identifying conserved M23 peptidases in *V. parahaemolyticus*, we tested their influence on cell morphology in a variety of deletion mutant combinations. As previously discussed: *nlpD*, *envC*, *shyA* and *shyC* all showed their distinct phenotype as it has been described in the literature (Uehara *et al.*, 2010; Dörr *et al.*, 2013; Möll *et al.*, 2014). The deletion of *vp1385* and *vpa1649* had no effect on cell morphology, as shown by the cell type and cell length distribution of the single deletion mutants. Similarly, the double deletion mutant of *vp1385* and *vpa1649* showed no morphological difference when compared to wildtype. While this indicates that these proteins have no visible effect under the tested conditions, we cannot exclude that they might be important under different conditions and then display a morphological phenotype. However, we did see an effect of VP1385 on peptidoglycan composition. Particularly, in the absence of *vp1385,* we found increased amounts of dimers and trimers at the expense of monomers in the PG profile. In this mutant background, there was less D,D-endopeptidase activity, resulting in an increase of cross-linkages compared to wildtype, indicating that VP1385 is a D,D-endopeptidase. The double deletion mutant of *vp1385* and *vpa1649* showed a similar PG profile to that of the *vp1385* single deletion. The effect of the double deletion was also presented by an increase in Polymyxin sensitivity when compared to single

deletions of either genes or the wildtype. This emphasizes that subtle changes in the peptidoglycan composition do not necessarily cause a distinct morphological phenotype, but non-the-less might affect cell wall integrity.

Upon the deletion of *vp0548* (*vcsP*), 25 % of the cell population formed chaining or elongated cells and in epistasis experiments, we showed that the deletion phenotype of Δ*vcsP* is unique when compared to its paralogues *vp1385* and *vpa1649*. We did not observe additive morphological effects, as the frequency of chaining or elongated cells did not increase in double or triple deletion backgrounds, but rather stayed around 25% like the single deletion of *vcsP*. The morphological phenotype had no effect on swarming and swimming motility as well as the ability to increase cell density when compared to wildtype. Interestingly however, in an environment where wildtype and Δ*vcsP* cells were challenged with each other, the Δ*vcsP* mutant was rapidly outcompeted, demonstrating that the chaining cells are at a disadvantage to form colonies, which reduces their dissemination ability. Upon the deletion of *vcsP*, in any combination with its paralogues, cells exhibited increasing sensitivity to Polymyxin antibiotics. The PG profile of the Δ*vcsP* strain showed increased amounts of dimers and trimers on behalf of monomers. Consequently, we found increased amounts of cross-linkages, which are mainly of the D,D kind, indicating that we identified VcsP as an D,D endopeptidase. The *vcsP H175A* mutant showed the same morphological phenotype, a very similar PG profile as well as sensitivity to Polymyxin antibiotics. These results strongly suggest that VcsP is an active M23 D,D-endopeptidase. To test that hypothesis *in vitro*, we aimed to purify different VcsP variants in order to check them in a dye release assay and on specific muropeptides. This would give *in vitro* proof of specific activity and might help determine if VcsP has any substrate preference. Unfortunately, so far, VcsP turned out to be difficult to purify and we are in the process of investigating improvements to solubility and increasing the yield during purification.

Some endopeptidases show spatio-temporal localization patterns that are important for their cellular activity (Möll *et al.*, 2014; Bartlett *et al.*, 2017). To test if VcsP also has such a regulated localization, we performed fluorescence microscopy on the active fusion protein VcsP-sfGFP. The fluorescent fusion protein is able to complement the deletion phenotype and we did not observe an effect on cell separation when over-expressing the VcsP-sfGFP fusion protein in the wildtype background. We observed the formation of fluorescent clusters in a sub-population of cells and the fluorescent clusters were predominantly localizing to the cell poles, although subpolar clusters were also observed. Often, the localization of a protein is directly correlated with the observed phenotype. For example, NlpD and EnvC localize to the division site to activate a single amidase,

which is required for cell division in *V. cholerae* (Möll *et al.*, 2014). Upon the deletion of NlpD and EnvC, the cell exhibits a chaining phenotype because the septal peptidoglycan cannot be disconnected, in order to separate the daughter cells. We showed that VcsP is also involved in cell separation; however, we did not see a predominant localization to mid cell. One explanation could be that VcsP is mostly active during cell elongation and that the loss of VcsP leaves the cells with a highly cross-linked PG mesh that cannot be disconnected in time during cell division. In that way, VcsP would not specifically localize to the division site but could still have an effect on cell separation. Another possibility is that VcsP is not directly involved in cell-separation, but rather is important to facilitate a passage through the PG mesh for other periplasmic or outer membrane components (Figure 27). EnvC of *H. influenzae* has been suggested to facilitate such a gateway through cross-linked PG and through this mechanism maintains the surface protein content. An *envC* mutant of that strain showed a drastic reduction of periplasmic protein abundance (Ercoli *et al.*, 2015). Similarly, lack of VcsP could lead to an overall decrease of protein abundance in the periplasm, which in turn passively creates a cell separation defect. This hypothesis could also explain the increased sensitivity of the Δ*vcsP* mutant to Polymyxin, because in that scenario the outer membrane would be compromised. This hypothesis can be tested by analyzing protein abundance of fractionated deletion mutant cells with mass-spectrometry in comparison to wildtype or by analyzing the LPS composition using silver staining methods. Another way to investigate the observed phenotypes of the *vcsP* mutant, is to perform synthetic lethal mutant screening. In this screening, a library of transposon insertions in wildtype and *ΔvcsP* cells is created. Afterwards, the frequency of transposon insertions is analyzed and compared between the wildtype and mutant. Genes, where a transposon insertion only occurs in the wildtype strain but not the mutant strain might encode for an interaction partner of VcsP or act together in the same pathway, resulting in a lethal combination. This screening has been shown to be successful in identifying genes involved in septal murein cleavage and cell division (Bernhardt *et al.*, 2004, 2005; Paradis-Bleau *et al.*, 2010).

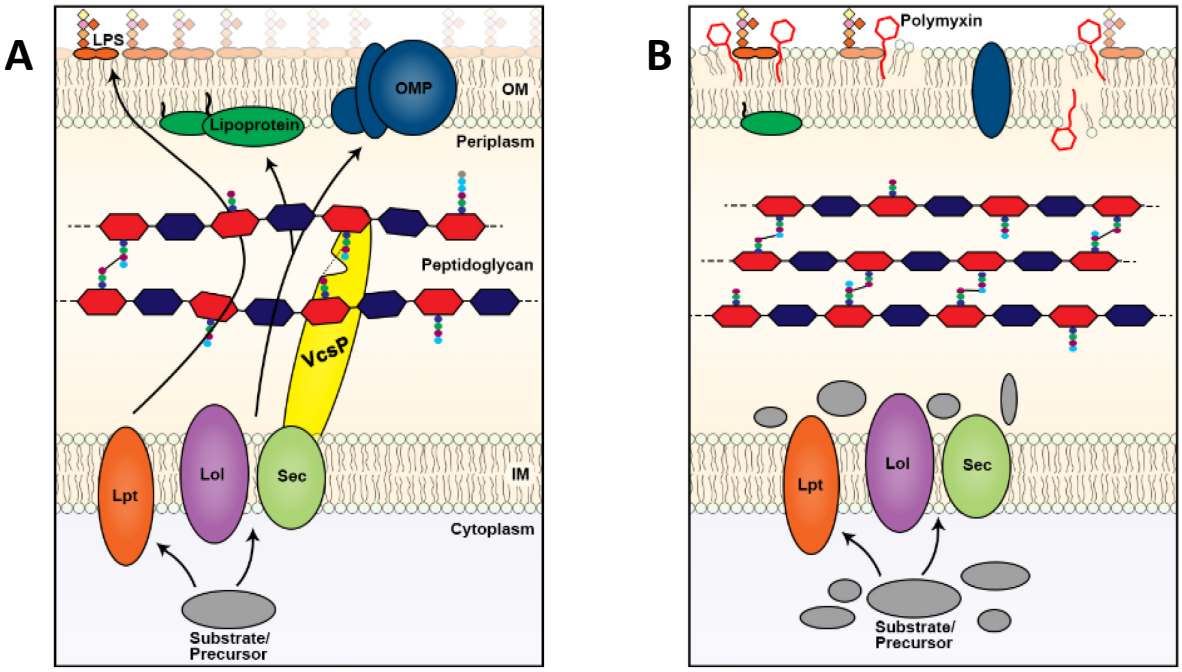

Figure 27: Possible model of VcsP function on cell wall biogenesis

(A) In wildtype cells, VcsP accociates with the protein translocation and integration complexes of the inner membrane and disconnects cross-linked stem peptides, relaxing the PG and creating space in the PG mesh. Through those spaces, proteins and other periplasmic/outer membrane components are guided to their final destination. (B) In the absence of VcsP, there are increasing amounts of PG that is highly cross-linked. It is more difficult for proteins and other outer membrane components to reach their destination. LPS accumulation might be reduced, resulting in a compromised outer membrane, more susceptible to e.g. Polymyxin antibiotics.

3.3 Screening for VcsP interaction partners

NlpD and EnvC M23 peptidases have distinct interaction partners in *E. coli* and other organisms (Peters *et al.*, 2011; Möll *et al.*, 2014). These partners are ultimately responsible for morphological phenotypes in the deletion background of given M23 peptidases. In order to find possible interaction partners of VcsP, we pursued two approaches. First, we had a detailed look into the genomic neighborhood of *vcsP* for possible interaction partners and second, we performed co-immunoprecipitation experiments.

VcsP is encoded next to a PilZ domain protein VP0549 and we showed that both genes are part of an operon and transcribed together. Nevertheless, upon deletion of *vp0549,* cells did not exhibit a chaining phenotype and the deletion mutant behaved like wildtype under all conditions tested. In order to test, if VcsP and VP0549 interact with each other, we performed a BACTH assay on both proteins and while we showed that both VcsP and VP0549 interact with themselves, we did not

observe their interaction with each other. The self-interaction of the PilZ domain protein VP0549 was not surprising, as it has been previously shown for other PilZ domain proteins to be able to form homodimers *in vitro* and *in vivo* (Benach *et al.*, 2007). Testing the self-interaction of VcsP, showed blue colony formation, however with little homogeneity and it has been shown for other M23 peptidases to be able to form homo- and hetero-dimers (Ichimura *et al.*, 2002; An *et al.*, 2016). Another way to show direct interaction between VcsP and VP0549 would be in co-immunoprecipitation experiments on *V. parahaemolyticus* cell lysate or with purified proteins. Although we have not found a functional connection between VcsP and VP0549 yet, we further characterized the PilZ domain protein. It has been shown previously that c-di-GMP signaling is also involved in call wall biogenesis, in that it regulates LPS modifications that improve immune evasion in the human pathogen *Pseudomonas aeruginosa* (McCarthy *et al.*, 2017). Additionally, in *Mycobacterium smegmatis* c-di-GMP regulates several target genes involved in growth, cell shape and cell division as well as the expression of lipid transport and metabolism genes (Li *et al.*, 2012; Gupta *et al.*, 2016). RgsP is an essential protein in *Rhizobiales* (class of α-proteobacteria) and it is able to bind and produce c-di-GMP through its GGDEF domain. It was shown that RgsP directly interacts with RgsM, a M23 domain containing protein, and that the deletion of either genes has an effect on cell morphology and biofilm formation (Schäper *et al.*, 2018). To determine if the PilZ domain protein VP0549 is able to bind c-di-GMP, as it has been described for other proteins of that family, we performed two different *in vitro* experiments. We showed that the wildtype variant of VP0549 is able to bind [^{32}P] radio-labeled c-di-GMP in a DRaCALA assay. Additionally, we utilized bio-layer interferometry (BLI) and showed that VP0549^{WT} binds c-di-GMP specifically and that the VP0549^{R9D} variant, as reported in literature (Ryjenkov *et al.*, 2006), was unable to bind c-di-GMP.

In a different approach to find possible interaction partners of VcsP, we performed a Co-IP experiment. Here we were able to find several proteins that are significantly enriched in the bait samples compared to the control samples. We found several proteins that are part of the RNA degradosome (Carpousis, 2007) as well as different cellular chaperons that prevent the aggregation of stress-denatured proteins and promote the refolding polypeptides generated under stress conditions (Langer *et al.*, 1992; Schröder *et al.*, 1993). The enrichment of these proteins strongly suggest that the overexpression of VcsP-FLAG causes stress response, possibly generating increasing amounts of *vcsP* mRNA and misfolded VcsP proteins. The degradosome, with RNase E as one of its components, is mainly responsible for the turnover of mRNA in bacterial cells (Deutscher, 2006). We used an inducible promoter to express VcsP-FLAG for the Co-IP experiments, which generates

an excess of coding mRNA, and in turn probably leads to the accumulation of unfolded protein. Because transcription and translation are a coupled process in bacteria (Kaberdin *et al.*, 2006; Proshkin *et al.*, 2010) we were able to pull down RNA degradosome components as well as protein chaperone complexes, all working together to manage this stress condition. In addition, this stress condition seems to be more prevalent when expressing VcsP-FLAG compared to sfGFP-FLAG. However, that might be due to the fact, that sfGFP can freely diffuse in the cytoplasm once it has been generated, whereas VcsP is designated for the translocation across the inner membrane. That creates even more stress for the cell, possibly overloading cellular translocation machineries. Indeed, we also found enriched in the pulldown experiments SecD (as well as other Sec proteins that were below the $\log_2$(FC) cutoff), which is suggested to be involved in the release of proteins from the Sec machinery after they have been translocated into the periplasm (Matsuyama *et al.*, 1993; Pogliano *et al.*, 1994; Guo *et al.*, 2018). Interestingly, in addition to SecD, we also found other proteins involved in cell envelope biogenesis: Ffh, is a component of signal recognition particle (SRP), which is involved in targeting and insertion of proteins into the inner membrane during co-translational translocation (Phillips *et al.*, 1992; Schlünzen *et al.*, 2005). Finding Ffh, as well as SecD, in this experiment suggests that VcsP is translocated using a signal recognition particle (SRP), however sequence analysis using the SignalP-5.0 software does not predict the presence of any signal sequence, neither for the Sec nor Tat pathway. BamA was significantly enriched and it is part of the of the Bam complex, which is responsible for inserting proteins into the outer membrane (Knowles *et al.*, 2009; Hussain *et al.*, 2018). This is an unusual candidate for an interaction partner of VcsP, since VcsP is likely located in the inner membrane whereas BamA is a large integral β-barrel protein located in the outer membrane. One possibility is that VcsP localizes close to protein translocation and integration complexes found in the inner membrane and through its lytic peptidase activity on PG, helps to create space in the PG mesh that is important for protein makeup of the periplasm (Figure 27). In the absence of VcsP the PG is heavily cross-linked, thereby affecting transport of proteins or LPS components across the periplasmic space. However, one cannot ignore the possibility that we pulldown entire stretches of inner and outer membrane together with our membrane anchored bait protein, which is the more likely scenario and an alternative method should be used to validate the Co-IP results.

3.4 Conclusions and future prospects

In this work, we characterized M23 peptidases encoded in *V. parahaemolyticus*, some of which showed conserved phenotypes as described in other organisms. However, we also found one specific M23 peptidase – VcsP – that showed a very interesting and distinct phenotype linked to cell wall biogenesis. In a Δ*vcsP* mutant, chaining cells were observed that are unable to perform the final separation of the mother and daughter cells. Analyzing the PG composition of *vcsP* deletion and *vcsP H175A* mutants, we found VcsP to be an active D,D endopeptidase, which would be further supported by *in vitro* verification.

Finding interaction partners or effectors of VcsP would give more clarity on its involvement in cell wall biogenesis. We started to address that with Co-IP experiments, however have not found clear candidates yet. Working with membrane-anchored proteins in Co-IP experiments is always delicate because the membrane association makes it difficult to determine if an enriched protein is a real interaction partner or just localized in close proximity on the membrane. Using a synthetic lethal screening to map transposon insertion frequencies could be a more promising approach. So far, we showed that VcsP is an active M23 endopeptidase by reproducing the phenotype in the absence of VcsP with an amino acid substitution of the M23 domains catalytic site *in vivo*. We started to work on the *in vitro* verification by trying to purify different variants of VcsP. In the future, further optimization will be required to obtain active protein, which will then be used to perform the dye release assay as well as hydrolyzing specific muropeptide standards. Interestingly, also VP1385, a VcsP paralogue, showed similar effects on the PG as VcsP, although the deletion of *vp1385* did not display a morphological phenotype. It will be interesting to see, if we can find a connection between both proteins, but also to perform *in vitro* assays on purified VP1385.

This study shed some light on M23 peptidases of *V. parahaemolyticus* in general, and additionally we elucidated a newly identified cell separation effector, which will help to understand PG remodeling in this organisms. VcsP forms a new clade of M23 peptidases involved in cell separation, suggesting that together these findings might also be applicable in other organisms and contribute to a better general understanding M23 endopeptidases.

4 Materials and Methods

4.1 Chemicals, equipment and software

Essential resources that were used during this work, such as reagents (Table 1), commercial purification kits (Table 2), hardware equipment (Table 3) and computer software (Table 4) are listed below. Information regarding their supplier/source is provided, as well as an identifier number, when available.

The chemicals and antibiotics used in this study were produced by the following companies (if not stated otherwise in the text): Merck (Darmstadt), Roth (Karlsruhe), Sigma-Aldrich (Taufkirchen), Alfa Aesar (Karlsruhe) and Invitrogen (Karlsruhe). Oligonucleotide synthesis was performed by Sigma-Aldrich (Taufkirchen) and DNA sequencing by Eurofins MWG Operon (Ebersberg).

Table 1: Reagents

Purpose	Enzyme/Kit	Reference
DNA amplification	Phusion High Fidelity DNA Polymerase	New England Biolabs (Frankfurt a. M.)
	Q5 Hot Start High Fidelity DNA Polymerase	
	Q5 High GC Enhancer	
	Q5 Reaction buffer	
	Desoxyribonucleotide (dNTP) Solution Mix	
Restrictive digestion	Endonucleases	New England Biolabs (Frankfurt a. M.)
		Fermentas (St. Leon-Rot)
	Alkaline Phosphatase Calf Intestinal (CIP)	New England Biolabs (Frankfurt a. M.)
Ligation	T4 Ligase	New England Biolabs (Frankfurt a. M.)
	10X Buffer for T4 DNA Ligase with 10mM ATP	

Purpose	Enzyme/Kit	Reference
DNA ladder	2-Log DNA Ladder (0.1-10.0KB)	New England Biolabs (Frankfurt a. M.)
Protein ladder	Color Pre-stained Protein Standard Broad Range (11-245 KDA)	New England Biolabs (Frankfurt a. M.)
Antibiotics	Chloramphenicol; Ampicillin sodium salt; Streptomycin sulfate; Kanamycin sulfate	Carl Roth GmbH + Co KG (Karlsruhe)
Growth medium	LB-Medium (Luria/Miller)	Carl Roth GmbH + Co KG (Karlsruhe)
	Difco Agar, Granulated	BD (Franklin Lakes, USA)
	Bacto Yeast Extract	
	Difco HI agar	
Assay component	2,2'-bipyridyl	Sigma-Aldrich (Steinheim)
	5-Bromo-4-Chloro-3-Indolyl-ß-D-Galactopyranoside (X-Gal)	Carl Roth GmbH + Co KG (Karlsruhe)
Protein induction	L(+)-Arabinose	Carl Roth GmbH + Co KG (Karlsruhe)
	Isopropyl β-D-1 thiogalactopyranoside (IPTG)	Peqlab (Erlangen)
Chemical competence	D(+) Saccharose	Carl Roth GmbH + Co KG (Karlsruhe)
PCR visualization	Ethidium bromide	Carl Roth GmbH + Co KG (Karlsruhe)
	Red-gal	Sigma-Aldrich (Steinheim)
	Gel loading dye purple 6X	New England Biolabs (Frankfurt a. M.)
PCR visualization and	peqGOLD Universal Agarose	Peqlab (Erlangen)
Microscopy	Agarose NEEP Ultra-Quality	Carl Roth GmbH + Co KG (Karlsruhe)
Protein visualization	Instant Blue	Expedeon (UK)
Cell cultivation and	Petri dish (round) 92x16mm	Sarstedt AG (Nümbrecht)
Assays	Petri dish (round) 150x20mm	
	96-well plates	Greiner Bio-One GmbH, Frickenhausen

Purpose	Enzyme/Kit	Reference
Microscopy	Microscopy slides	Carl Roth GmbH + Co KG (Karlsruhe)
	Cover slips	
MS coupled Co-IP	Microspin C18 columns	The Nest Group Inc. (USA)

Table 2: Purification Kits

Purpose	Enzyme/Kit	Reference
PCR product purification	NucleoSpin® Gel and PCR Clean-up	Macherey-Nagel (Düren)
Plasmid purification	NucleoSpin® Plasmid	Macherey-Nagel (Düren)

Table 3: Equipment

Purpose	Types	Reference
Centrifugation	SORVALL RC 6+	Thermo Electron (Dreieich)
	Multifuge 1 s-R	
	Biofuge pico	
	Centrifuge 5424 (R)	Eppendorf (Hamburg)
PCR	Mastercycler personal	Eppendorf (Hamburg)
	Mastercycler epgradient	
Thermomixer	Thermomixer compact	Eppendorf (Hamburg)
	Thermomixer comfort	
Agarose gel photography	E-BOX VX 2	Peqlab (Erlangen)
UV table	UVT_20 LE	Herolab (Wiesloch)
Spectral photometer	Nanodrop ND-1000	Nanodrop (Wilmington, USA)
	Ultrospec 2100 pro	Amersham Biosciences (München)
Plate Reader	Infinite M200 Pro	Tecan (Crailsheim)
Western Blotting and	TransBlot Turbo Transfer System	Bio-Rad (München)
imaging	LAS-4000 Luminescence Analyser	Fujifilm (Düsseldorf)

Purpose	Types	Reference
Cell disruption	Sonopuls mini20	Bandelin (Berlin)
	UP200st Ultrasonic Processor	Hielscher (Teltow)
	French pressure cell press	SLM instruments (Urbana, USA)
Electroporation	Gene Pulser Xcell	Bio-Rad (München)
Microscopy	Eclipse Ti inverted microscope	Nikon (Düsseldorf)
	with a 100x lens and	
	Zyla sCMOS cooled camera	Andor Technology Ltd. (Belfast, UK)
	Zeiss Axio Imager M1 with	Carl Zeiss AG (Jena)
	α Plan-Fluar 100x/1.45 Oil DIC	
	Cascade:1K CCD camera	Teledyne Photometrics (Tucson, USA)

Table 4: Software and online tools

Software and Function	URL	Reference
KEGG sequence database	http://www.genome.jp/kegg/kegg2.html	(Ogata *et al.*, 1999)
NCBI sequence database	http://www.ncbi.nlm.nih.gov/	(Ostell *et al.*, 1998)
UniProt sequence database	http://www.uniprot.org/	(Apweiler *et al.*, 2004)
BLAST sequence comparison	http://blast.ncbi.nlm.nih.gov/Blast.cgi	(Altschul *et al.*, 1990)
SMART protein domain prediction	http://smart.embl-heidelberg.de/	(Schultz *et al.*, 1998)
MEROPS peptidase database	https://www.ebi.ac.uk/merops/	(Rawlings *et al.*, 2008)
iTol phylogenetic tree	http://itol.embl.de	(Letunic *et al.*, 2019)
MetaMorph v7.5 Microscopy analysis		Molecular Devices (Union City, CA)
ImageJ-Fiji v1.49j10 Microscopy analysis	http://rsbweb.nih.gov/ij	(Rueden *et al.*, 2017)

NIS-Elements 4.60.00 Microscopy analysis		Nikon (Düsseldorf)
Oligo Calc Primer design	http://biotools.nubic.northwestern.edu/OligoCalc.html	(Kibbe, 2007)
Perseus v1.5.2.6 MS analysis		(Tyanova *et al.*, 2016)
Scaffold v4.8.9 MS analysis	http://www.proteomesoftware.com/products/scaffold/	Proteome Software (USA)
Microsoft Office 2016		Microsoft (Redmond, USA)
Mendeley v1.19.3 Reference library	https://www.mendeley.com/reference-management/reference-manager	Mendeley (London, UK)
GraphPad Prism v6.07 Statistical analysis and blot generation		Prism Software (Irvine, USA)

4.2 Media, buffers and solutions

Media and additives described in the following tables will be sterilized either by autoclaving them at 121 °C and 1 bar positive pressure for 20 minutes or by filtration trough 0.22 µm pores (Millipore (Schwalbach/Ts.); Sarstedt (Nümbrecht)). Additives like antibiotics or inducing agents are added after sterilization, under sterile conditions.

Table 5: Media and Buffer

Media/Buffer	**Composition (per Liter)**
Lysogeny Broth (LB)	10 g tryptone 5 g yeast extract 10 g NaCl
LB agar	LB medium + 15 g agar
Transformation & Storage Solution (TSS) (Chung *et al.*, 1989)	10 g tryptone 5 g yeast extract 10 g NaCl 100 g PEG 5 ml DMSO 50 mM MgCl2 or MgSO4 pH 6.5

Media/Buffer	Composition (per Liter)
Difco Heart Infusion (HI) Agar (BD, Franklin Lakes, USA)	10 g beef-heart infusion (from 500g) 10 g tryptone 5 g NaCl 15 g agar
HI swarming assay additives	4 mM CaCl2 50 µM di-pyridyl (solution in 100 % ethanol)
Phosphate buffered saline 10x (PBS)	25.6 g Na2HPO4·7H2O 80 g NaCl 2 g KCl 2 g KH2PO4
2x TY	16 g tryptone 10 g yeast extract 5 g NaCl

Table 6: Antibiotics concentrations for *E. coli* growth media

Antibiotic	Final concentration	Solvent
Ampicillin	100 µg/ml	H_2O
Chloramphenicol	20 µg/ml	100 % ethanol
Kanamycin-sulfate	50 µg/ml	H_2O

Table 7: Antibiotics concentrations for *V. parahaemolyticus* growth media

Antibiotic	Final concentration	Solvent
Ampicillin	100 µg/ml	H_2O
Chloramphenicol	5 µg/ml	100 % ethanol

4.3 Microbiological methods

4.3.1 Growth conditions

In all experiments, unless stated otherwise, *V. parahaemolyticus* and *E. coli* were grown in LB medium or on LB agar plates at 37°C containing antibiotics with concentrations indicated in Table 6 and Table 7.

4.3.2 Construction of bacterial strains

Deletion of genes in *V. parahaemolyticus* was performed through the principle of homologous recombination. *E. coli* strain DH5αλpir was used for standard cloning and E. coli strain SM10λpir was for conjugative transfer of pDM4 derivatives from *E. coli* to *V. parahaemolyticus* (Miller *et al.*, 1988). The procedure is described as follows.

Both the donor *E. coli* strain (SM10λpir) harboring the corresponding plasmid (pDM4 derivative) and the recipient *V. parahaemolyticus* strain were grown in LB until the cultures reach an OD_{600} of approximately 0.5. 1 ml of each of these cultures was then harvested and the obtained pellet was resuspended in 100 µl of LB. 40 µl of each of these suspensions was then mixed together in a separate tube. From this, triplicates of 20 µl of the mixture were spotted on LB-agar plates and incubated at 37 °C. The grown spots were then scraped off and resuspended in 1ml of LB medium. Dilution series of the aforementioned suspension were plated on LB+Amp+Cm plates and incubated at 37 °C. Single colonies that were obtained from these dilution series were then restreaked onto fresh LB agar plates supplemented with ampicillin and chloramphenicol and once again incubated at 37 °C. The colonies thus obtained were the single crossovers and if the next step is not carried out immediately after, the single crossovers obtained can be suspended in glycerol and stored at -80 °C for storage.

The single crossovers obtained above were grown in LB broth containing chloramphenicol, shaking at 37 °C for at least 5-6 hours. From this grown culture, 50 µl was taken out and mixed with a solution containing 2 ml of LB broth and 1 ml of 33% sucrose solution. This mixture was grown shaking at 37 °C for around 20-24 hours. Dilution series of this grown culture were then plated on to LB agar plates containing 33% sucrose and incubated overnight at 30 °C. The colonies thus obtained were streaked on to both LB agar plates supplemented with both ampicillin and chloramphenicol and LB agar plates supplemented only with ampicillin. Those colonies that were found to be sensitive to

chloramphenicol were further tested by colony PCR to assess for the corresponding deletion. If positive results were obtained through agarose gel electrophoresis, the respective patches were further re-streaked onto LB agar plates supplemented with ampicillin and incubated at 37 °C to obtain single colonies. These single colonies were once again tested with colony PCR to assess for deletion of the gene. The PCRs were performed alongside genomic DNA of *V. parahaemolyticus* to assess for the size shift in the DNA band, indicative of the deletion.

The aforementioned procedure of conjugative transfer/ homologous recombination was also carried out to obtain insertions within the genome of *V. parahaemolyticus*. Colony PCR of the positive patches and colonies at the end of the double crossover step were performed alongside genomic DNA to assess for an increase in the desired DNA band, indicative of an insertion within the genome.

Strain	**Description/genotype**	**Reference**
Vibrio parahaemolyticus		
RIMD2210633	Clinical isolate, wildtype	(Makino *et al.*, 2003)
JH32	*Δvp0548* (*ΔvcsP*)	This work
JH2	*Δvpa1548*	(Heering *et al.*, 2016)
SR58	*Δvp2225*	(Ringgaard *et al.*, 2014)
JH35	*Ω*PLAC*::lacZ*	This work
JH47	*Ωvp0548* H175A	This work
JH40	*Δvp1385*	This work
JH39	*Δvpa1649*	This work
JH51	*Δvp1385, Δvpa1649*	This work
JH43	*Δvp1385, Δvp0548*	This work
JH42	*Δvpa1649, Δvp0548*	This work
JH48	*Δvp1385, Δvp0548, Δvpa1649*	This work
JH54	*Δvpa0517*	This work
JH52	*Δvp2471*	This work
JH55	*Δvp2834, Δvp2554*	This work
JH46	*Δvp2834*	This work

Strain	Description/genotype	Reference
JH36	*Δvp0549*	This work
Escherichia coli		
SM10 λ pir	KmR, thi-1, thr, leu, tonA, lacY, supE, recA::RP4-2- Tc::Mu, pir	(Miller *et al.*, 1988)
DH5 λ pir	sup E44, ΔlacU169 (ΦlacZΔM15), recA1, endA1, hsdR17, thi-1, gyrA96, relA1, λpir phage lysogen	(Platt *et al.*, 2000)
TOP10	F-, mcrA, Δ(mrr-hsdRMS-mcrBC), ϕ80lacZΔM15, lacX74, nupG, recA1, araD139, Δ(ara-leu)7697, galE15, galK16, rpsL(StrR), endA1 λ-	Invitrogen (Karlsruhe)
BTH101	F-, cya-99, araD139, galE15, galK16, rpsL1 (StrR), hsdR2, mcrA1, mcrB1	Euromedex (FR)
BL21 (DE3)	F-, ompT, hsdS(rB– mB–), dcm+, TetR, gal, λ(DE3), endA, Hte	(Studier *et al.*, 1986)

4.3.3 Strain storage

For the long-term storage of strains, glycerol stocks were made. 1 mL of densely grown bacterial cultures were stored, supplemented with 16% (v/v) glycerol, at - 80 °C.

4.3.4 Separation and detection of DNA using agarose gel electrophoresis

1% agarose gels prepared with 0.5X TAE buffer and supplemented with 0.005% (v/v) of ethidium bromide were used to separate the DNA fragments by agarose gel electrophoresis. 6X Gel loading dye purple (New England Biolabs) was added to DNA samples before loading the samples into the agarose gel wells. To be able to estimate the size of the DNA fragment, a 2-log DNA ladder (New England Biolabs) was loaded in the gel along with the samples of interest. Detection of DNA bands was obtain using the E-BOX VX2 imaging system (PeqLab). If needed, DNA fragments of interest were cutted and removed for further use.

4.3.5 Restriction digestion and ligation of DNA

Restriction of DNA fragments was performed using the appropriate restriction endonuclease (1µL/ µg of DNA fragment) and the corresponding buffer. Reaction was carried out at 37°C for at least 1 h. Next, in the case of the vector, to avoid sef-ligation, 1 µL of calf intestine alkaline phosphatase (CIP) was added and the reaction was carried out for at least 1 more hour at 37°C. Restricted DNA was directly purified by using the NucleoSpin Gel and PCR Clean-up kit (Machenery-Nagel).

Ligation reactions were performed in 20 µL total volume, using 1 µL T4 DNA ligase and the corresponding buffer (New England Biolabs). Approximately 1:5 ratio of the digested vector DNA and of insert DNA were added and the reaction was kept at 16°C between 2-3 h. Ligation mixtures were then transform into *E. coli* strains DH5αλpir.

4.3.6 Preparation of chemically competent *E. coli* cells

Cells growing in a 20 mL LB culture were harvested at OD_{600}=0.6 by centrifugation. The cell pellet was resuspended in ice-cold TSS buffer (Chung *et al.*, 1989), in 1/10 of the original cell culture volume. The culture was aliquoted, the tubes frozen with liquid nitrogen and and stored at -80°C.

4.3.7 Transformation of chemically competent *E. coli* cells

1-2 µL of the corresponding plasmid was added to 50 µL of the (above-obtained) chemically competent *E. coli* cells. After approximately 30 minutes on ice, the cells were heat-shock, placed at 42°C for 1 minute and immediatly transferred back to ice and resuspended in 500 µl of LB medium. The cells were then shaken for 1 h at 37°C followed by centrifugation. The pelletized cells were ressupended in 100 µL of LB and plated onto LB-agar plates containing the relevant antibiotic.

4.3.8 Preparation of electro-competent *V. parahaemolyticus* cells

To prepare electro-competent cells of *V. parahaemolyticus,* 200 mL of inoculated LB liquid culture were incubated at 37° C until it reached OD_{600}=1. After centrifugation for 10 min at 4700 rpm at 4° C, cells were kept on ice. The pellet was washed twice with ice-cold freshly prepared 273mM sucrose solution. The sucrose solution was buffered using KOH to keep pH at 7.2-7.4. After the two washes,

the cells were re-suspended in sucrose solution with glycerol added to 1/10 of the original cell culture volume. Aliquots of 50µl were frozen in liquid nitrogen and then at -80° C.

4.3.9 Transformation of electro-competent *V. parahaemolyticus* cells

5 µL of the corresponding plasmid was added to 100 µL of the (above-obtained) electro-competent *V. parahaemolyticus* cells. After approximately 1 h on ice, the cells were transferred into a pre-chilled electroporation cuvette. Electroporation was carried out using a MicroPulser electroporator (Bio-Rad) at the following conditions: voltage 2200, µF 25 and 200 Ω and immediately after cells were resuspended in 1 mL of LB medium. The cells were then transferred back into a 1.5 mL Eppendorf tube and shaken for at least 2 hours at 37 °C, followed by centrifugation. The pelletized cells were ressupended in 100 µL of LB and plated onto LB-agar plates containing the relevant antibiotic.

4.3.10 Swarming assay

To perform swarming assays, a liquid culture of *V. parahaemolyticus* was grown in LB medium to an OD_{600} between 0.1-0.5 and subsequently spotted onto swarm agar plates (Table 5). The swarm agar plates (agar (40 g L^{-1} Difco Heart Infusion Agar (BD) supplemented with 4 mM CaCl2 and 50 mM 2,2'-bipyridyl (Sigma Aldrich)) were dried 10 min at 37 °C before spotting the liquid culture. After letting the spot of liquid culture dry for 4 min at RT, plates were sealed with clear plastic tape and incubated overnight at 24° C. Afterwards, the colony diameter was measured.

4.3.11 Swimming assay

To perform swimming assays, a liquid culture of *V. parahaemolyticus* was grown in LB medium to an $OD_{600} \approx 1$ and subsequently spotted on LB agar 0.3 % plates, with a toothpick. The plates were incubated overnight at 30 °C for 15 h. Afterwards, the diameter of the swimming colony was measured.

4.3.12 Growth curve

Bacterial cultures were grown to stationary phase and afterwards their OD_{600} was normalized to 1. Samples were diluted 1/1000 and triplicates of 200 µL were placed in a 96 well plate. The OD_{600} was measured over time in a microplate reader every 15 min for 18h, at 37 °C. The mean values of replicates with standard deviation are plotted against time.

4.3.13 Competition Assay

To test competition between wildtype and another strain, liquid medium was inoculated with a 1:1 ratio of wildtype cells, which are *lacZ+* and form blue colonies on LB agar supplemented with X-gal, and a second strain, which are *lacZ-* and forms white colonies. Afterwards, dilution series of triplicates were plated and the CFU/ml were determined, which represents the input. The same cell mixture was incubated for 4 and 24 hours as five replicates, and the CFU/ml were determined. To calculate the competitive index, the ratio of wildtype^{lac+} over second strain at a certain time point was multiplied by the input ratio of wildtype^{lac+} over the second strain. A competitive index close to one indicates that the two strains are proliferating similarly.

4.3.14 Bacterial two hybrid assay

In order to detect protein-protein interactions by reconstituting certain proteins in *E. coli*, the bacterial two hybrid (BACTH) assay was employed (Karimova *et al.*, 1998). The assay makes use of the T18 and T25 domains of the adenylate cyclase within the organism, *Bordetella pertussis*. In order to carry out the experiment, plasmids that encode either the T18 domain (pUT18 or pUT18C) or the T25 domain (pKNT25 or pKT25) were purified and the corresponding genes whose products are to be tested for interaction were fused to the aforementioned plasmids. The plasmids in the study were all provided by the manufacturer (Euromedex, FR).

After designing the appropriate constructs, two plasmids (one encoding for the T18 and the other encoding for the T25 domain), carrying either N-terminal or C-terminal fusions of the gene of interest were co-transformed into the *E. coli* strain, BTH101. The reason for using this particular strain of *E. coli* is that it lacks the *cyaA* gene which in turn encodes for the catalytic domain of adenylate cyclase. Therefore, on its own this strain is unable to produce the messenger molecule, cyclic adenosine monophosphate (cAMP). Interaction between the genes used in the

aforementioned co-transformation experiment in turn results in bringing the T18 and the T25 domains closer to each other and subsequently, reconstitution of the catalytic domain of the adenylate cyclase enzyme. As a result of this, the strain is able to produce cAMP which is then able to activate transcription of the lac operon and subsequently, expression of β-galactosidase (β-gal). This can be visualized by employing the indicator, X-gal which is in turn cleaved by the β-gal enzyme and resulting in the formation of blue colonies.

The experimental workflow of a typical BACTH assay in the laboratory is described as follows. 20-25 ng of the purified plasmid DNA (from both T18 and T25) were used for transformation into BTH101. The transformed cells were in turn plated onto LB agar plates with the following antibiotics: 100 µg/ml of ampicillin, 50 µg/ml of kanamycin. In order to permit blue-white screening, the plates were also supplemented with 500 µM of IPTG and 80 µg/ml of X-gal. The plates were then incubated at 30 °C for a period not lasting longer than 2 days. From each of these plates, three colonies (standing for three replicates) were selected and resuspended into 1 ml of LB medium containing the aforementioned antibiotics. The Eppendorf tubes were then shaken at 30 °C for at least 2 hours. They were then spotted onto LB-agar plates containing the aforementioned antibiotics and indicators and incubated at 30 °C for a maximum period of 2 days. Pictures were taken of the above plates at regular intervals. In all cases, co-transformation of pUT18C-zip and pKNT25-zip (Euromedex, FR) into *E.coli* BTH101 was carried out and this served as the positive control. On the other hand, transformations were also done with empty vectors which in turn served as negative controls.

4.4 Molecular biological methods

4.4.1 Isolation of genomic DNA from *V. parahaemolyticus*

A small portion of cells grown overnight in a LB plate containing ampicillin, was resuspended in distilled water and boiled for 10-12 minutes. After centrifugation at 10,000 rpm for 10 minutes, the supernatant was then transferred to a fresh Eppendorf tube.

4.4.2 Isolation of plasmid DNA from *E. coli*

For plasmid isolation, *E. coli* strain containing the desired plasmid was grown in 5 mL of LB supplemented with the required antibiotic overnight at 37 °C shaking. Plasmid DNA was extracted by using the NucleoSpin Plasmid kit (Macherey-Nagel). The plasmid DNA concentration was measured using a Nanodrop spectrophotometer.

4.4.3 Polymerase chain reaction (PCR)

Amplification of DNA fragment was carried out either with Q5 Hot Start High Fidelity DNA Polymerase or Phusion High-Fidelity DNA Polymerase. In case of colony PCR, the total reaction volume used was 20 µL, otherwise the volume used was 50 µL. The composition of the PCR mixtures for Q5 Hot Start Polymerase and Phusion Polymerase are shown in **Error! Reference source not found.** and **Error! Reference source not found.**, respectively. The temperature of annealing was chosen according to the primer meting temperature, and the extension time was chosen according to the size of the fragment to be amplified (usually 1 minute per kilobase). For colony PCR with E. coli, the colony of interest was suspended in the PCR reaction mixture. For V. parahaemolyticus, genomic DNA was obtained by the method described above and used as template.

Table 8. Q5 PCR reaction composition

Reagents	Volumes (µl)
10mM dNTPs	1
5X Q5 reaction buffer	10
5X Q5 High GC enhancer	10
0.5 µM forward primer	2
0.5 µM reverse primer	2
Polymerase	0.5
Template DNA	1
Nuclease-free water	Up to 50 µl

Table 9. Phusion PCR reaction composition

Reagents	Volumes (µl)
10mM dNTPs	1
10X Buffer	5
0.5 µM forward primer	2
0.5 µM reverse primer	2
Polymerase	1
Template DNA	1
Nuclease-free water	Up to 50 µl

4.4.4 Separation and detection of DNA using agarose gel electrophoresis

1 % agarose gels prepared with 0.5X TAE buffer and supplemented with 0.005 % (v/v) of ethidium bromide were used to separate the DNA fragments by agarose gel electrophoresis. 6X Gel loading dye purple (New England Biolabs) was added to DNA samples before loading the samples into the agarose gel wells. To be able to estimate the size of the DNA fragment, a 2-log DNA ladder (New England Biolabs) was loaded in the gel along with the samples of interest. Detection of DNA bands was obtain using the E-BOX VX2 imaging system (PeqLab). If needed, DNA fragments of interest were cut and removed for further use.

4.4.5 Restriction digestion and ligation of DNA

Restriction of DNA fragments was performed using the appropriate restriction endonuclease (1µL/ µg of DNA fragment) and the corresponding buffer. Reaction was carried out at 37°C for at least 1 h. Next, in the case of the vector, to avoid sef-ligation, 1 µL of calf intestine alkaline phosphatase (CIP) was added and the reaction was carried out for at least 1 more hour at 37°C. Restricted DNA was directly purified by using the NucleoSpin Gel and PCR Clean-up kit (Machenery-Nagel).

Ligation reactions were performed in 20 µL total volume, using 1 µL T4 DNA ligase and the corresponding buffer (New England Biolabs). Approximately 1:5 ratio of the digested vector DNA and of insert DNA were added and the reaction was kept at 16°C between 2-3 h. Ligation mixtures were then transform into *E. coli* strain DH5αλpir.

4.4.6 Preparation of chemically competent *E. coli* cells

Cells growing in a 20 mL LB culture were harvested at OD_{600} = 0.6 by centrifugation. The cell pellet was resuspended in ice-cold TSS buffer (Table 5), in 1/10 of the original cell culture volume. The culture was aliquoted, the tubes frozen with liquid nitrogen and stored at -80°C.

4.4.7 Transformation of chemically competent *E. coli* cells

1-2 µL of the corresponding plasmid was added to 50 µL of the chemically competent *E. coli* cells (section 4.4.6). After approximately 30 minutes on ice, the cells were heat-shock, placed at 42°C for

1 minute and immediately transferred back to ice and resuspended in 500 µl of LB medium. The cells were then shaken for 1 h at 37°C followed by centrifugation. The pelletized cells were resuspended in 100 µL of LB and plated onto LB-agar plates containing the relevant antibiotic.

4.4.8 Preparation of electro-competent *V. parahaemolyticus* cells

To prepare electro-competent cells of *V. parahaemolyticus*, 200 mL of inoculated LB liquid culture were incubated at 37° C until it reached OD_{600} = 1. After centrifugation for 10 min at 4700 rpm at 4° C, cells were kept on ice. The pellet was washed twice with ice-cold and freshly prepared 273mM sucrose solution. The sucrose solution was buffered using KOH to keep pH at 7.2-7.4. After the two washes, the cells were resuspended in sucrose solution with glycerol added to 1/10 of the original cell culture volume. Aliquots of 50µl were frozen in liquid nitrogen and then stored at -80° C.

4.4.9 Transformation of electro-competent *V. parahaemolyticus* cells

5 µL of the corresponding plasmid was added to 100 µL of the (section 4.4.8) electro-competent *V. parahaemolyticus* cells. After approximately 1 h on ice, the cells were transferred into a pre-chilled electroporation cuvette. Electroporation was carried out using a MicroPulser electroporator (Bio-Rad) at the following conditions: voltage 2200, µF 25 and 200 Ω and immediately after, the cells were resuspended in 1 mL of LB medium. The cells were then transferred into a 2.0 mL Eppendorf tube and shaken for at least 2 hours at 37 °C, followed by centrifugation. The pelletized cells were resuspended in 100 µL of LB and plated onto LB-agar plates containing the relevant antibiotic.

4.4.10 Plasmids

The plasmids used in this study are listed in Table 10. Primers used are listed in Table 11. *E. coli* strains DH5αλpir and SM10λpir were used for cloning. *E. coli* strain SM10λpir was used to transfer DNA into *V. parahaemolyticus* by conjugation (Miller *et al.*, 1988). Construction of *V. parahaemolyticus* deletion mutants was performed with standard allele exchange techniques using derivatives of plasmid pDM4 (Donnenberg *et al.*, 1991).

4.4.10.1. Construction of plasmids

pJH070

The up- and downstream regions flanking *vp0549* were amplified using primer pairs 851/852 and 853/854, respectively, using V. parahaemolyticus RIMD 2210633 chromosomal DNA as template. In a third PCR, using primers 851/854 and products of the first two PCR reactions as template, the flanking regions were fused together. The resulting product was inserted into the XbaI site of pDM4, resulting in plasmid pJH070.

pJH081

A plasmid region encoding for *lacZα* under the control of the *lac* promotor in the pUC19 vector was amplified using primers 580/581. The PCR product was inserted into pDM4 suicide vector digested with Eco53kI/SalI, resulting in plasmid pJH081.

pJH088

The up- and downstream regions flanking *vp0548* were amplified using primer pairs 1662/1663 and 1664/1665, respectively, using *V. parahaemolyticus* chromosomal DNA as template. In a third PCR, using primers 1662/1665 and products of the first two PCR reactions as template, the flanking regions were fused together. The resulting product was digested with SphI/XbaI and was inserted into the equivalent site of pJH081, resulting in plasmid pJH088.

pJH100

V. parahaemolyticus genomic DNA was used as a template to amplify the region encoding *vp0548* using primer pair 1671/2844. In a second PCR, primers 2729/2730 were used to amplify *sfgfp* from a plasmid. In a third PCR, both PCR products were used as a template to fuse them together using primers 1671/2730. The resulting product was digested with XbaI/ SphI and was inserted into the equivalent site of pBAD33, resulting in plasmid pJH100.

pJH101

The up- and downstream regions flanking *vp0548* were amplified using primer pairs 1662/2985 and 2971/1665, respectively, using *V. parahaemolyticus* chromosomal DNA as template. Primer pair 2492/3042 was used to amplify the H175A variant of *vp0548* from a plasmid. In a fourth PCR, using primers 1662/3042 and products of the first and third PCR reactions as template were fused together. In a final PCR reaction using primers 1662/1665, the second and fourth PCR products were used as template and fused together into the final PCR product. The resulting product was digested with SphI/XbaI and was inserted into the equivalent site of pJH081, resulting in plasmid pJH101.

pJH102

The up- and downstream regions flanking *vp1385* were amplified using primer pairs 2865/2866 and 2867/2868, respectively, using *V. parahaemolyticus* chromosomal DNA as template. In a third PCR, using primers 2865/2868 and products of the first two PCR reactions as template, the flanking regions were fused together. The resulting product was digested with XbaI and was inserted into the equivalent site of pJH081, resulting in plasmid pJH102.

pJH103

The up- and downstream regions flanking *vpa1649* were amplified using primer pairs 2860/2861 and 2862/2863, respectively, using *V. parahaemolyticus* chromosomal DNA as template. In a third PCR, using primers 2860/2863 and products of the first two PCR reactions as template, the flanking regions were fused together. The resulting product was digested with XbaI and was inserted into the equivalent site of pJH081, resulting in plasmid pJH103.

pJH097 and pJH098

A truncated variant of *vp0548* from nucleotide 130 until the end of the gene was amplified using primer pair 3167/3168 and using *V. parahaemolyticus* RIMD 2210633 or strain JH47 (*vp0548* H175A variant) as template. The resulting products was inserted into the EcoRI/XbaI site of pMalE-c2x, resulting in plasmids pJH097 and pJH098, respectively.

pJH104 and pJH106

The encoding sequence of *vp0549 was* amplified using primer pair 1673/1674 and using *V. parahaemolyticus* RIMD 2210633 chromosomal DNA as template. The resulting product was inserted into the XbaI/KpnI sites of pUT18C and pKT25, resulting in plasmids pJH104 and pJH106, respectively.

pJH105 and pJH107

The encoding sequence of *vp0549 was* amplified using primer pair 1669/1670 and using *V. parahaemolyticus* RIMD 2210633 chromosomal DNA as template. The resulting product was inserted into the XbaI/KpnI sites of pUT18 and pKNT25, resulting in plasmids pJH105 and pJH107, respectively.

pJH108 and pJH109

A truncated variant of *vp0548* from nucleotide 130 until the end of the gene was amplified using primer pair 1667/1668 and using *V. parahaemolyticus* RIMD 2210633 chromosomal DNA as template. The resulting product was inserted into the XbaI/KpnI sites of pUT18 and pKNT25, resulting in plasmids pJH108 and pJH109, respectively.

pJH110 and pJH111

The encoding sequence of *vp0548 was* amplified using primer pair 1671/1672 and using *V. parahaemolyticus* RIMD 2210633 chromosomal DNA as template. The resulting product was inserted into the XbaI/KpnI sites of pUT18C and pKT25, resulting in plasmids pJH110 and pJH111, respectively.

pJH112

Only the M23 domain encoding sequence of *vp0548* was amplified using primer pair 3179/3180 and using *V. parahaemolyticus* RIMD 2210633 chromosomal DNA as template. The resulting product was inserted into the EcoRI/XbaI site of pMalE-c2x, resulting in plasmid pJH112.

pJH113

Only the M23 domain encoding sequence of *vp0548* was amplified using primer pair 3182/3180 and using strain JH47 (*vp0548* H175A variant) chromosomal DNA as template. The resulting product was inserted into the EcoRI/XbaI site of pMalE-c2x, resulting in plasmid pJH113.

pJH114

The encoding sequence of *vp0549 was* amplified using primer pair 1832/1833 and using *V. parahaemolyticus* RIMD 2210633 chromosomal DNA as template. The resulting product was inserted into the NcoI/XhoI sites of pET28b(+), resulting in plasmid pJH114.

pJH115

Primers 1991/1992 were used to perform rolling circle PCR on pJH114 as a template, resulting in plasmid pJH115.

pJH116

A truncated variant of *vp0548* from nucleotide 130 until the end of the gene was amplified using primer pair 3115/2879 and using *V. parahaemolyticus* RIMD 2210633 chromosomal DNA as template. The resulting product was inserted into the NcoI/XhoI sites of pET28b(+), resulting in plasmid pJH116.

pJH117

Primers 2597/2598 were used to perform rolling circle PCR on pJH116 as a template, resulting in plasmid pJH117.

pJH118

Only the M23 domain encoding sequence of *vp0548* was amplified using primer pair 3177/3178 and using *V. parahaemolyticus* RIMD 2210633 chromosomal DNA as template. The resulting product was inserted into the NcoI/XhoI sites of pET28b(+), resulting in plasmid pJH118.

pJH119

Only the M23 domain encoding sequence of *vp0548* was amplified using primer pair 3177/3178 and using strain JH47 (*vp0548* H175A variant) chromosomal DNA as template. The resulting product was inserted into the NcoI/XhoI sites of pET28b(+), resulting in plasmid pJH119.

pJH120

The up- and downstream regions flanking *vpa0517* were amplified using primer pairs 3081/3082 and 3083/3084, respectively, using *V. parahaemolyticus* RIMD 2210633 chromosomal DNA as template. In a third PCR, using primers 3081/3084 and products of the first two PCR reactions as template, the flanking regions were fused together. The resulting product was digested with XbaI and was inserted into the equivalent site of pJH081, resulting in plasmid pJH120.

pJH121

The up- and downstream regions flanking *vp2471* were amplified using primer pairs 3086/3087 and 3088/3089, respectively, using *V. parahaemolyticus* RIMD 2210633 chromosomal DNA as template. In a third PCR, using primers 3086/3089 and products of the first two PCR reactions as template, the flanking regions were fused together. The resulting product was digested with SphI and was inserted into the equivalent site of pJH081, resulting in plasmid pJH121.

pJH122

The up- and downstream regions flanking *vp2554* were amplified using primer pairs 3120/3121 and 3122/3123, respectively, using *V. parahaemolyticus* RIMD 2210633 chromosomal DNA as template. In a third PCR, using primers 3120/3123 and products of the first two PCR reactions as template, the flanking regions were fused together. The resulting product was digested with XbaI and was inserted into the equivalent site of pJH081, resulting in plasmid pJH122.

pJH123

The up- and downstream regions flanking *vp2834* were amplified using primer pairs 2959/2960 and 2961/2962, respectively, using *V. parahaemolyticus* RIMD 2210633 chromosomal DNA as template. In a third PCR, using primers 2959/2962 and products of the first two PCR reactions as template, the flanking regions were fused together. The resulting product was digested with XbaI and was inserted into the equivalent site of pJH081, resulting in plasmid pJH123.

pJH124

The encoding sequence of *sfgfp was* amplified from a plasmid using primer pair 2064/2875. Primer 2875 includes the coding sequence of the FLAG tag. The resulting product was inserted into the XbaI/KpnI sites of pBAD33, resulting in plasmid pJH124.

pJH125

The encoding sequence of *sfgfp was* amplified from a plasmid using primer pair 1671/2845. Primer 2845 includes the coding sequence of the FLAG tag. The resulting product was inserted into the XbaI/SphI sites of pBAD33, resulting in plasmid pJH125.

4.4.10.2. List of plasmids

Table 10: List of plasmids

Plasmid	Description/genotype	Reference
pDM4	*mobRK2*, *oriR6K* (pir requiring), *sacBR* of *B. subtilis*	(Donnenberg *et al.*, 1991)
pBAD33	PBAD::	(Guzman *et al.*, 1995)
pET28b(+)	PT7::His6	Merck (Darmstadt)
pKNT25	PLAC::t25	(Karimova *et al.*, 1998)
pUT18	PLAC::t18	(Karimova *et al.*, 1998)
pKT25	PLAC::t25	(Karimova *et al.*, 1998)
pUT18C	PLAC::t18	(Karimova *et al.*, 1998)
pPM001	PBAD::*yfp-ftsZ* (*vp0464*)	(Muraleedharan *et al.*, 2018)
pJH070	PDM4::*Δvp0549*	This work
pJH081	PDM4::PLAC::*MCS-lacZα*	This work
pJH088	PDM4::*Δvp0548* (*vcsP*)	This work
pJH097	PTAC::*malE-vp0548*Δ1-129 (WT)	This work
pJH098	PTAC::*malE-vp0548*Δ1-129 (H175A)	This work
pJH100	PBAD::*vp0548-sfgfp*	This work
pJH101	PDM4::*Ωvp0548* H175A	This work
pJH102	PDM4::*Δvp1385*	This work

Plasmid	Description/genotype	Reference
pJH103	PDM4::*Δvpa1649*	This work
pJH104	PLAC::*vp0549-t18*	This work
pJH105	PLAC::*t18-vp0549*	This work
pJH106	PLAC::*vp0549-t25*	This work
pJH107	PLAC::*t25-vp0549*	This work
pJH108	PLAC::*t18-vp0548*Δ1-129	This work
pJH109	PLAC::*t25-vp0548*Δ1-129	This work
pJH110	PLAC::*vp0548-t18*	This work
pJH111	PLAC::*vp0548-t25*	This work
pJH112	PTAC::*malE-vp0548*(517-807) (WT)	This work
pJH113	PTAC::*malE-vp0548*(517-807) (H175A)	This work
pJH114	PT7::His6-*vp0549* (WT)	This work
pJH115	PT7::His6-*vp0549* (R9D)	This work
pJH116	PT7::*vp0548*Δ1-129-His6 (WT)	This work
pJH117	PT7::*vp0548*Δ1-129-His6 (H175A)	This work
pJH118	PT7::*vp0548*(517-807)-His6 (WT)	This work
pJH119	PT7::*vp0548*(517-807)-His6 (H175A)	This work
pJH120	PDM4::*Δvpa0517* (*shyA*)	This work
pJH121	PDM4::*Δvp2471* (*shyC*)	This work
pJH122	PDM4::Δvp2554 (*nlpD*)	This work
pJH123	PDM4::Δvp2834 (*envC*)	This work
pJH124	PBAD::*sfgfp*-FLAG	This work
pJH125	PBAD::*vp0548*-FLAG	This work

4.5 Biochemical methods

4.5.1 SDS polyacrylamide gel electrophoresis (SDS-PAGE)

To separate proteins under denaturing conditions SDS-PAGE with 12% or 15% polyacrylamide gels was performed. To denature proteins, the protein samples were mixed with loading buffer (10% (v/v) glycerol, 60 mM Tris-HCl pH 6.8, 2% (w/v) SDS, 100 mM DTT, 3 mM EDTA, 0.005% (w/v)

bromophenol blue) and heated for 10 min. at 98 °C before loading on the gel. Gel electrophoresis was performed in Bio-Rad electrophoresis chambers (Bio-Rad, München) at 120-150 V in 1x Tris/Glycine SDS (TGS) running buffer (Bio-Rad). Size of proteins was determined by comparison to the protein marker, the Color Pre-stained Protein Standard (New England Biolabs). Proteins were visualized by staining with Instant Blue protein staining solution (Expedeon).

4.5.2 Immonublot analysis

Protein solutions or proteins from cell extracts were separated in the gel by SDS-PAGE and transferred to a nitrocellulose membrane using „TransBlot® TurboTM Transfer System“ from Bio-Rad at 1.3 A, 25 V for 7 min with transfer buffer (300 mM Tris and 300 mM Glycin, and 0.05% SDS, pH 9.0). After transfer, the membrane was blocked in 5% non-fat milk powder (w/v) in 1 x TBST buffer (0.05% (v/v) Tween 20, 20 mM Tris-HCl, 137 mM NaCl pH 7.0) for 1 h or over night at 4 °C. After washing with 1 x TBST buffer, the primary antibody was added in proper dilutions in 1 x TBST supplemented with 2% non-fat milk powder over night at 4 °C. Next, membranes were washed again with 1 x TBST buffer and incubated with secondary antibody coupled with horseradish peroxidase (HRP) for 1h at 4 °C. After washing with 1 x TBST buffer the blot was developed with the Luminata Western HRP Substrate (Merck Millipore) and visualized with the luminescent image analyzer LAS-4000 (Fujifilm).

4.5.3 Co-immunoprecipitation and mass-spectroscopy

A minimum of three biological replicates were performed for each experiment. A single *V. parahaemolyticus* colony was inoculated into 5 ml LB medium, with the appropriate antibiotics and approximately 30 minutes later L-arabinose (for pBAD33 derivatives) was added to induce protein production. Upon reaching an OD of approximately 1.0, the cultures were diluted into 200 ml of LB already containing the antibiotics and inducers to an initial OD of 0.05. The cultures were grown until they reach an OD of 1.5 and afterwards harvested by centrifugation and the pellet was resuspended in 10 ml of lysis buffer (50 mM HEPES, 150 mM NaCl and 5 mM EDTA) pre-mixed with protease inhibitors (cOmplete EDTA free, Sigma-Aldrich). NP-40 (Sigma-Aldrich) was added to a final concentration of 0.5%. This was followed by ultrasonication to break open the cells (Amplitude 100%, three 20s pulses) after which the samples were incubated at 4 °C on an overhead rotator to

ensure uniform mixing. Immediately after this, another step of ultrasonication (same conditions) was performed, followed by centrifugation for 10 minutes. The supernatant was then mixed with 20 µl of anti-FLAG magnetic beads (Sigma-Aldrich) and incubated for an hour with rotation at 4 °C.

The beads were then washed four times with 700 µl of 100 mM ammoniumbicarbonate (Sigma-Aldrich). For elution, an on-bead digestion was performed by adding 200 µl trypsin-containing elution buffer 1 (1.0 M urea, 100 mM ammoniumbicarbonate, 1 µg trypsin (Promega)) to each sample. After 30 min shaking incubation (1400 rpm) at 30 °C, the supernatant containing digested proteins was collected. Beads were then washed twice with 80 µL of elution buffer 2 (1.0 M urea, 100 mM ammoniumbicarbonate, 5 mM Tris(2-carboxyethyl)phosphin (TCEP)) (Thermo Scientific) and the supernatant was added to the first elution fraction. Digestion was allowed to proceed overnight at 30°C.

Following digestion, the peptides were incubated with 10 mM iodoacetamide (IAA, Sigma-Aldrich) for 30 min at 25°C in the dark. The peptides were acidified with 1% trifluoroacetic acid (TFA, Thermo Scientific) and desalted using solid-phase extraction (SPE) on C18-Microspin columns (Harvard Apparatus). SPE columns were prepared by adding acetonitrile (ACN), followed by column equilibration with 0.1% TFA. Peptides were loaded on equilibrated Microspin columns and washed twice with 5% ACN/0.1% TFA. After peptide elution using 50% ACN/0.1% TFA, peptides were dried in a rotating concentrator (Thermo Scientific), reconstituted in 0.1% TFA, sonicated (Vial-Tweeter Sonotrode, Hielscher Ultrasonics) and subjected to liquid chromatography-mass spectrometry (LC-MS) analysis.

LC-MS analysis of the peptide samples was carried out on a Q-Exactive Plus instrument connected to an Ultimate 3000 RSLC nano and a nanospray flex ion source (Thermo Scientific). Peptide separation was performed on a reverse phase HPLC column (75 µm x 42 cm) packed in-house with C18 resin (2.4 µm). The peptides were loaded onto a PepMap 100 precolumn (Thermo Scientific) and then eluted by a linear ACN gradient from 2-35% solvent B over 60 minutes (solvent A: 0.15% formic acid; solvent B: 99.85% ACN in 0.15% formic acid). The following parameters were used for testing: a flow rate of 300 nl/min, spray voltage of 2.5 kV and heated capillary temperature of 300 °C. The peptides were analyzed in positive ion mode. Survey full-scan MS spectra (m/z = 375-1500) were acquired in the Orbitrap with a resolution of 70,000 full width at half maximum at a theoretical m/z 200 after accumulation of a maximum of 3 × 106 ions in the Orbitrap. Based on the survey scan, up to 10 most intense ions were subject to fragmentation using high collision dissociation (HCD) at

27% normalized collision energy. Fragmented spectra were acquired at a resolution of 17,500. The ion accumulation time was set to 50 ms for both MS survey and MS/MS scans. To increase the efficiency of MS/MS attempts, the charged state screening modus was enabled to exclude unassigned and singly charged ions. The dynamic exclusion duration was set to 30 sec.

The Perseus tool (Tyanova *et al.*, 2016) was employed to analyze the data obtained through LC-MS. The reference *V. parahaemolyticus* proteome was chosen and the replicates were grouped together to analyze variance. Furthermore, in order to generate volcano plots, the P-values were calculated using a standard Student's T-test and fold changes were generated upon comparison of the peptide levels of different bait and control samples.

4.5.4 Protein purification

To purify the proteins, the appropriate plasmids were introduced into *E. coli* BL21 (DE3) (Studier *et al.*, 1986). The cultures were grown in 0.5 l or 1 l LB or 2xTY medium containing appropriate antibiotics at 37 °C to an OD_{600} of 0.5-0.7. The protein expression was induced by addition of IPTG to a final concentration of 0.1 mM and cells were grown overnight at 18 °C.

The cells were harvested by centrifugation at 10 000 x rpm for 10 min at 4 °C and resuspended in 25 ml lysis buffer (50 mM Tris pH 8.0, 150 mM NaCl, 1 mM DTT, 10 mM imidazole, 10% glycerol) with added protease inhibitors (c0mplete Protease Inhibitor Cocktail Tablets, Roche). Cells were lysed using a French pressure cell and centrifuged at 20 000 rpm for 1h at 4 °C to collect cell debris. The supernatant containing soluble proteins was used for the protein purification.

His_6-tagged proteins were purified using Ni^{2+}-NTA-agarose columns (Qiagen) according to the manufacturers instructions. The supernatant was mixed with appropriate amounts of the beads and was loaded on a Pierce centrifuge column. After collecting the flow through, the column was washed twice with 20 ml lysis buffer with 20 mM imidazole. Bound protein was eluted with imidazol gradient from 50 mM to 500 mM in several steps.

MalE-tagged proteins were purified using amylose resin (New England Biolabs) according to the manufacturers instructions. The supernatant was mixed with appropriate amounts of the beads and was loaded on a Pierce centrifuge column. After collecting the flow through, the column was washed twice with 20 ml column buffer 1 (20mM Tris-HCL, pH 7.4; 0.2 M NaCl; 1mM DTT; 1 mM EDTA). Bound protein was eluted with column buffer 1 (added 10 mM Maltose) in several steps.

4.5.5 DRaCALA

C-di-GMP binding was determined using a DRaCALA assay (Differential Radial Capillary Action of Ligand Assay) with ^{32}P-labeled c-di-GMP. Briefly, ^{32}P-labeled c-di-GMP was prepared as described by (Skotnicka *et al.*, 2015), mixed with 20 µM protein and incubated for 10 min at room temperature in binding buffer (10 mM Tris, pH 8.0, 100 mM NaCl, 5 mM $MgCl_2$). 10 µl of this reaction mixture was transferred to a nitrocellulose filter (GE Healthcare), allowed to dry and imaged using a STORM 840 scanner (Amersham Biosciences) and Image Quant 5.2 software.

4.5.6 Bio-layer interferometry (BLI)

Interaction analyses of proteins of interest were performed in real time by bio-layer interferometry using the BLItz system (forteBio, USA). A Streptavidin SA biosensor (forteBio, USA) is incubated first with biotinylated c-di-GMP and afterwards with the protein of interest. While measuring the reflection of white light, some wavelengths show constructive or destructive interference. If the protein of interest binds c-di-GMP in this setup, binding-specific shifts in the interference pattern can be measured and quantified. The 500 nM biotinylated c-di-GMP in SEC buffer (20 mM Hepes-Na, pH 7.5, 200 mM NaCl, 20 mM MgCl2, 20 mM KCl) supplemented with 0.01% (wt/vol) Tween 20 was immobilized onto the biosensors for 120 s, and unbound molecules were washed off for 30 s with reaction buffer (25 mM HEPES/NaOH, pH 7.5, 150 mM NaCl, 10% [v/v] glycerol, 10 µM BSA, 0.01% [v/v] Triton X-100). The association and dissociation traces were recorded.

4.6 Oligonucleotides (primers)

Table 11: List of primers

Primer	Primer Name	Primer Sequence
580	pDM4-Plac+lacZ-cw	ataacaatttgtggaattcccgggagagctaacgcaattaatgtgagtt agctc
581	pDM4-Plac+lacZ-ccw	agtgtatatcaagcttatcgataccgtcgaaaataccgcatcaggcgcc attc

Primer	Primer Name	Primer Sequence
851	del-VP0549-a	gagctcaggttacccgcatgcaagatctatgagatgggtgacacagtg aa
852	del-VP0549-b	aggcgttgatttatttttcccctaatcttttctccgtcatattgc
853	del-VP0549-c	agagcgcaatatgacggagaaaagattaggggaaaaata aatcaa
854	del-VP0549-d	gagtacgcgtcactagtggggcccttctagttaagtgtgcgacctagaa a
1662	del-VP0548-a	cccccgcatgcacgcacatcatcgactaccg
1662	del-VP0548-a	cccccgcatgcacgcacatcatcgactaccg
1663	del-VP0548-b	gaatgacatcagttaataatcgtgatttttttagacataattattgt
1664	del-VP0548-c	acgattattaactgatgtcattc
1665	del-VP0548-d	ccccctctagactatcaggttaccaagtgaaagt
1667	T18-VP0548t-a	ccccctctagaggctgcatatttgaaccagcaacagattc
1668	T18-VP0548t-b	cccccggtacctcagttaataatcgtttcgttg
1669	T18-VP0549-a	ccccctctagaggctgcaacggagaaaagacgctttt
1670	T18-VP0549-b	cccccggtaccttatttttcccctaaatcagaa
1671	VP0548-T18-a	ccccctctagaatgtctaaaaaaatcatcatgcag
1671	VP0548-T18-a	ccccctctagaatgtctaaaaaaatcatcatgcag
1671	VP0548-T18-a	ccccctctagaatgtctaaaaaaatcatcatgcag
1672	VP0548-T18-b	cccccggtaccgctgcagcgttaataatcgtttcgttgttg
1673	VP0549-T18-a	ccccctctagaatgacggagaaaagacgct
1674	VP0549-T18-b	cccccggtaccgctgcagctttttcccctaaatcagaaagatg
1832	pET28b+His6-VP0549-a	ccccccccatggcccatcatcatcatcatcacacggagaaaagacgcttt t
1833	pET28b+His6-VP0549-b	cccccctcgagttatttttcccctaaatcagaa
1991	RC-VP0549_R9D-cw	ggagaaaagacgcttttcagatatcatctaccaagctcca
1992	RC-VP0549_R9D-ccw	tggagcttggtagatgatatctgaaaagcgtcttttctcc
2064	Sfgfp-vpa1044-a	cccccggtaccatgagcaaaggagaagaacttttc
2492	del-VP0549-2-c	atgtctaaaaaaatcatcatgcaga
2494	OM-VP0549-a	ctaccaagctccagctcagttag
2495	OM-VP0549-b	cgattcagaagttcgttattgcc
2496	OM-VP0549+VP0549-a	acatcggcattgaaagcattagc

Primer	Primer Name	Primer Sequence
2497	OM-VP0549+VP0549-b	ctgattatgaatctgttgctggt
2498	OM-VP0548-a	cggcagctatagattctgcggtt
2499	OM-VP0548-b	tgacattgaacttgttcaagtga
2597	RC-VP0548-H175A-a	ctcaggcagaagacacgtggccaccggtatcgatttgacc
2598	RC-VP0548-H175A-b	ggtcaaatcgataccggtggccacgtgtcttctgcctgag
2729	linker-sfGFP cw	gacatcctcgagctcatgagcaaaggagaagaacttttcac
2730	sfGFP+stop ccw	Cccccgcatgcttatttgtagagctcatccatgccatg
2844	VP0548-[linker-sfGFP] ccw	tgctcatgagctcgaggatgtcgttaataatcgtttcgttgttgt
2845	VP0548-FLAG ccw	cccgcatgcttatttatcatcatcatctttgtaatcgttaataatcgtttcgttgttgt
2860	del-vpa1649-a	ccctctagaatccgtcaaacagatcgatc
2861	del-vpa1649-b	gtcaatctggacgtcgttttcatgtcgtaatgatcgtattct
2862	del-vpa1649-c	aaaacgacgtccagattgac
2863	del-vpa1649-d	ccctctagatttgaatcgcaggtggatc
2865	del-vp1385-a	ccctctagaattggtgtggtttcattgaca
2866	del-vp1385-b	gaattatggtttggctaaatgaaaactgtgcttagaag
2867	del-vp1385-c	gccaaaccataattccgga
2868	del-vp1385-d	ccctctagaattggattggtgttttctatca
2875	sfGFP-FLAG-STOP-ccw	ccctctagattatttatcatcatcatctttgtaatctttgtagagctcatccatgc
2879	VP0548-HIS6-b (pET28b+)	cccctcgaggttaataatcgtttcgttgttgt
2959	del-vp2834-a	ccctctagaagagcaagagcctatgttgg
2960	del-vp2834-b	tgggtgattttgttttcgcac
2961	del-vp2834-c	gcgaaaacaaaatcacccattacctgacttatttacttgtag
2962	del-vp2834-d	ccctctagagtttagagcaagcattggct
2971	ins-vp0548-SD-luc8-e	tgtcattcgcttgaaatagaaag
2985	ins-vp0548-sfGFP-b	gcatgatgatttttttagacataattattgttacttaaataggcgtt
3042	ins-vp0548-H175A-d	ttcaagcgaatgacagttaataatcgtttcgttgttg
3081	del-vpa0517-a	ccctctagagagtgtatgcggtgatcctatt
3082	del-vpa0517-b	taagagcctaaacaggggaattactatctcctttcaaac
3083	del-vpa0517-c	ctgtttaggctcttaatcgaaac

Primer	Primer Name	Primer Sequence
3084	del-vpa0517-d	ccctctagactgaaagtcatgagctttacgtg
3086	del-vp2471-a	cccgcatgccgtctagaccaacaagaagc
3087	del-vp2471-b	ttttttacttttccgtgaggtacttgattgctaaattaa
3088	del-vp2471-c	acggaaaagtaaaaagaggca
3089	del-vp2471-d	cccgcatgcgcctataaccaactttgctc
3115	vp0548-HIS-trunk-a	ccatggcctatttgaaccagcaacagattc
3120	del-vp2554-a	ccctctagaatccgcgtgggcatgatatc
3121	del-vp2554-b	aagttgtttttcaaagtcctaacctcagatccttaagcc
3122	del-vp2554-c	gactttgaaaaacaacttgcgaaa
3123	del-vp2554-d	ccctctagagatgtcatcatcttgagtcgac
3167	pMAL-c2x-vp0548t-a	cccgaattctatttgaaccagcaacagattc
3168	pMAL-c2x-vp0548t-b	ccctctagatcagttaataatcgtttcgttgt
3177	vp0548-M23-HIS-a	cccccatggcccacgtgcataccggtatcg
3178	vp0548-M23-HIS-b	cccctcgagagggttaagtgtgcgacct
3178	vp0548-M23-HIS-b	cccctcgagagggttaagtgtgcgacct
3179	pMAL-c2x-vp0548-M23-a	cccgaattccacgtgcataccggtatcg
3180	pMAL-c2x-vp0548-M23-b	ccctctagatcaagggttaagtgtgcgacct
3180	pMAL-c2x-vp0548-M23-b	ccctctagatcaagggttaagtgtgcgacct
3181	vp0548-M23-H175A-HIS-a	cccccatggcccacgtggctaccggtatcg
3182	pMAL-c2x-vp0548-H175A-M23-a	cccgaattccacgtggctaccggtatcg

4.7 Microscopy

4.7.1 Phase contrast (fluorescence) Microscopy

Phase contrast fluorescence microscopy of *V. parahaemolyticus* cells was carried out in several steps: 5 mL LB supplemented with the required antibiotic was inoculated with a colony of cells harboring the relevant plasmid and grown to OD600 = 0.1 at 37 °C; then expression of fluorescent fusion proteins was induced by adding L-arabinose to a final concentration of 0.2 %. The cultures were incubated for an additional 2 h. Afterwards cell culture was mounted onto agarose pads (1%

agarose, 20% PBS, 10% LB) on microscope slides. For non-fluorescent microscopy, cell cultures were grown to an OD_{600} of 1.5 and then imaged. The cell were mounted onto an agarose pad and imaged in phase contrast using the Zeiss Axio Imager M1, with a Zeiss αPlan-Fluar 100x/1.45 Oil DIC objective (Carl Zeiss AG) and equipped with a Cascade:1K CCD camera (Photometrics).

4.7.2 Image analysis

Image analysis was carried out essentially as described by (Heering and Ringgaard, 2016; Alvarado et al., 2017; Heering et al., 2017). DIC/PH3 and the corresponding fluorescent channel were loaded in MetaMorph Offline (Molecular Devices) for analysis. Cells were marked using the Multi-line tool to acquire cell length measurements. In addition, the number of constrictions and foci were noted for each cell. The sample size is indicated in the figure description. All images´ scale bar corresponds to 5 µm. Statistical analyses and plots were generated using GraphPad Prism, v6.07, software (Prism Software, Irvine, CA).

4.7.3 Transmission electron microscopy

V. parahaemolyticus strains were grown in LB to an OD_{600} of 0.5, a volume of 200µl harvested by gentle centrifugation (5min at 5000xg) and carefully resuspended in 50µl LB. Aliquots of 3 µl were directly applied to a plasma-cleaned R2/2 copper Quantifoil grid (Quantifoil Micro Tools, Jena, Germany). Grids were plunge frozen using a Leica EM GP (Leica microsystems, Wetzlar, Germany) grid plunger. Blotting time was set to 1 s at 20°C and 95% humidity. Grids were stored in liquid nitrogen until imaging.

Transmission electron microscopy images were recorded using the Talos L120C (Thermo Scientific™) microscope equipped with a 4k × 4k Ceta CMOS camera. Acceleration voltage was set to 120kV and magnification as indicated in the figure panels.

4.8 Peptidoglycan purification and analysis

Peptidoglycan (PG) samples were analyzed as described previously (Desmarais *et al.*, 2013; Alvarez *et al.*, 2016). In brief, samples were boiled in SDS 5% for 2h and saccule were repeatedly washed

with MilliQ water by ultracentrifugation (110.000 rpm, 10 min, 20 °C). The samples were treated with muramidase (100 µg/mL) for 15 hours at 37 °C. Muramidase digestion was stopped by boiling and, coagulated proteins were removed by centrifugation (10 min, 14.000 rpm). The supernatants were first adjusted to pH 8.5-9.0 with sodium borate buffer and then sodium borohydride was added to a final concentration of 10 mg/mL. After reduction for 30 min at room temperature, the samples pH was adjusted to pH 3.5 with orthophosphoric acid.

UPLC analyses of muropeptides were performed on a Waters UPLC system (Waters Corporation, USA) equipped with an ACQUITY UPLC BEH C18 Column, 130Å, 1.7 µm, 2.1mm X 150mm (Waters, USA) and a dual wavelength absorbance detector. Elution of muropeptides was detected at 204 nm. Muropeptides were separated at 45 °C using a linear gradient from buffer A (formic acid 0.1% in water) to buffer B (formic acid 0.1% in acetonitrile) in a 18 minutes run, with a 0.25 mL/min flow.

Relative total PG amounts were calculated by comparison of the total intensities of the chromatograms (total area) from three biological replicas normalized to the same OD_{600} and extracted with the same volumes. Quantification of muropeptides was based on their relative abundances (relative area of the corresponding peak) normalized to their molar ratio.

4.9 Bioinformatics Analysis

Nucleotide and amino acid sequences were obtained from the national center for biotechnology information (NCBI) (Ostell *et al.*, 1998) and the KEGG2 database (Ogata *et al.*, 1999). Sequence alignments were conducted using the BlastN- or BlastP-algorithm at NCBI or ClustalOmega (Sievers *et al.*, 2014). Conserved domains of proteins were identified using the SMART database (Schultz *et al.*, 1998).

The phylogenetic tree was generated using BlastP algorithm on the KEGG2 database with an E-value threshold 10.0 with 200 results for VcsP, NlpD and ShyA as reference sequences. Taxonomic lineage as well as 5000bp up-/downstream sequences were extracted from the KEGG2 database based on the BlastP results. Clustal Omega was used to generate the multiple sequence alignment as well as the phylogenetic tree using standard settings. “Percent identity matrix” was also generated using the Clustal Omega tool. iTol phyl. tree visualization (Letunic *et al.*, 2019) tool was used to customize the phylogenetic tree and add additional information. Microsoft Excel software was used to extract conserved motif from the provided protein sequences as well as to extract the “percent identity score” values.

5 Supplementary Materials

Table 12: Significantly enriched proteins in a Co-IP experiment

Statistically significantly (FDR=0.01 S0=0.2) enriched proteins in either bait (VcsP-FLAG) or control (sfGFP-FLAG) Co-IP experiment.

Protein	Bait VS. Control log_2(FC)	Description
VP0548	11.0	Putative ToxR-activated protein TagE
RNE	7.5	Ribonuclease E
GroL1	2.4	60 kDa chaperonin 1
PNP	6.5	Polyribonucleotide nucleotidyltransferase
GroL2	3.4	60 kDa chaperonin 2
ENO	1.5	Enolase
AtpA	1.0	ATP synthase subunit alpha
DnaJ	2.3	Chaperone protein DnaJ
RplA	0.8	50S ribosomal protein L1
VP0921	2.4	Peptidylprolyl isomerase
RhlB	7.2	ATP-dependent RNA helicase RhlB
AtpH	1.2	ATP synthase subunit delta
VP0018	2.8	16 kDa heat shock protein A
SecD	2.1	Protein translocase subunit SecD
VP0485	4.9	Uncharacterized protein
VP1440	1.5	Uncharacterized protein
BamA	2.7	Outer membrane protein assembly factor BamA
VP1014	2.2	ATP-dependent Clp protease, ATP-binding subunit ClpA
Ffh	1.7	Signal recognition particle protein
VP0610	2.2	Uncharacterized protein
VPA0921	2.8	NAD(P) transhydrogenase subunit beta
HflC	1.3	Protein HflC
VP0107	1.2	DNA polymerase I

Protein	Bait VS. Control log_2(FC)	Description
VP0434	1.0	Uncharacterized protein
MalT	1.5	HTH-type transcriptional regulator MalT
VP2935	1.8	RNA-binding protein
GFP	-4.9	Green fluorescent protein
RplK	-0.8	50S ribosomal protein L11
VP2833	-1.7	Serine acetyltransferase
VP1380	-2.2	Uncharacterized protein
VP0712	-3.1	Uncharacterized protein
VP0598	-3.1	Iron-binding protein IscA
VP0567	-2.1	Putative protease
AcpP	-1.9	Acyl carrier protein
VP1949	-2.2	UPF0263 protein VP1949
MnmG	-2.5	tRNA uridine 5-carboxymethylaminomethyl modification enzyme MnmG
MsrA	-1.8	Peptide methionine sulfoxide reductase MsrA
RibA	-2.8	GTP cyclohydrolase-2
VPA1175	-2.6	Putative thiosulfate sulfurtransferase SseA
GlpE	-2.5	Thiosulfate sulfurtransferase GlpE
SthA	-2.5	Soluble pyridine nucleotide transhydrogenase

Table 13: Muropeptide analysis experiment 1

Analysis of purified PG from wildtype and Δ*vcsP* strains, with average (AVG) amounts in percent and standard deviation (SD) from three experimental replicates.

Muropeptide	**wildtype**		**Δ*vcsP***	
	AVG	**SD**	**AVG**	**SD**
M3 (%)	7.24	0.50	4.54	1.14
$M4^{G}$ (%)	2.83	0.07	2.04	0.27
M4 (%)	63.49	4.03	55.34	1.82
M2 (%)	5.81	3.79	4.28	2.27
$M3^{Lpp}$ (%)	2.00	0.29	1.37	0.22
D33 (%)	0.43	0.02	0.41	0.04
D43 (%)	0.00	0.00	4.87	0.73
D34 (%)	0.48	0.04	0.94	0.12
D44 (%)	13.14	0.25	17.93	1.71
D45 (%)	0.32	0.01	0.56	0.07
$M4^{Anh}$ (%)	0.64	0.09	0.72	0.06
T344 (%)	0.04	0.04	1.54	0.84
T444 (%)	0.59	0.06	0.77	0.17
$D44^{Anh}$ (%)	2.73	0.31	5.13	0.49
$T444^{Anh}$ (%)	0.27	0.04	0.39	0.09
Total (%)	100	13.37	122.98	14.73
Monomers (%)	82.01	0.49	68.28	3.91
Dimers (%)	17.10	0.53	29.03	3.50
Trimers (%)	0.90	0.08	2.70	0.92
Anhydro (%)	3.64	0.33	6.25	0.48
Chain length (units)	27.72	2.49	16.11	1.26
Total Crosslink (%)	18.90	0.47	34.42	4.48
LD-crosslink (%)	1.20	0.44	4.08	1.54
DD-crosslink (%)	17.70	0.63	30.00	3.63

Table 14: Muropeptide analysis experiment 2

Analysis of purified PG from wildtype and *vcsP* H175A strains, with average (AVG) amounts in percent and standard deviation (SD) from three experimental replicates.

Muropeptide	**wildtype**		***vcsP* H175A**	
	AVG	**SD**	**AVG**	**SD**
M3 (%)	5.65	0.19	2.52	0.40
$M4^{G}$ (%)	3.32	0.32	2.61	0.27
M4 (%)	55.30	0.32	45.71	1.19
M2 (%)	1.73	0.15	2.12	0.12
$M3^{Lpp}$ (%)	1.75	0.09	1.18	0.35
D33 (%)	1.12	0.04	1.11	0.20
D43 (%)	0.96	0.03	4.08	1.42
D34 (%)	0.49	0.35	2.26	0.17
D44 (%)	22.26	0.39	25.71	0.59
D45 (%)	0.00	0.00	0.45	0.33
$M4^{Anh}$ (%)	0.56	0.05	0.86	0.06
T344 (%)	0.06	0.09	1.68	0.19
T444 (%)	1.35	0.05	1.72	0.17
$D44^{Anh}$ (%)	4.62	0.12	7.11	0.16
$T444^{Anh}$ (%)	0.48	0.34	1.86	0.32
Total (%)	100	9.51	134.5	10.07
Monomers (%)	66.50	0.75	54.66	1.04
Dimers (%)	29.78	0.16	40.15	1.38
Trimers (%)	1.90	0.44	4.84	0.56
Anhydro (%)	5.66	0.25	9.84	0.46
Chain length (units)	17.69	0.81	10.19	0.49
Total Crosslink (%)	33.59	0.86	49.83	2.32
LD-crosslink (%)	1.73	0.17	5.31	2.00
DD-crosslink (%)	31.86	1.01	44.52	0.84

Table 15: Muropeptide analysis experiment 3

Analysis of purified PG from wildtype, Δ*vpa1649* and Δ*vp1385* strains, with average (AVG) amounts in percent and standard deviation (SD) from three experimental replicates.

Muropeptide	**wildtype**		**Δ*vpa1649***		**Δ*vp1385***	
	AVG	**SD**	**AVG**	**SD**	**AVG**	**SD**
M3 (%)	7.90	0.05	7.10	0.24	4.31	0.22
$M4^{G}$ (%)	3.32	0.09	3.54	0.13	2.39	0.12
M4 (%)	54.19	0.76	55.46	0.16	46.49	2.68
M2 (%)	1.07	0.04	1.05	0.06	0.71	0.03
$M3^{Lpp}$ (%)	1.79	0.02	1.63	0.02	1.42	0.04
D33 (%)	0.95	0.07	1.01	0.03	0.85	0.07
D43 (%)	0.18	0.25	0.00	0.00	8.69	1.18
D34 (%)	0.93	0.11	0.83	0.05	0.88	0.13
D44 (%)	21.51	0.63	21.98	0.63	17.33	1.80
D45 (%)	0.77	0.06	0.78	0.22	0.99	0.28
$M4^{Anh}$ (%)	0.00	0.00	0.00	0.00	4.55	1.80
T344 (%)	0.36	0.01	0.19	0.13	3.87	1.53
T444 (%)	1.37	0.06	1.16	0.17	1.57	0.49
$D44^{Anh}$ (%)	4.89	0.08	4.74	0.26	5.13	0.08
$T444^{Anh}$ (%)	0.77	0.16	0.54	0.24	0.86	0.14
Total (%)	100.00	1.49	112.80	2.62	98.22	4.97
Monomers (%)	66.48	0.77	67.15	0.36	58.43	1.25
Dimers (%)	29.23	0.56	29.34	0.17	33.85	0.88
Trimers (%)	2.49	0.21	1.88	0.49	6.30	2.16
Anhydro (%)	5.65	0.24	5.28	0.50	10.54	2.02
Chain length (units)	17.72	0.74	19.10	1.69	9.85	1.88
Total Crosslink (%)	34.21	0.95	33.10	0.83	46.45	3.44
LD-crosslink (%)	2.60	0.12	2.21	0.25	9.46	3.00
DD-crosslink (%)	31.61	0.83	30.90	0.64	37.00	0.43

Table 15: Muropeptide analysis experiment 3, continued

Analysis of purified PG from wildtype, Δ*vpa1649* and Δ*vp1385* strains, with average (AVG) amounts in percent and standard deviation (SD) from three experimental replicates.

Muropeptide	***Δvpa1649 Δvp1385***		***ΔvcsP Δvp1385 Δvpa1649***	
	AVG	**SD**	**AVG**	**SD**
M3 (%)	1.17	0.05	1.25	0.13
$M4^{G}$ (%)	1.23	0.33	1.38	0.07
M4 (%)	42.40	0.21	36.86	0.60
M2 (%)	1.43	0.31	1.11	0.02
$M3^{Lpp}$ (%)	0.16	0.16	0.37	0.04
D33 (%)	0.00	0.00	0.00	0.00
D43 (%)	10.04	0.97	11.56	1.08
D34 (%)	0.91	0.25	1.14	0.30
D44 (%)	13.64	2.25	16.52	2.71
D45 (%)	0.30	0.30	0.98	0.30
$M4^{Anh}$ (%)	6.46	0.31	6.54	0.84
T344 (%)	5.92	0.69	8.36	0.32
T444 (%)	2.34	0.54	3.04	0.60
$D44^{Anh}$ (%)	11.76	0.00	8.98	1.04
$T444^{Anh}$ (%)	2.27	0.34	1.90	0.52
Total (%)	134.96	2.65	139.44	2.76
Monomers (%)	52.68	1.21	47.15	0.25
Dimers (%)	36.64	1.23	39.17	0.80
Trimers (%)	10.53	0.18	13.31	0.93
Anhydro (%)	20.48	0.65	17.41	1.91
Chain length (units)	4.89	0.16	5.81	0.59
Total Crosslink (%)	57.70	0.87	65.79	1.10
LD-crosslink (%)	12.76	1.64	17.86	0.64
DD-crosslink (%)	31.61	0.83	30.90	0.64

6 References

Aaron, M. *et al.* (2007) 'The tubulin homologue FtsZ contributes to cell elongation by guiding cell wall precursor synthesis in *Caulobacter crescentus*', *Molecular Microbiology*, 64(4), pp. 938–952. doi: 10.1111/j.1365-2958.2007.05720.x.

Abel, S. *et al.* (2013) 'Bi-modal Distribution of the Second Messenger c-di-GMP Controls Cell Fate and Asymmetry during the *Caulobacter* Cell Cycle', *PLoS Genetics*, 9(9), p. e1003744. doi: 10.1371/journal.pgen.1003744.

Adams, D. W. and Errington, J. (2009) 'Bacterial cell division: assembly, maintenance and disassembly of the Z ring', *Nat Rev Microbiol*, 7(9), pp. 642–653. doi: 10.1038/nrmicro2198.

Alberti, L. and Harshey, R. M. (1990) 'Differentiation of *Serratia marcescens 274* into swimmer and swarmer cells.', *Journal of Bacteriology*, 172(8), pp. 4322–4328. doi: 10.1128/jb.172.8.4322-4328.1990.

Alexander, C. and Rietschel, E. T. (2001) 'Bacterial lipopolysaccharides and innate immunity.', *Journal of endotoxin research*, 7(3), pp. 167–202.

Altschul, S. F. *et al.* (1990) 'Basic local alignment search tool', *J Mol Biol*, 215(3), pp. 403–410. doi: 10.1016/S0022-2836(05)80360-2.

Alvarez, L. *et al.* (2016) 'Ultra-Sensitive, High-Resolution Liquid Chromatography Methods for the High-Throughput Quantitative Analysis of Bacterial Cell Wall Chemistry and Structure', in *Methods in Molecular Biology*, pp. 11–27. doi: 10.1007/978-1-4939-3676-2_2.

Alyahya, S. A. *et al.* (2009) 'RodZ, a component of the bacterial core morphogenic apparatus', *Proceedings of the National Academy of Sciences*, 106(4), pp. 1239–1244. doi: 10.1073/pnas.0810794106.

An, D. R. *et al.* (2016) 'Structural Basis of the Heterodimer Formation between Cell Shape-Determining Proteins Csd1 and Csd2 from *Helicobacter pylori*', *PLOS ONE*. Edited by E. A. Permyakov, 11(10), p. e0164243. doi: 10.1371/journal.pone.0164243.

Apweiler, R. *et al.* (2004) 'UniProt: the Universal Protein knowledgebase', *Nucleic Acids Res*, 32(Database issue), pp. D115-9. doi: 10.1093/nar/gkh131.

Arends, S. J. R., Kustusch, R. J. and Weiss, D. S. (2009) 'ATP-Binding Site Lesions in FtsE Impair Cell Division', *Journal of Bacteriology*, 191(12), pp. 3772–3784. doi: 10.1128/JB.00179-09.

Arnold, T. M., Forrest, G. N. and Messmer, K. J. (2007) 'Polymyxin antibiotics for gram-negative infections', *American Journal of Health-System Pharmacy*, 64(8), pp. 819–826. doi: 10.2146/ajhp060473.

Arora, A. *et al.* (2000) 'Refolded Outer Membrane Protein A of *Escherichia coli* Forms Ion Channels with Two

Conductance States in Planar Lipid Bilayers', *Journal of Biological Chemistry*, 275(3), pp. 1594–1600. doi: 10.1074/jbc.275.3.1594.

Babu, M. M. *et al.* (2006) 'A Database of Bacterial Lipoproteins (DOLOP) with Functional Assignments to Predicted Lipoproteins', *Journal of Bacteriology*, 188(8), pp. 2761–2773. doi: 10.1128/JB.188.8.2761-2773.2006.

Bartlett, T. M. *et al.* (2017) 'A Periplasmic Polymer Curves Vibrio cholerae and Promotes Pathogenesis', *Cell*, 168(1–2), p. 172–185.e15. doi: 10.1016/j.cell.2016.12.019.

Beacham, I. R. (1979) 'Periplasmic enzymes in gram-negative bacteria', *International Journal of Biochemistry*. Elsevier, 10(11), pp. 877–883.

Behrens, S. (2001) 'The SurA periplasmic PPIase lacking its parvulin domains functions in vivo and has chaperone activity', *The EMBO Journal*, 20(1), pp. 285–294. doi: 10.1093/emboj/20.1.285.

Benach, J. *et al.* (2007) 'The structural basis of cyclic diguanylate signal transduction by PilZ domains', *The EMBO Journal*, 26(24), pp. 5153–5166. doi: 10.1038/sj.emboj.7601918.

Bendezú, F. O. *et al.* (2009) 'RodZ (YfgA) is required for proper assembly of the MreB actin cytoskeleton and cell shape in *E. coli*', *The EMBO Journal*, 28(3), pp. 193–204. doi: 10.1038/emboj.2008.264.

Berendt, S. *et al.* (2012) 'Cell Wall Amidase AmiC1 Is Required for Cellular Communication and Heterocyst Development in the Cyanobacterium *Anabaena PCC 7120* but Not for Filament Integrity', *Journal of Bacteriology*, 194(19), pp. 5218–5227. doi: 10.1128/JB.00912-12.

Berg, B. van den *et al.* (2004) 'X-ray structure of a protein-conducting channel', *Nature*, 427(6969), pp. 36–44. doi: 10.1038/nature02218.

Berks, B. C., Palmer, T. and Sargent, F. (2003) 'The Tat protein translocation pathway and its role in microbial physiology', in *Advances in Microbial Physiology*, pp. 187–254. doi: 10.1016/S0065-2911(03)47004-5.

Bernhardt, T. G. and de Boer, P. A. J. (2005) 'SlmA, a Nucleoid-Associated, FtsZ Binding Protein Required for Blocking Septal Ring Assembly over Chromosomes in *E. coli*', *Molecular Cell*, 18(5), pp. 555–564. doi: 10.1016/j.molcel.2005.04.012.

Bernhardt, T. G. and De Boer, P. A. J. (2003) 'The *Escherichia coli* amidase AmiC is a periplasmic septal ring component exported via the twin-arginine transport pathway', *Molecular Microbiology*, 48(5), pp. 1171–1182. doi: 10.1046/j.1365-2958.2003.03511.x.

Bernhardt, T. G. and De Boer, P. A. J. (2004) 'Screening for synthetic lethal mutants in *Escherichia coli* and identification of EnvC (YibP) as a periplasmic septal ring factor with murein hydrolase activity', *Molecular Microbiology*, 52(5), pp. 1255–1269. doi: 10.1111/j.1365-2958.2004.04063.x.

Bernstein, H. D. (2000) 'The biogenesis and assembly of bacterial membrane proteins', *Current Opinion in Microbiology*, 3(2), pp. 203–209. doi: 10.1016/S1369-5274(00)00076-X.

Bitto, E. and McKay, D. B. (2003) 'The Periplasmic Molecular Chaperone Protein SurA Binds a Peptide Motif That Is Characteristic of Integral Outer Membrane Proteins', *Journal of Biological Chemistry*, 278(49), pp. 49316–49322. doi: 10.1074/jbc.M308853200.

Bochtler, M. *et al.* (2004) 'Similar active sites in lysostaphins and D-Ala-D-Ala metallopeptidases.', *Protein science : a publication of the Protein Society*, 13(4), pp. 854–861. doi: 10.1110/ps.03515704.

Boël, G. *et al.* (2014) 'The ABC-F protein EttA gates ribosome entry into the translation elongation cycle', *Nature Structural & Molecular Biology*, 21(2), pp. 143–151. doi: 10.1038/nsmb.2740.

Bonis, M. *et al.* (2010) 'A M23B family metallopeptidase of *Helicobacter pylori* required for cell shape, pole formation and virulence', *Molecular Microbiology*, 78(4), pp. 809–819. doi: 10.1111/j.1365-2958.2010.07383.x.

Bornikoel, J. *et al.* (2018) 'LytM factor Alr3353 affects filament morphology and cell-cell communication in the multicellular cyanobacterium *Anabaena sp. PCC 7120*', *Molecular Microbiology*, 108(2), pp. 187–203. doi: 10.1111/mmi.13929.

Bratton, B. P. *et al.* (2018) 'MreB polymers and curvature localization are enhanced by RodZ and predict *E. coli*'s cylindrical uniformity', *Nature Communications*, 9(1), p. 2797. doi: 10.1038/s41467-018-05186-5.

Budd, A. *et al.* (2004) 'Bacterial α2-macroglobulins: colonization factors acquired by horizontal gene transfer from the metazoan genome?', *Genome biology*, 5(1), p. R38.

Buist, G. *et al.* (2008) 'LysM, a widely distributed protein motif for binding to (peptido)glycans', *Molecular Microbiology*, 68(4), pp. 838–847. doi: 10.1111/j.1365-2958.2008.06211.x.

Cabeen, M. T. and Jacobs-Wagner, C. (2005) 'Bacterial cell shape', *Nat.Rev.Microbiol.*, 3(8), pp. 601–610. doi: 10.1038/nrmicro1205.

Carlos, J. L. *et al.* (2002) 'Bacterial Type I Signal Peptidases', in *Enzymes*, pp. 27–55. doi: 10.1016/S1874-6047(02)80003-8.

Carpousis, A. J. (2007) 'The RNA Degradosome of *Escherichia coli* : An mRNA-Degrading Machine Assembled on RNase E', *Annual Review of Microbiology*, 61(1), pp. 71–87. doi: 10.1146/annurev.micro.61.080706.093440.

Cava, F. *et al.* (2011) 'Distinct pathways for modification of the bacterial cell wall by non-canonical D-amino acids', *The EMBO Journal*, 30(16), pp. 3442–3453. doi: 10.1038/emboj.2011.246.

Chambers, H. F. (2003) 'Solving *Staphylococcal* resistance to β-lactams', *Trends in Microbiology*, 11(4), pp.

145–148. doi: 10.1016/S0966-842X(03)00046-5.

Chao, G. *et al.* (2010) 'Distribution of Genes Encoding Four Pathogenicity Islands (VPaIs), T6SS, Biofilm, and Type I Pilus in Food and Clinical Strains of *Vibrio parahaemolyticus* in China', *Foodborne Pathogens and Disease*, 7(6), pp. 649–658. doi: 10.1089/fpd.2009.0441.

Chen, R. and Henning, U. (1996) 'Aperiplasmic protein (Skp) of *Escherichia coli* selectively binds a class of outer membrane proteins', *Molecular Microbiology*, 19(6), pp. 1287–1294. doi: 10.1111/j.1365-2958.1996.tb02473.x.

Cho, H. *et al.* (2016) 'Bacterial cell wall biogenesis is mediated by SEDS and PBP polymerase families functioning semi-autonomously', *Nature Microbiology*, 1(10), p. 16172. doi: 10.1038/nmicrobiol.2016.172.

Cho, H., Uehara, T. and Bernhardt, T. G. (2014) 'Beta-Lactam Antibiotics Induce a Lethal Malfunctioning of the Bacterial Cell Wall Synthesis Machinery', *Cell*, 159(6), pp. 1300–1311. doi: 10.1016/j.cell.2014.11.017.

Chung, C. T., Niemela, S. L. and Miller, R. H. (1989) 'One-Step Preparation of Competent *Escherichia coli* - Transformation and Storage of Bacterial-Cells in the Same Solution', *Proc Natl Acad Sci U S A*, 86(7), pp. 2172–2175. doi: DOI 10.1073/pnas.86.7.2172.

Cohen, D. N. *et al.* (2009) 'Shared Catalysis in Virus Entry and Bacterial Cell Wall Depolymerization', *Journal of Molecular Biology*, 387(3), pp. 607–618. doi: 10.1016/j.jmb.2009.02.001.

Confer, A. W. and Ayalew, S. (2013) 'The OmpA family of proteins: Roles in bacterial pathogenesis and immunity', *Veterinary Microbiology*, 163(3–4), pp. 207–222. doi: 10.1016/j.vetmic.2012.08.019.

Cookson, B. T. *et al.* (1989) 'Biological activities and chemical composition of purified tracheal cytotoxin of *Bortella pertussis*', *Infection and Immunity*, 57(7), pp. 2223–2229.

Corbin, B. D. *et al.* (2007) 'Interaction between Cell Division Proteins FtsE and FtsZ', *Journal of Bacteriology*, 189(8), pp. 3026–3035. doi: 10.1128/JB.01581-06.

Cowan, S. W. *et al.* (1992) 'Crystal structures explain functional properties of two *E. coli* porins', *Nature*, 358(6389), pp. 727–733. doi: 10.1038/358727a0.

Crawshaw, A. D. *et al.* (2014) 'A mother cell-to-forespore channel: Current understanding and future challenges', *FEMS Microbiology Letters*, pp. 129–136. doi: 10.1111/1574-6968.12554.

Daniel, R. A. and Errington, J. (2003) 'Control of Cell Morphogenesis in Bacteria', *Cell*, 113(6), pp. 767–776. doi: 10.1016/S0092-8674(03)00421-5.

Daniels, N. A. *et al.* (2000) '*Vibrio parahaemolyticus* Infections in the United States, 1973–1998', *The Journal of Infectious Diseases*. Oxford University Press, 181(5), pp. 1661–1666. doi: 10.1086/315459.

DePamphilis, M. L. and Adler, J. (1971) 'Fine structure and isolation of the hook-basal body complex of flagella

from *Escherichia coli* and *Bacillus subtilis*.', *Journal of Bacteriology*, 105(1), pp. 384–395.

Derouaux, A. *et al.* (2008) 'The Monofunctional Glycosyltransferase of *Escherichia coli* Localizes to the Cell Division Site and Interacts with Penicillin-Binding Protein 3, FtsW, and FtsN', *Journal of Bacteriology*, 190(5), pp. 1831–1834. doi: 10.1128/JB.01377-07.

Desmarais, S. M. *et al.* (2013) 'Peptidoglycan at its peaks: how chromatographic analyses can reveal bacterial cell wall structure and assembly', *Molecular Microbiology*, 89(1), pp. 1–13. doi: 10.1111/mmi.12266.

Desvaux, M. *et al.* (2006) 'Protein cell surface display in Gram-positive bacteria: from single protein to macromolecular protein structure', *FEMS Microbiology Letters*, 256(1), pp. 1–15. doi: 10.1111/j.1574-6968.2006.00122.x.

Deutscher, M. P. (2006) 'Degradation of RNA in bacteria: comparison of mRNA and stable RNA', *Nucleic Acids Research*, 34(2), pp. 659–666. doi: 10.1093/nar/gkj472.

Dominguez-Escobar, J. *et al.* (2011) 'Processive Movement of MreB-Associated Cell Wall Biosynthetic Complexes in Bacteria', *Science*, 333(6039), pp. 225–228. doi: 10.1126/science.1203466.

Domínguez-Gil, T. *et al.* (2016) 'Activation by Allostery in Cell-Wall Remodeling by a Modular Membrane-Bound Lytic Transglycosylase from *Pseudomonas aeruginosa*', *Structure*, 24(10), pp. 1729–1741. doi: 10.1016/j.str.2016.07.019.

Donnenberg, M. S. and Kaper, J. B. (1991) 'Construction of an eae deletion mutant of enteropathogenic *Escherichia coli* by using a positive-selection suicide vector.', *Infection and immunity*.

Dörr, T. *et al.* (2013) 'Substrate specificity of an elongation-specific peptidoglycan endopeptidase and its implications for cell wall architecture and growth of *Vibrio cholerae*', *Molecular Microbiology*, 89(5), pp. 949–962. doi: 10.1111/mmi.12323.

Dörr, T. *et al.* (2014) 'Differential requirement for PBP1a and PBP1b in in vivo and in vitro fitness of *Vibrio cholerae*', *Infection and Immunity*, 82(5), pp. 2115–2124. doi: 10.1128/IAI.00012-14.

Dramsi, S. *et al.* (2008) 'Covalent attachment of proteins to peptidoglycan', *FEMS Microbiology Reviews*, 32(2), pp. 307–320. doi: 10.1111/j.1574-6976.2008.00102.x.

Dunn, A. K. and Stabb, E. V. (2008) 'The twin arginine translocation system contributes to symbiotic colonization of *Euprymna scolopes* by *Vibrio fischeri*', *FEMS Microbiology Letters*, 279(2), pp. 251–258. doi: 10.1111/j.1574-6968.2007.01043.x.

Egan, A. J. F. *et al.* (2014) 'Outer-membrane lipoprotein LpoB spans the periplasm to stimulate the peptidoglycan synthase PBP1B', *Proceedings of the National Academy of Sciences*, 111(22), pp. 8197–8202. doi: 10.1073/pnas.1400376111.

Eliseev, R., Alexandrov, A. and Gunter, T. (2004) 'High-yield expression and purification of p18 form of Bax as an MBP-fusion protein', *Protein Expression and Purification*, 35(2), pp. 206–209. doi: 10.1016/j.pep.2004.01.015.

Ellwood, D. C. and Tempest, D. W. (1968) 'Teichoic Acids of *Bacillus subtilis var niger* and *Bacillus subtilis w23* grown in a chemostat', in *Biochemical Journal*. PORTLAND PRESS 59 PORTLAND PLACE, LONDON W1N 3AJ, ENGLAND, p. P40.

Ercoli, G. *et al.* (2015) 'LytM Proteins Play a Crucial Role in Cell Separation, Outer Membrane Composition, and Pathogenesis in Nontypeable *Haemophilus influenzae*', *mBio*. Edited by J. Parkhill, 6(2), pp. e02575-14. doi: 10.1128/mBio.02575-14.

Errington, J. (2013) 'L-form bacteria, cell walls and the origins of life', *Open Biology*, 3(1), p. 120143. doi: 10.1098/rsob.120143.

Falke, J. J. and Kim, S.-H. (2000) 'Structure of a conserved receptor domain that regulates kinase activity: the cytoplasmic domain of bacterial taxis receptors', *Current Opinion in Structural Biology*, 10(4), pp. 462–469. doi: 10.1016/S0959-440X(00)00115-9.

Fernández-Tornero, C. *et al.* (2001) 'A novel solenoid fold in the cell wall anchoring domain of the pneumococcal virulence factor LytA', *Nature Structural Biology*, 8(1), pp. 1020–1024. doi: 10.1038/nsb724.

Firczuk, M. and Bochtler, M. (2007) 'Folds and activities of peptidoglycan amidases', *FEMS Microbiology Reviews*, pp. 676–691. doi: 10.1111/j.1574-6976.2007.00084.x.

Fitzgerald, D. M., Bonocora, R. P. and Wade, J. T. (2014) 'Comprehensive Mapping of the *Escherichia coli* Flagellar Regulatory Network', *PLoS Genetics*. Edited by L. Søgaard-Andersen, 10(10), p. e1004649. doi: 10.1371/journal.pgen.1004649.

Foster, S. J., Smith, T. J. and Blackman, S. A. (2000) 'Autolysins of *Bacillus subtilis*: multiple enzymes with multiple functions', *Microbiology*, 146(2), pp. 249–262. doi: 10.1099/00221287-146-2-249.

Fujino, T. *et al.* (1953) 'On the bacteriological examination of shirasu food poisoning', *Med. J. Osaka Univ*, 2(3), pp. 299–304.

Galli, E., Paly, E. and Barre, F.-X. (2017) 'Late assembly of the *Vibrio cholerae* cell division machinery postpones septation to the last 10% of the cell cycle', *Scientific Reports*, 7(1), p. 44505. doi: 10.1038/srep44505.

Galperin, M. Y. *et al.* (2012) 'Genomic determinants of sporulation in *Bacilli* and *Clostridia*: Towards the minimal set of sporulation-specific genes', *Environmental Microbiology*, 14(11), pp. 2870–2890. doi: 10.1111/j.1462-2920.2012.02841.x.

Gan, L., Chen, S. and Jensen, G. J. (2008) 'Molecular organization of Gram-negative peptidoglycan',

Proceedings of the National Academy of Sciences, 105(48), pp. 18953–18957. doi: 10.1073/pnas.0808035105.

Georgopoulos, C. (1992) 'The emergence of the chaperone machines', *Trends in Biochemical Sciences*, 17(1), pp. 295–299. doi: 10.1016/0968-0004(92)90439-G.

Gerding, M. A. *et al.* (2007) 'The trans -envelope Tol-Pal complex is part of the cell division machinery and required for proper outer-membrane invagination during cell constriction in *E. coli*', *Molecular Microbiology*, 63(4), pp. 1008–1025. doi: 10.1111/j.1365-2958.2006.05571.x.

Gessmann, D. *et al.* (2014) 'Outer membrane -barrel protein folding is physically controlled by periplasmic lipid head groups and BamA', *Proceedings of the National Academy of Sciences*, 111(16), pp. 5878–5883. doi: 10.1073/pnas.1322473111.

Gething, M.-J. and Sambrook, J. (1992) 'Protein folding in the cell', *Nature*, 355(6355), pp. 33–45. doi: 10.1038/355033a0.

Giles, D. K. *et al.* (2011) 'Remodelling of the *Vibrio cholerae* membrane by incorporation of exogenous fatty acids from host and aquatic environments', *Molecular Microbiology*, 79(3), pp. 716–728. doi: 10.1111/j.1365-2958.2010.07476.x.

Glauner, B., Höltje, J. V and Schwarz, U. (1988) 'The composition of the murein of *Escherichia coli.*', *The Journal of biological chemistry*, 263(21), pp. 10088–95.

Gohlke, U. *et al.* (2005) 'The TatA component of the twin-arginine protein transport system forms channel complexes of variable diameter', *Proceedings of the National Academy of Sciences*, 102(30), pp. 10482–10486. doi: 10.1073/pnas.0503558102.

Guo, L. *et al.* (2018) 'secA , secD , secF , yajC, and yidC contribute to the adhesion regulation of *Vibrio alginolyticus*', *MicrobiologyOpen*, 7(2), p. e00551. doi: 10.1002/mbo3.551.

Gupta, K. R. *et al.* (2016) 'Regulation of Growth, Cell Shape, Cell Division, and Gene Expression by Second Messengers (p)ppGpp and Cyclic Di-GMP in *Mycobacterium smegmatis*', *Journal of Bacteriology*. Edited by A. M. Stock, 198(9), pp. 1414–1422. doi: 10.1128/JB.00126-16.

Guzman, L. M. *et al.* (1995) 'Tight regulation, modulation, and high-level expression by vectors containing the arabinose P(BAD) promoter', *Journal of Bacteriology*, 177(14), pp. 4121–4130. doi: 0021-9193/95/$04.00+0.

Haney, S. A. *et al.* (2001) 'Genetic Analysis of the *Escherichia coli* FtsZ·ZipA Interaction in the Yeast Two-hybrid System', *Journal of Biological Chemistry*, 276(15), pp. 11980–11987. doi: 10.1074/jbc.M009810200.

Harshey, R. M. and Matsuyama, T. (1994) 'Dimorphic transition in *Escherichia coli* and *Salmonella typhimurium*: surface-induced differentiation into hyperflagellate swarmer cells', *Proceedings of the National Academy of Sciences of the United States of America*, 91(18), pp. 8631–8635. doi: 10.1073/pnas.91.18.8631.

Hayhurst, E. J. *et al.* (2008) 'Cell wall peptidoglycan architecture in *Bacillus subtilis*', *Proceedings of the National Academy of Sciences*, 105(38), pp. 14603–14608. doi: 10.1073/pnas.0804138105.

He, F. *et al.* (2009) 'Molecular Basis of ChvE Function in Sugar Binding, Sugar Utilization, and Virulence in *Agrobacterium tumefaciens*', *Journal of Bacteriology*, 191(18), pp. 5802–5813. doi: 10.1128/JB.00451-09.

He, H. *et al.* (2011) 'Functional Characterization of *Vibrio alginolyticus* Twin-Arginine Translocation System: Its Roles in Biofilm Formation, Extracellular Protease Activity, and Virulence Towards Fish', *Current Microbiology*, 62(4), pp. 1193–1199. doi: 10.1007/s00284-010-9844-6.

Heering, J., Alvarado, A. and Ringgaard, S. (2017) 'Induction of Cellular Differentiation and Single Cell Imaging of *Vibrio parahaemolyticus* Swimmer and Swarmer Cells', *Journal of Visualized Experiments*, 123(123), p. e55842. doi: 10.3791/55842.

Heering, J. and Ringgaard, S. (2016) 'Differential Localization of Chemotactic Signaling Arrays during the Lifecycle of *Vibrio parahaemolyticus*', *Frontiers in Microbiology*, 7(NOV), p. 1767. doi: 10.3389/fmicb.2016.01767.

Hegde, S. S. and Shrader, T. E. (2001) 'FemABX Family Members Are Novel Nonribosomal Peptidyltransferases and Important Pathogen-specific Drug Targets', *Journal of Biological Chemistry*, 276(10), pp. 6998–7003. doi: 10.1074/jbc.M008591200.

Heidrich, C. *et al.* (2001) 'Involvement of N-acetylmuramyl-l-alanine amidases in cell separation and antibiotic-induced autolysis of *Escherichia coli*', *Molecular Microbiology*, 41(1), pp. 167–178. doi: 10.1046/j.1365-2958.2001.02499.x.

Heidrich, C. *et al.* (2002) 'Effects of multiple deletions of murein hydrolases on viability, septum cleavage, and sensitivity to large toxic molecules in *Escherichia coli*', *Journal of Bacteriology*, 184(22), pp. 6093–6099. doi: 10.1128/JB.184.22.6093-6099.2002.

Heijenoort, J. v. (2001) 'Formation of the glycan chains in the synthesis of bacterial peptidoglycan', *Glycobiology*, 11(3), p. 25R–36R. doi: 10.1093/glycob/11.3.25R.

Hengge, R. (2009) 'Principles of c-di-GMP signalling in bacteria', *Nature reviews. Microbiology*, 7(4), pp. 263–273. doi: 10.1038/nrmicro2109.

Higgins, D. and Dworkin, J. (2012) 'Recent progress in Bacillus subtilis sporulation', *FEMS Microbiology Reviews*, pp. 131–148. doi: 10.1111/j.1574-6976.2011.00310.x.

Höltje, J. V. *et al.* (1975) 'Novel type of murein transglycosylase in Escherichia coli', *Journal of Bacteriology*, 124(3), pp. 1067–1076.

Höltje, J. V (1998) 'Growth of the stress-bearing and shape-maintaining murein sacculus of *Escherichia coli.*',

Microbiology and molecular biology reviews : MMBR, 62(1), pp. 181–203.

Horsburgh, G. J., Atrih, A. and Foster, S. J. (2003) 'Characterization of LytH, a differentiation-associated peptidoglycan hydrolase of *Bacillus subtilis* involved in endospore cortex maturation', *Journal of Bacteriology*, 185(13), pp. 3813–3820. doi: 10.1128/JB.185.13.3813-3820.2003.

Huber, D. and Bukau, B. (2008) 'DegP: a Protein "Death Star"', *Structure*, 16(7), pp. 989–990. doi: 10.1016/j.str.2008.06.004.

Hübscher, J. *et al.* (2007) 'Living with an imperfect cell wall: compensation of femAB inactivation in *Staphylococcus aureus*', *BMC Genomics*, 8(1), p. 307. doi: 10.1186/1471-2164-8-307.

Hung, W., Jane, W.-N. and Wong, H. (2013) 'Association of a d-Alanyl-d-Alanine Carboxypeptidase Gene with the Formation of Aberrantly Shaped Cells during the Induction of Viable but Nonculturable *Vibrio parahaemolyticus*', *Applied and Environmental Microbiology*, 79(23), pp. 7305–7312. doi: 10.1128/AEM.01723-13.

Hussain, S. and Bernstein, H. D. (2018) 'The Bam complex catalyzes efficient insertion of bacterial outer membrane proteins into membrane vesicles of variable lipid composition', *Journal of Biological Chemistry*, 293(8), pp. 2959–2973. doi: 10.1074/jbc.RA117.000349.

Ichimura, T. *et al.* (2002) 'Proteolytic Activity of YibP Protein in *Escherichia coli*', *Journal of Bacteriology*, 184(10), pp. 2595–2602. doi: 10.1128/JB.184.10.2595-2602.2002.

Ikeda, M. *et al.* (1989) 'Structural similarity among *Escherichia coli* FtsW and RodA proteins and *Bacillus subtilis* SpoVE protein, which function in cell division, cell elongation, and spore formation, respectively.', *Journal of Bacteriology*, 171(11), pp. 6375–6378. doi: 10.1128/jb.171.11.6375-6378.1989.

Jacobs, C. *et al.* (1994) 'Bacterial cell wall recycling provides cytosolic muropeptides as effectors for beta-lactamase induction.', *The EMBO Journal*, 13(19), pp. 4684–4694. doi: 10.1002/j.1460-2075.1994.tb06792.x.

Jacobs, C. *et al.* (1995) 'AmpD, essential for both ß-lactamase regulation and cell wall recycling, is a novel cytosolic N-acetylmuramyl-L-alanine amidase', *Molecular Microbiology*, 15(3), pp. 553–559. doi: 10.1111/j.1365-2958.1995.tb02268.x.

Jean, N. L. *et al.* (2014) 'Elongated Structure of the Outer-Membrane Activator of Peptidoglycan Synthesis LpoA: Implications for PBP1A Stimulation', *Structure*, 22(7), pp. 1047–1054. doi: 10.1016/j.str.2014.04.017.

Jones, L. J. F., Carballido-López, R. and Errington, J. (2001) 'Control of cell shape in bacteria: Helical, actin-like filaments in *Bacillus subtilis*', *Cell*, 104(6), pp. 913–922. doi: 10.1016/S0092-8674(01)00287-2.

Jude, B. A. (2008) *Characterization of factors critical for initial stages of* Vibrio cholerae *intestinal colonization.* Dartmouth College. doi: 10.1349/ddlp.1660.

Kaberdin, V. R. and Bläsi, U. (2006) 'Translation initiation and the fate of bacterial mRNAs', *FEMS Microbiology Reviews*, 30(6), pp. 967–979. doi: 10.1111/j.1574-6976.2006.00043.x.

Kamio, Y. and Nikaido, H. (1976) 'Outer membrane of *Salmonella typhimurium*: accessibility of phospholipid head groups to phospholipase C and cyanogen bromide activated dextran in the external medium', *Biochemistry*, 15(12), pp. 2561–2570. doi: 10.1021/bi00657a012.

Karimova, G. *et al.* (1998) 'A bacterial two-hybrid system based on a reconstituted signal transduction pathway', *Proc Natl Acad Sci U S A*, 95(10), pp. 5752–5756.

Kato, J., Suzuki, H. and Hirota, Y. (1985) 'Dispensability of either penicillin-binding protein-1a or -1b involved in the essential process for cell elongation in *Escherichia coli.*', *Molecular & general genetics*, 200(2), pp. 272–277. doi: 10.1007/BF00425435.

Kerff, F. *et al.* (2010) 'Specific Structural Features of the N-Acetylmuramoyl-l-Alanine Amidase AmiD from *Escherichia coli* and Mechanistic Implications for Enzymes of This Family', *Journal of Molecular Biology*, 397(1), pp. 249–259. doi: 10.1016/j.jmb.2009.12.038.

Kibbe, W. A. (2007) 'OligoCalc: an online oligonucleotide properties calculator', *Nucleic Acids Research*, 35(Web Server), pp. W43–W46. doi: 10.1093/nar/gkm234.

Kim, Y. K. and McCarter, L. L. (2007) 'ScrG, a GGDEF-EAL protein, participates in regulating swarming and sticking in *Vibrio parahaemolyticus*', *J Bacteriol*, 189(11), pp. 4094–4107. doi: Doi 10.1128/Jb.01510-06.

Kirov, S. M. *et al.* (2002) 'Lateral flagella and swarming motility in *Aeromonas species*', *Journal of Bacteriology*, 184(2), pp. 547–555. doi: 10.1128/JB.184.2.547-555.2002.

Knowles, T. J. *et al.* (2009) 'Membrane protein architects: the role of the BAM complex in outer membrane protein assembly', *Nature Reviews Microbiology*, 7(3), pp. 206–214. doi: 10.1038/nrmicro2069.

Korepanova, A. *et al.* (2007) 'Expression of membrane proteins from *Mycobacterium tuberculosis* in *Escherichia coli* as fusions with maltose binding protein', *Protein Expression and Purification*, 53(1), pp. 24–30. doi: 10.1016/j.pep.2006.11.022.

Korndörfer, I. P. *et al.* (2006) 'The Crystal Structure of the Bacteriophage PSA Endolysin Reveals a Unique Fold Responsible for Specific Recognition of Listeria Cell Walls', *Journal of Molecular Biology*, 364(4), pp. 678–689. doi: 10.1016/j.jmb.2006.08.069.

Koronakis, V. *et al.* (2000) 'Crystal structure of the bacterial membrane protein TolC central to multidrug efflux and protein export', *Nature*, 405(6789), pp. 914–919. doi: 10.1038/35016007.

Koronakis, V., Eswaran, J. and Hughes, C. (2004) 'Structure and Function of TolC: The Bacterial Exit Duct for Proteins and Drugs', *Annual Review of Biochemistry*, 73(1), pp. 467–489. doi:

10.1146/annurev.biochem.73.011303.074104.

Krojer, T. *et al.* (2008) 'Structural basis for the regulated protease and chaperone function of DegP', *Nature*, 453(7197), pp. 885–890. doi: 10.1038/nature07004.

Kubori, T. (1998) 'Supramolecular Structure of the *Salmonella typhimurium* Type III Protein Secretion System', *Science*, 280(5363), pp. 602–605. doi: 10.1126/science.280.5363.602.

Kumar, A. *et al.* (2013) 'The structure of Rv3717 reveals a novel amidase from M*ycobacterium tuberculosis*', *Acta Crystallographica Section D: Biological Crystallography*, 69(12), pp. 2543–2554. doi: 10.1107/S0907444913026371.

Kumar, S. *et al.* (2019) 'The bacterial lipid II flippase MurJ functions by an alternating-access mechanism', *Journal of Biological Chemistry*, 294(3), pp. 981–990. doi: 10.1074/jbc.RA118.006099.

Kuru, E. *et al.* (2012) 'In situ probing of newly synthesized peptidoglycan in live bacteria with fluorescent D-amino acids', *Angewandte Chemie - International Edition*, 51(50), pp. 12519–12523. doi: 10.1002/anie.201206749.

Lam, H. *et al.* (2009) 'D-amino acids govern stationary phase cell wall remodeling in bacteria', *Science*, 325(5947), pp. 1552–1555. doi: 10.1126/science.1178123.

Lange, R. and Hengge-Aronis, R. (1994) 'The *nlpD* gene is located in an operon with rpoS on the *Escherichia coli* chromosome and encodes a novel lipoprotein with a potential function in ceil wall formation', *Molecular Microbiology*, 13(4), pp. 733–743. doi: 10.1111/j.1365-2958.1994.tb00466.x.

Langer, T. *et al.* (1992) 'Successive action of DnaK, DnaJ and GroEL along the pathway of chaperone-mediated protein folding', *Nature*, 356(6371), pp. 683–689. doi: 10.1038/356683a0.

Lapage, G. (1945) 'Mode of Action of Penicillin', *Nature*, 156(3957), pp. 272–273. doi: 10.1038/156272a0.

Lapidot, A. and Irving, C. S. (1979a) 'Comparative in vivo nitrogen-15 nuclear magnetic resonance study of the cell wall components of five Gram-positive bacteria', *Biochemistry*. ACS Publications, 18(4), pp. 704–714.

Lapidot, A. and Irving, C. S. (1979b) 'Nitrogen-15 and carbon-13 dynamic nuclear magnetic resonance study of chain segmental motion of the peptidoglycan pentaglycine chain of 15N-Gly-and 13C2-Gly-labeled *Staphylococcus aureus* cells and isolated cell walls', *Biochemistry*. ACS Publications, 18(9), pp. 1788–1796.

Lawler, M. L. and Brun, Y. V. (2007) 'Advantages and mechanisms of polarity and cell shape determination in *Caulobacter crescentus*', *Current Opinion in Microbiology*, pp. 630–637. doi: 10.1016/j.mib.2007.09.007.

Leake, M. C. *et al.* (2008) 'Variable stoichiometry of the TatA component of the twin-arginine protein transport system observed by in vivo single-molecule imaging', *Proceedings of the National Academy of Sciences*, 105(40), pp. 15376–15381. doi: 10.1073/pnas.0806338105.

Leclercq, S. *et al.* (2017) 'Interplay between Penicillin-binding proteins and SEDS proteins promotes bacterial cell wall synthesis', *Scientific Reports*, 7(1), p. 43306. doi: 10.1038/srep43306.

Letunic, I. and Bork, P. (2019) 'Interactive Tree Of Life (iTOL) v4: recent updates and new developments', *Nucleic Acids Research*, 47(W1), pp. W256–W259. doi: 10.1093/nar/gkz239.

Li, S. L., Norioka, S. and Sakiyama, F. (1990) 'Molecular cloning and nucleotide sequence of the beta-lytic protease gene from Achromobacter lyticus.', *Journal of bacteriology*, 172(11), pp. 6506–11.

Li, W. and He, Z.-G. (2012) 'LtmA, a novel cyclic di-GMP-responsive activator, broadly regulates the expression of lipid transport and metabolism genes in *Mycobacterium smegmatis*', *Nucleic Acids Research*, 40(22), pp. 11292–11307. doi: 10.1093/nar/gks923.

Lupoli, T. J. *et al.* (2014) 'Lipoprotein activators stimulate escherichia coli penicillin-binding proteins by different mechanisms', *Journal of the American Chemical Society*, 136(1), pp. 52–55. doi: 10.1021/ja410813j.

Luzzatto, L., Apirion, D. and Schlessinger, D. (1968) 'Mechanism of action of streptomycin in *E. coli*: interruption of the ribosome cycle at the initiation of protein synthesis.', *Proceedings of the National Academy of Sciences*, 60(3), pp. 873–880. doi: 10.1073/pnas.60.3.873.

MacAlister, T. J. *et al.* (1972) 'Distribution of alkaline phosphatase within the periplasmic space of gram-negative bacteria', *Journal of bacteriology*, 111(3), pp. 827–832.

Machuca, M. A. *et al.* (2017) '*Helicobacter pylori* chemoreceptor TlpC mediates chemotaxis to lactate', *Scientific Reports*, 7(1), p. 14089. doi: 10.1038/s41598-017-14372-2.

Macnab, R. M. (2003) 'How Bacteria Assemble Flagella', *Annual Review of Microbiology*, 57(1), pp. 77–100. doi: 10.1146/annurev.micro.57.030502.090832.

Makino, K. *et al.* (2003) 'Genome sequence of *Vibrio parahaemolyticus*: a pathogenic mechanism distinct from that of V. cholerae', *Lancet*, 361(9359), pp. 743–749. doi: 10.1016/S0140-6736(03)12659-1.

Malinverni, J. C. *et al.* (2006) 'YfiO stabilizes the YaeT complex and is essential for outer membrane protein assembly in *Escherichia coli*', *Molecular Microbiology*, 61(1), pp. 151–164. doi: 10.1111/j.1365-2958.2006.05211.x.

Manat, G. *et al.* (2015) 'Membrane Topology and Biochemical Characterization of the *Escherichia coli* BacA Undecaprenyl-Pyrophosphate Phosphatase', *PLOS ONE*. Edited by E. Cascales, 10(11), p. e0142870. doi: 10.1371/journal.pone.0142870.

Matias, V. R. F. *et al.* (2003) 'Cryo-Transmission Electron Microscopy of Frozen-Hydrated Sections of *Escherichia coli* and *Pseudomonas aeruginosa*', *Journal of Bacteriology*, 185(20), pp. 6112–6118. doi: 10.1128/JB.185.20.6112-6118.2003.

Matsuyama, S., Fujita, Y. and Mizushima, S. (1993) 'SecD is involved in the release of translocated secretory proteins from the cytoplasmic membrane of *Escherichia coli.*', *The EMBO Journal*, 12(1), pp. 265–270. doi: 10.1002/j.1460-2075.1993.tb05652.x.

Matteï, P. J., Neves, D. and Dessen, A. (2010) 'Bridging cell wall biosynthesis and bacterial morphogenesis', *Current Opinion in Structural Biology*. doi: 10.1016/j.sbi.2010.09.014.

McCarter, L. L. (2004) 'Dual flagellar systems enable motility under different circumstances', *Journal of Molecular Microbiology and Biotechnology*, 7(1–2), pp. 18–29. doi: 10.1159/000077866.

McCarthy, R. R. *et al.* (2017) 'Cyclic-di-GMP regulates lipopolysaccharide modification and contributes to *Pseudomonas aeruginosa* immune evasion', *Nature Microbiology*, 2(6), p. 17027. doi: 10.1038/nmicrobiol.2017.27.

Meeske, A. J. *et al.* (2015) 'MurJ and a novel lipid II flippase are required for cell wall biogenesis in *Bacillus subtilis*', *Proceedings of the National Academy of Sciences*, 112(20), pp. 6437–6442. doi: 10.1073/pnas.1504967112.

Meeske, A. J. *et al.* (2016) 'SEDS proteins are a widespread family of bacterial cell wall polymerases', *Nature*, 537(7622), pp. 634–638. doi: 10.1038/nature19331.

Meisner, J. *et al.* (2012) 'Structure of the basal components of a bacterial transporter', *Proceedings of the National Academy of Sciences*, 109(14), pp. 5446–5451. doi: 10.1073/pnas.1120113109.

Meisner, J. and Moran, C. P. (2011) 'A LytM domain dictates the localization of proteins to the mother cell-forespore interface during bacterial endospore formation', *Journal of Bacteriology*, 193(3), pp. 591–598. doi: 10.1128/JB.01270-10.

Mengin-Lecreulx, D., Van Heijenoort, J. and Park, J. T. (1996) 'Identification of the *mpl* gene encoding UDP-N-acetylmuramate: L-alanyl- γ-D-glutamyl-meso-diaminopimelate ligase in *Escherichia coli* and its role in recycling of cell wall peptidoglycan', *Journal of Bacteriology*, 178(18), pp. 5347–5352.

Miller, V. L. and Mekalanos, J. J. (1988) 'A novel suicide vector and its use in construction of insertion mutations: osmoregulation of outer membrane proteins and virulence determinants in *Vibrio cholerae* requires toxR.', *Journal of Bacteriology*, 170(6), pp. 2575–2583. doi: 10.1128/jb.170.6.2575-2583.1988.

Mitchell, P. (1961) 'Approaches to the analysis of specific membrane transport', *Biological structure and function*. Academic Press, 2(1), pp. 581–599.

Miyadai, H. *et al.* (2004) 'Effects of Lipoprotein Overproduction on the Induction of DegP (HtrA) Involved in Quality Control in the *Escherichia coli* Periplasm', *Journal of Biological Chemistry*, 279(38), pp. 39807–39813. doi: 10.1074/jbc.M406390200.

Miyagishima, S. *et al.* (2014) 'DipM is required for peptidoglycan hydrolysis during chloroplast division', *BMC Plant Biology*, 14(1), p. 57. doi: 10.1186/1471-2229-14-57.

Mohammadi, T. *et al.* (2011) 'Identification of FtsW as a transporter of lipid-linked cell wall precursors across the membrane', *The EMBO Journal*, 30(8), pp. 1425–1432. doi: 10.1038/emboj.2011.61.

Möll, A. *et al.* (2010) 'DipM, a new factor required for peptidoglycan remodelling during cell division in *Caulobacter crescentus*', *Molecular Microbiology*, 77(1), pp. 90–107. doi: 10.1111/j.1365-2958.2010.07224.x.

Möll, A. *et al.* (2014) 'Cell separation in *Vibrio cholerae* is mediated by a single amidase whose action is modulated by two nonredundant activators', *Journal of Bacteriology*, 196(22), pp. 3937–3948. doi: 10.1128/JB.02094-14.

Möll, A. *et al.* (2015) 'A D, D-carboxypeptidase is required for *Vibrio cholerae* halotolerance', *Environmental Microbiology*, 17(2), pp. 527–540. doi: 10.1111/1462-2920.12779.

Morath, S., von Aulock, S. and Hartung, T. (2005) 'Structure/function relationships of lipoteichoic acids', *Journal of endotoxin research*. Sage Publications Sage UK: London, England, 11(6), pp. 348–356.

Moslavac, S. *et al.* (2005) 'Conserved pore-forming regions in polypeptide- transporting proteins', *FEBS Journal*, 272(6), pp. 1367–1378. doi: 10.1111/j.1742-4658.2005.04569.x.

Müller, M. (2005) 'Twin-arginine-specific protein export in *Escherichia coli*', *Research in Microbiology*, 156(2), pp. 131–136. doi: 10.1016/j.resmic.2004.09.016.

Mullineaux, C. W. *et al.* (2006) 'Diffusion of Green Fluorescent Protein in Three Cell Environments in *Escherichia Coli*', *Journal of Bacteriology*, 188(10), pp. 3442–3448. doi: 10.1128/JB.188.10.3442-3448.2006.

Murakami, S. *et al.* (2006) 'Crystal structures of a multidrug transporter reveal a functionally rotating mechanism', *Nature*, 443(7108), pp. 173–179. doi: 10.1038/nature05076.

Muraleedharan, S. *et al.* (2018) 'A cell length-dependent transition in MinD-dynamics promotes a switch in division-site placement and preservation of proliferating elongated *Vibrio parahaemolyticus* swarmer cells', *Molecular Microbiology*, 109(3), pp. 365–384. doi: 10.1111/mmi.13996.

Narita, S. -i. *et al.* (2002) 'Disruption of lolCDE, Encoding an ATP-Binding Cassette Transporter, Is Lethal for *Escherichia coli* and Prevents Release of Lipoproteins from the Inner Membrane', *Journal of Bacteriology*, 184(5), pp. 1417–1422. doi: 10.1128/JB.184.5.1417-1422.2002.

Narita, S. and Tokuda, H. (2006) 'An ABC transporter mediating the membrane detachment of bacterial lipoproteins depending on their sorting signals', *FEBS Letters*, 580(4), pp. 1164–1170. doi: 10.1016/j.febslet.2005.10.038.

Natale, P., Brüser, T. and Driessen, A. J. M. (2008) 'Sec- and Tat-mediated protein secretion across the bacterial

cytoplasmic membrane—Distinct translocases and mechanisms', *Biochimica et Biophysica Acta (BBA) - Biomembranes*, 1778(9), pp. 1735–1756. doi: 10.1016/j.bbamem.2007.07.015.

Neuhaus, F. C. and Baddiley, J. (2003) 'A Continuum of Anionic Charge: Structures and Functions of D-Alanyl-Teichoic Acids in Gram-Positive Bacteria', *Microbiology and Molecular Biology Reviews*, 67(4), pp. 686–723. doi: 10.1128/MMBR.67.4.686-723.2003.

Newton, A. *et al.* (2012) 'Increasing Rates of Vibriosis in the United States, 1996–2010: Review of Surveillance Data From 2 Systems', *Clinical Infectious Diseases*, 54(suppl_5), pp. S391–S395. doi: 10.1093/cid/cis243.

Nikaido, H. (2003) 'Molecular Basis of Bacterial Outer Membrane Permeability Revisited', *Microbiology and Molecular Biology Reviews*, 67(4), pp. 593–656. doi: 10.1128/MMBR.67.4.593-656.2003.

Oates, J. *et al.* (2005) 'The *Escherichia coli* Twin-arginine Translocation Apparatus Incorporates a Distinct Form of TatABC Complex, Spectrum of Modular TatA Complexes and Minor TatAB Complex', *Journal of Molecular Biology*, 346(1), pp. 295–305. doi: 10.1016/j.jmb.2004.11.047.

Ogata, H. *et al.* (1999) 'KEGG: Kyoto Encyclopedia of Genes and Genomes', *Nucleic Acids Res*, 27(1), pp. 29–34.

Oku, Y. *et al.* (2009) 'Pleiotropic Roles of Polyglycerolphosphate Synthase of Lipoteichoic Acid in Growth of *Staphylococcus aureus* Cells', *Journal of Bacteriology*, 191(1), pp. 141–151. doi: 10.1128/JB.01221-08.

Okuda, S., Freinkman, E. and Kahne, D. (2012) 'Cytoplasmic ATP Hydrolysis Powers Transport of Lipopolysaccharide Across the Periplasm in *E. coli*', *Science*, 338(6111), pp. 1214–1217. doi: 10.1126/science.1228984.

Ostell, J. M. and Kans, J. A. (1998) 'The NCBI data model.', *Methods of biochemical analysis*, 39(1), pp. 121–44.

Paetzel, M. (2019) 'Bacterial Signal Peptidases', in *Subcellular Biochemistry*, pp. 187–219. doi: 10.1007/978-3-030-18768-2_7.

Paradis-Bleau, C. *et al.* (2010) 'Lipoprotein cofactors located in the outer membrane activate bacterial cell wall polymerases', *Cell*, 143(7), pp. 1110–1120. doi: 10.1016/j.cell.2010.11.037.

Paredes-Sabja, D., Shen, A. and Sorg, J. A. (2014) 'Clostridium difficile spore biology: Sporulation, germination, and spore structural proteins', *Trends in Microbiology*, pp. 406–416. doi: 10.1016/j.tim.2014.04.003.

Park, J. T. and Uehara, T. (2008) 'How Bacteria Consume Their Own Exoskeletons (Turnover and Recycling of Cell Wall Peptidoglycan)', *Microbiology and Molecular Biology Reviews*, 72(2), pp. 211–227. doi: 10.1128/MMBR.00027-07.

de Pedro, M. A. *et al.* (1997) 'Murein segregation in *Escherichia coli*.', *Journal of Bacteriology*, 179(9), pp.

2823–2834. doi: 10.1128/jb.179.9.2823-2834.1997.

de Pedro, M. A. *et al.* (2001) 'Constitutive Septal Murein Synthesis in *Escherichia coli* with Impaired Activity of the Morphogenetic Proteins RodA and Penicillin-Binding Protein 2', *Journal of Bacteriology*, 183(14), pp. 4115–4126. doi: 10.1128/JB.183.14.4115-4126.2001.

Peters, K. *et al.* (2016) 'The Redundancy of Peptidoglycan Carboxypeptidases Ensures Robust Cell Shape Maintenance in *Escherichia coli*', *mBio*, 7(3), pp. e00819-16. doi: 10.1128/mBio.00819-16.

Peters, N. T. *et al.* (2013) 'Structure-function analysis of the LytM domain of EnvC, an activator of cell wall remodelling at the *Escherichia coli* division site', *Molecular Microbiology*, 89(4), pp. 690–701. doi: 10.1111/mmi.12304.

Peters, N. T., Dinh, T. and Bernhardt, T. G. (2011) 'A Fail-Safe Mechanism in the Septal Ring Assembly Pathway Generated by the Sequential Recruitment of Cell Separation Amidases and Their Activators', *Journal of Bacteriology*, 193(18), pp. 4973–4983. doi: 10.1128/JB.00316-11.

Phillips, G. J. and Silhavy, T. J. (1992) 'The *E. coli ffh* gene is necessary for viability and efficient protein export', *Nature*, 359(6397), pp. 744–746. doi: 10.1038/359744a0.

Platt, R. *et al.* (2000) 'Genetic System for Reversible Integration of DNA Constructs and lacZ Gene Fusions into the *Escherichia coli* Chromosome', *Plasmid*, 43(1), pp. 12–23. doi: 10.1006/plas.1999.1433.

van der Ploeg, R. *et al.* (2013) 'Colocalization and interaction between elongasome and divisome during a preparative cell division phase in *Escherichia coli*', *Molecular Microbiology*, 87(5), pp. 1074–1087. doi: 10.1111/mmi.12150.

Pogliano, J. A. and Beckwith, J. (1994) 'SecD and SecF facilitate protein export in *Escherichia coli*.', *The EMBO Journal*, 13(3), pp. 554–561. doi: 10.1002/j.1460-2075.1994.tb06293.x.

Pollack, J. H. and Neuhaus, F. C. (1994) 'Changes in wall teichoic acid during the rod-sphere transition of *Bacillus subtilis 168*.', *Journal of Bacteriology*, 176(23), pp. 7252–7259. doi: 10.1128/jb.176.23.7252-7259.1994.

Potluri, L.-P., de Pedro, M. A. and Young, K. D. (2012) '*Escherichia coli* low-molecular-weight penicillin-binding proteins help orient septal FtsZ, and their absence leads to asymmetric cell division and branching', *Molecular Microbiology*, 84(2), pp. 203–224. doi: 10.1111/j.1365-2958.2012.08023.x.

Pratt, J. T. *et al.* (2007) 'PilZ domain proteins bind cyclic diguanylate and regulate diverse processes in *Vibrio cholerae*', *Journal of Biological Chemistry*, 282(17), pp. 12860–12870. doi: 10.1074/jbc.M611593200.

Pratt, R. F. (2008) 'Substrate specificity of bacterial DD-peptidases (penicillin-binding proteins)', *Cellular and Molecular Life Sciences*, 65(14), pp. 2138–2155. doi: 10.1007/s00018-008-7591-7.

Priyadarshini, R., De Pedro, M. A. and Young, K. D. (2007) 'Role of peptidoglycan amidases in the development and morphology of the division septum in *Escherichia coli*', *Journal of Bacteriology*, 189(14), pp. 5334–5347. doi: 10.1128/JB.00415-07.

Proshkin, S. *et al.* (2010) 'Cooperation Between Translating Ribosomes and RNA Polymerase in Transcription Elongation', *Science*, 328(5977), pp. 504–508. doi: 10.1126/science.1184939.

Raetz, C. R. H. and Dowhan, W. (1990) 'Biosynthesis and function of phospholipids in *Escherichia coli*', *Journal of Biological Chemistry*, 265(3), pp. 1235–1238.

Raetz, C. R. H. and Whitfield, C. (2002) 'Lipopolysaccharide Endotoxins', *Annual Review of Biochemistry*, 71(1), pp. 635–700. doi: 10.1146/annurev.biochem.71.110601.135414.

Ragumani, S. *et al.* (2008) 'Crystal structure of a putative lysostaphin peptidase from *Vibrio cholerae*', *Proteins: Structure, Function and Genetics*, 72(3), pp. 1096–1103. doi: 10.1002/prot.22095.

Randall, L. L. and Hardy, S. J. S. (2002) 'SecB, one small chaperone in the complex milieu of the cell', *Cellular and Molecular Life Sciences*, 59(10), pp. 1617–1623. doi: 10.1007/PL00012488.

Rather, P. N. (2005) 'Swarmer cell differentiation in *Proteus mirabilis*', *Environmental Microbiology*, pp. 1065–1073. doi: 10.1111/j.1462-2920.2005.00806.x.

Rawlings, N. D. *et al.* (2008) 'MEROPS: the peptidase database.', *Nucleic acids research*. England, 36(Database issue), pp. D320-5. doi: 10.1093/nar/gkm954.

Reith, J. and Mayer, C. (2011) 'Peptidoglycan turnover and recycling in Gram-positive bacteria', *Applied Microbiology and Biotechnology*, 92(1), pp. 1–11. doi: 10.1007/s00253-011-3486-x.

Remans, K. *et al.* (2010) 'Genome-wide analysis and literature-based survey of lipoproteins in *Pseudomonas aeruginosa*', *Microbiology*, 156(9), pp. 2597–2607. doi: 10.1099/mic.0.040659-0.

Ringgaard, S. *et al.* (2014) 'ParP prevents dissociation of CheA from chemotactic signaling arrays and tethers them to a polar anchor', *Proc Natl Acad Sci U S A*, 111(2), pp. E255-64. doi: 10.1073/pnas.1315722111.

Rizzitello, A. E., Harper, J. R. and Silhavy, T. J. (2001) 'Genetic Evidence for Parallel Pathways of Chaperone Activity in the Periplasm of *Escherichia coli*', *Journal of Bacteriology*, 183(23), pp. 6794–6800. doi: 10.1128/JB.183.23.6794-6800.2001.

Rocaboy, M. *et al.* (2013) 'The crystal structure of the cell division amidase amic reveals the fold of the AMIN domain, a new peptidoglycan binding domain', *Molecular Microbiology*, 90(2), pp. 267–277. doi: 10.1111/mmi.12361.

Rodrigues, C. D. A. *et al.* (2013) 'Peptidoglycan hydrolysis is required for assembly and activity of the transenvelope secretion complex during sporulation in *Bacillus subtilis*', *Molecular Microbiology*, 89(6), pp.

1039–1052. doi: 10.1111/mmi.12322.

Rohrer, S. and Berger-Bachi, B. (2003) 'FemABX Peptidyl Transferases: a Link between Branched-Chain Cell Wall Peptide Formation and -Lactam Resistance in Gram-Positive Cocci', *Antimicrobial Agents and Chemotherapy*, 47(3), pp. 837–846. doi: 10.1128/AAC.47.3.837-846.2003.

Rojas, E. R. *et al.* (2018) 'The outer membrane is an essential load-bearing element in Gram-negative bacteria', *Nature*, 559(7715), pp. 617–621. doi: 10.1038/s41586-018-0344-3.

Romeis, T. and Höltje, J. V (1994) 'Specific interaction of penicillin-binding proteins 3 and 7/8 with soluble lytic transglycosylase in *Escherichia coli.*', *Journal of Biological Chemistry*. ASBMB, 269(34), pp. 21603–21607.

Rose, R. W. *et al.* (2002) 'Adaptation of protein secretion to extremely high-salt conditions by extensive use of the twin-arginine translocation pathway', *Molecular Microbiology*, 45(4), pp. 943–950. doi: 10.1046/j.1365-2958.2002.03090.x.

Rowlett, V. W. *et al.* (2017) 'Impact of Membrane Phospholipid Alterations in *Escherichia coli* on Cellular Function and Bacterial Stress Adaptation', *Journal of Bacteriology*. Edited by V. J. DiRita, 199(13), pp. e00849-16. doi: 10.1128/JB.00849-16.

Rueden, C. T. *et al.* (2017) 'ImageJ2: ImageJ for the next generation of scientific image data', *BMC Bioinformatics*, 18(1), p. 529. doi: 10.1186/s12859-017-1934-z.

Ruiz, N. (2008) 'Bioinformatics identification of MurJ (MviN) as the peptidoglycan lipid II flippase in *Escherichia coli*', *Proceedings of the National Academy of Sciences*, 105(40), pp. 15553–15557. doi: 10.1073/pnas.0808352105.

Ryan, R. P. *et al.* (2006) 'Cell-cell signaling in *Xanthomonas campestris* involves an HD-GYP domain protein that functions in cyclic di-GMP turnover.', *Proceedings of the National Academy of Sciences of the United States of America*, 103(17), pp. 6712–6717. doi: 10.1073/pnas.0600345103.

Ryjenkov, D. A. *et al.* (2006) 'The PilZ domain is a receptor for the second messenger c-di-GMP: The PilZ domain protein YcgR controls motility in enterobacteria', *Journal of Biological Chemistry*, 281(41), pp. 30310–30314. doi: 10.1074/jbc.C600179200.

Saikawa, N., Akiyama, Y. and Ito, K. (2004) 'FtsH exists as an exceptionally large complex containing HflKC in the plasma membrane of *Escherichia coli*', *Journal of Structural Biology*, 146(1–2), pp. 123–129. doi: 10.1016/j.jsb.2003.09.020.

Sandkvist, M., Morales, V. and Bagdasarian, M. (1993) 'A protein required for secretion of cholera toxin through the outer membrane of *Vibrio cholerae*', *Gene*, 123(1), pp. 81–86. doi: https://doi.org/10.1016/0378-1119(93)90543-C.

Sankaran, K. and Wu, H. C. (1994) 'Lipid modification of bacterial prolipoprotein. Transfer of diacylglyceryl moiety from phosphatidylglycerol', *Journal of Biological Chemistry*, 269(31), pp. 19701–19706.

Saraswat, M. *et al.* (2013) 'Preparative Purification of Recombinant Proteins: Current Status and Future Trends', *BioMed Research International*, 2013, pp. 1–18. doi: 10.1155/2013/312709.

Sauvage, E. *et al.* (2008) 'The penicillin-binding proteins: structure and role in peptidoglycan biosynthesis', *FEMS Microbiology Reviews*, 32(2), pp. 234–258. doi: 10.1111/j.1574-6976.2008.00105.x.

Schäper, S. *et al.* (2017) 'AraC-like transcriptional activator CuxR binds c-di-GMP by a PilZ-like mechanism to regulate extracellular polysaccharide production', *Proceedings of the National Academy of Sciences*, 114(24), pp. E4822–E4831. doi: 10.1073/pnas.1702435114.

Schäper, S. *et al.* (2018) 'Seven-transmembrane receptor protein RgsP and cell wall-binding protein RgsM promote unipolar growth in *Rhizobiales*', *PLOS Genetics*. Edited by G. P. Copenhaver, 14(8), p. e1007594. doi: 10.1371/journal.pgen.1007594.

Scheurwater, E. M., Pfeffer, J. M. and Clarke, A. J. (2007) 'Production and purification of the bacterial autolysin N-acetylmuramoyl-l-alanine amidase B from *Pseudomonas aeruginosa*', *Protein Expression and Purification*, 56(1), pp. 128–137. doi: 10.1016/j.pep.2007.06.009.

Schirmer, T. *et al.* (1995) 'Structural basis for sugar translocation through maltoporin channels at 3.1 A resolution', *Science*, 267(5197), pp. 512–514. doi: 10.1126/science.7824948.

Schlünzen, F. *et al.* (2005) 'The Binding Mode of the Trigger Factor on the Ribosome: Implications for Protein Folding and SRP Interaction', *Structure*, 13(11), pp. 1685–1694. doi: 10.1016/j.str.2005.08.007.

Schneider, T. and Sahl, H. G. (2010) 'An oldie but a goodie - cell wall biosynthesis as antibiotic target pathway', *International Journal of Medical Microbiology*, pp. 161–169. doi: 10.1016/j.ijmm.2009.10.005.

Schröder, H. *et al.* (1993) 'DnaK, DnaJ and GrpE form a cellular chaperone machinery capable of repairing heat-induced protein damage.', *The EMBO Journal*, 12(11), pp. 4137–4144. doi: 10.1002/j.1460-2075.1993.tb06097.x.

Schroeder, U. *et al.* (1994) 'Peptidase D of *Escherichia coli K-12*, a metallopeptidase of low substrate specificity', *FEMS Microbiology Letters*, 123(1–2), pp. 153–159. doi: 10.1111/j.1574-6968.1994.tb07215.x.

Schultz, J. *et al.* (1998) 'SMART, a simple modular architecture research tool: identification of signaling domains', *Proc Natl Acad Sci U S A*, 95(11), pp. 5857–5864.

Scott, J. R. and Barnett, T. C. (2006) 'Surface Proteins of Gram-Positive Bacteria and How They Get There', *Annual Review of Microbiology*, 60(1), pp. 397–423. doi: 10.1146/annurev.micro.60.080805.142256.

Sham, L.-T. *et al.* (2014) 'MurJ is the flippase of lipid-linked precursors for peptidoglycan biogenesis', *Science*,

345(6193), pp. 220–222. doi: 10.1126/science.1254522.

Shen, Q.-T. *et al.* (2009) 'Bowl-shaped oligomeric structures on membranes as DegP's new functional forms in protein quality control', *Proceedings of the National Academy of Sciences*, 106(12), pp. 4858–4863. doi: 10.1073/pnas.0811780106.

Shockman, G. D. and Barren, J. F. (1983) 'Structure, Function, and Assembly of Cell Walls of Gram-Positive Bacteria', *Annual Review of Microbiology*, 37(1), pp. 501–527. doi: 10.1146/annurev.mi.37.100183.002441.

Sievers, F. and Higgins, D. G. (2014) 'Clustal Omega', in *Current Protocols in Bioinformatics*. Hoboken, NJ, USA: John Wiley & Sons, Inc., p. 3.13.1-3.13.16. doi: 10.1002/0471250953.bi0313s48.

Singh, S. K. *et al.* (2012) 'Three redundant murein endopeptidases catalyse an essential cleavage step in peptidoglycan synthesis of *Escherichia coli K12*', *Molecular Microbiology*, 86(5), pp. 1036–1051. doi: 10.1111/mmi.12058.

Sjodt, M. *et al.* (2018) 'Structure of the peptidoglycan polymerase RodA resolved by evolutionary coupling analysis', *Nature*, 556(7699), pp. 118–121. doi: 10.1038/nature25985.

Sklar, J. G., Wu, T., Kahne, D., *et al.* (2007) 'Defining the roles of the periplasmic chaperones SurA, Skp, and DegP in *Escherichia coli*', *Genes & Development*, 21(19), pp. 2473–2484. doi: 10.1101/gad.1581007.

Sklar, J. G., Wu, T., Gronenberg, L. S., *et al.* (2007) 'Lipoprotein SmpA is a component of the YaeT complex that assembles outer membrane proteins in *Escherichia coli*', *Proceedings of the National Academy of Sciences*, 104(15), pp. 6400–6405. doi: 10.1073/pnas.0701579104.

Skotnicka, D. *et al.* (2015) 'c-di-GMP regulates type IV pili-dependent-motility in *Myxococcus xanthus*', *Journal of bacteriology*, 198(1), pp. 77–90. doi: 10.1128/JB.00281-15.

Skotnicka, D. *et al.* (2016) 'A Minimal Threshold of c-di-GMP Is Essential for Fruiting Body Formation and Sporulation in *Myxococcus xanthus*', *PLoS Genet*. Public Library of Science, 12(5), p. e1006080.

Smith, S. M. *et al.* (2017) 'TatA complexes exhibit a marked change in organisation in response to expression of the TatBC complex', *Biochemical Journal*, 474(9), pp. 1495–1508. doi: 10.1042/BCJ20160952.

Söderström, B. *et al.* (2016) 'Coordinated disassembly of the divisome complex in *Escherichia coli*', *Molecular Microbiology*, 101(3), pp. 425–438. doi: 10.1111/mmi.13400.

Spencer, J. *et al.* (2010) 'Crystal Structure of the LasA Virulence Factor from *Pseudomonas aeruginosa*: Substrate Specificity and Mechanism of M23 Metallopeptidases', *Journal of Molecular Biology*, 396(4), pp. 908–923. doi: 10.1016/j.jmb.2009.12.021.

Spratt, B. G. (1975) 'Distinct penicillin binding proteins involved in the division, elongation, and shape of *Escherichia coli K12*.', *Proceedings of the National Academy of Sciences*, 72(8), pp. 2999–3003. doi:

10.1073/pnas.72.8.2999.

Stohl, E. A. *et al.* (2016) 'The gonococcal NlpD protein facilitates cell separation by activating peptidoglycan cleavage by AmiC', *Journal of Bacteriology*, 198(4), pp. 615–622. doi: 10.1128/JB.00540-15.

Studier, F. W. and Moffatt, B. A. (1986) 'Use of bacteriophage T7 RNA polymerase to direct selective high-level expression of cloned genes', *Journal of Molecular Biology*, 189(1), pp. 113–130. doi: 10.1016/0022-2836(86)90385-2.

Suginaka, H., Blumberg, P. M. and Strominger, J. L. (1972) 'Multiple penicillin-binding components in *Bacillus subtilis*, *Bacillus cereus*, *Staphylococcus aureus*, and *Escherichia coli*', *Journal of Biological Chemistry*. ASBMB, 247(17), pp. 5279–5288.

Sycuro, L. K. *et al.* (2010) 'Peptidoglycan crosslinking relaxation promotes *Helicobacter pylori*'s helical shape and stomach colonization', *Cell*, 141(5), pp. 822–833. doi: 10.1016/j.cell.2010.03.046.

Symmons, M. F. *et al.* (2009) 'The assembled structure of a complete tripartite bacterial multidrug efflux pump', *Proceedings of the National Academy of Sciences*, 106(17), pp. 7173–7178. doi: 10.1073/pnas.0900693106.

Taguchi, A. *et al.* (2019) 'FtsW is a peptidoglycan polymerase that is functional only in complex with its cognate penicillin-binding protein', *Nature Microbiology*, 4(4), pp. 587–594. doi: 10.1038/s41564-018-0345-x.

Talmon, E. and Kleinschmidt, J. H. (2016) 'The periplasmic domain of the barrel assembly machinery protein A (BamA) from Escherichia coli assists folding of outer membrane protein A', *Thesis*.

Terrak, M. *et al.* (1999) 'The catalytic, glycosyl transferase and acyl transferase modules of the cell wall peptidoglycan-polymerizing penicillin-binding protein 1b of *Escherichia coli*', *Molecular Microbiology*, 34(2), pp. 350–364. doi: 10.1046/j.1365-2958.1999.01612.x.

Tidhar, A. *et al.* (2009) 'The NlpD Lipoprotein Is a Novel *Yersinia pestis* Virulence Factor Essential for the Development of Plague', *PLoS ONE*, 4(9), p. e7023. doi: 10.1371/journal.pone.0007023.

Tischler, A. D. and Camilli, A. (2004) 'Cyclic diguanylate (c-di-GMP) regulates *Vibrio cholerae* biofilm formation', *Molecular Microbiology*, 53(3), pp. 857–869. doi: 10.1111/j.1365-2958.2004.04155.x.

Ton-That, H. *et al.* (1998) 'Anchor Structure of *Staphylococcal* Surface Proteins', *Journal of Biological Chemistry*, 273(44), pp. 29143–29149. doi: 10.1074/jbc.273.44.29143.

Trimble, M. J. and McCarter, L. L. (2011) 'Bis-(3'-5')-cyclic dimeric GMP-linked quorum sensing controls swarming in *Vibrio parahaemolyticus*', *Proc Natl Acad Sci U S A*, 108(44), pp. 18079–18084. doi: 10.1073/pnas.1113790108.

Truebestein, L. and Leonard, T. A. (2016) 'Coiled-coils: The long and short of it', *BioEssays*, 38(9), pp. 903–916.

doi: 10.1002/bies.201600062.

Tsukazaki, T. *et al.* (2011) 'Structure and function of a membrane component SecDF that enhances protein export', *Nature*, 474(7350), pp. 235–238. doi: 10.1038/nature09980.

Tyanova, S. *et al.* (2016) 'The Perseus computational platform for comprehensive analysis of (prote)omics data', *Nature Methods*, 13(9), pp. 731–740. doi: 10.1038/nmeth.3901.

Typas, A. *et al.* (2010) 'Regulation of peptidoglycan synthesis by outer-membrane proteins', *Cell*, 143(7), pp. 1097–1109. doi: 10.1016/j.cell.2010.11.038.

Typas, A. *et al.* (2012) 'From the regulation of peptidoglycan synthesis to bacterial growth and morphology', *Nature Reviews Microbiology*, 10(2), pp. 123–136. doi: 10.1038/nrmicro2677.

Uehara, T. *et al.* (2010) 'Daughter cell separation is controlled by cytokinetic ring-activated cell wall hydrolysis', *EMBO Journal*, 29(8), pp. 1412–1422. doi: 10.1038/emboj.2010.36.

Uehara, T., Dinh, T. and Bernhardt, T. G. (2009) 'LytM-domain factors are required for daughter cell separation and rapid ampicillin-induced lysis in *Escherichia coli*', *Journal of Bacteriology*, 191(16), pp. 5094–5107. doi: 10.1128/JB.00505-09.

Uehara, T. and Park, J. T. (2003) 'Identification of MpaA, an Amidase in *Escherichia coli* That Hydrolyzes the -D-Glutamyl-meso-Diaminopimelate Bond in Murein Peptides', *Journal of Bacteriology*, 185(2), pp. 679–682. doi: 10.1128/JB.185.2.679-682.2003.

Uehara, T. and Park, J. T. (2007) 'An Anhydro-N-Acetylmuramyl-L-Alanine Amidase with Broad Specificity Tethered to the Outer Membrane of *Escherichia coli*', *Journal of Bacteriology*, 189(15), pp. 5634–5641. doi: 10.1128/JB.00446-07.

Vasconcelos, G. J., Stang, W. J. and Laidlaw, R. H. (1975) 'Isolation of *Vibrio parahaemolyticus* and *Vibrio alginolyticus* from estuarine areas of Southeastern Alaska.', *Applied microbiology*, 29(4), pp. 557–9.

Viala, J. *et al.* (2004) 'Nod1 responds to peptidoglycan delivered by the Helicobacter pylori cag pathogenicity island', *Nature Immunology*, 5(1), pp. 1166–1174. doi: 10.1038/ni1131.

Vollmer, W., Joris, B., *et al.* (2008) 'Bacterial peptidoglycan (murein) hydrolases', *FEMS Microbiology Reviews*, 32(2), pp. 259–286. doi: 10.1111/j.1574-6976.2007.00099.x.

Vollmer, W. and Bertsche, U. (2008) 'Murein (peptidoglycan) structure, architecture and biosynthesis in *Escherichia coli*', *Biochimica et Biophysica Acta (BBA) - Biomembranes*, 1778(9), pp. 1714–1734. doi: 10.1016/j.bbamem.2007.06.007.

Vollmer, W., von Rechenberg, M. and Höltje, J.-V. (1999) 'Demonstration of Molecular Interactions between the Murein Polymerase PBP1B, the Lytic Transglycosylase MltA, and the Scaffolding Protein MipA of

Escherichia coli', *Journal of Biological Chemistry*, 274(10), pp. 6726–6734. doi: 10.1074/jbc.274.10.6726.

Voulhoux, R. (2001) 'Involvement of the twin-arginine translocation system in protein secretion via the type II pathway', *The EMBO Journal*, 20(23), pp. 6735–6741. doi: 10.1093/emboj/20.23.6735.

Walton, T. A. *et al.* (2009) 'The cavity-chaperone Skp protects its substrate from aggregation but allows independent folding of substrate domains', *Proceedings of the National Academy of Sciences*, 106(6), pp. 1772–1777. doi: 10.1073/pnas.0809275106.

Weiser, J. N. *et al.* (1995) 'Identification and characterization of a cell envelope protein of *Haemophilus influenzae* contributing to phase variation in colony opacity and nasopharyngeal colonization', *Molecular Microbiology*, 17(3), pp. 555–564. doi: 10.1111/j.1365-2958.1995.mmi_17030555.x.

Weiss, D. S. *et al.* (1999) 'Localization of FtsI (PBP3) to the septal ring requires its membrane anchor, the Z ring, FtsA, FtsQ, and FtsL', *Journal of Bacteriology*, 181(2), pp. 508–520.

Weiss, D. S. (2015) 'Last but not least: new insights into how FtsN triggers constriction during *Escherichia coli* cell division', *Molecular Microbiology*, 95(6), pp. 903–909. doi: 10.1111/mmi.12925.

Wu, T. *et al.* (2005) 'Identification of a Multicomponent Complex Required for Outer Membrane Biogenesis in *Escherichia coli*', *Cell*, 121(2), pp. 235–245. doi: 10.1016/j.cell.2005.02.015.

Xie, K. and Dalbey, R. E. (2008) 'Inserting proteins into the bacterial cytoplasmic membrane using the Sec and YidC translocases', *Nature Reviews Microbiology*, 6(3), pp. 234–244. doi: 10.1038/nrmicro3595.

Yakhnina, A. A., McManus, H. R. and Bernhardt, T. G. (2015) 'The cell wall amidase AmiB is essential for *Pseudomonas aeruginosa* cell division, drug resistance and viability', *Molecular Microbiology*, 97(5), pp. 957–973. doi: 10.1111/mmi.13077.

Yamaguchi, K., Yu, F. and Inouye, M. (1988) 'A single amino acid determinant of the membrane localization of lipoproteins in *E. coli*', *Cell*, 53(3), pp. 423–432. doi: 10.1016/0092-8674(88)90162-6.

Yang, D. C. *et al.* (2012) 'A conformational switch controls cell wall-remodelling enzymes required for bacterial cell division', *Molecular Microbiology*, 85(4), pp. 768–781. doi: 10.1111/j.1365-2958.2012.08138.x.

Yang, J. *et al.* (2013) 'Transcriptional activation of the mrkA promoter of the *Klebsiella pneumoniae* type 3 fimbrial operon by the c-di-GMP-dependent MrkH protein', *PLoS ONE*, 8(11), p. e79038. doi: 10.1371/journal.pone.0079038.

Yao, X. *et al.* (1999) 'Thickness and elasticity of gram-negative murein sacculi measured by atomic force microscopy', *Journal of Bacteriology*, 181(22), pp. 6865–6875.

Yeagle, P. L. (2016) 'Membrane Proteins', in Yeagle, P. L. B. T.-T. M. of C. (Third E. (ed.) *The Membranes of Cells*. Boston: Elsevier, pp. 219–268. doi: 10.1016/B978-0-12-800047-2.00010-3.

Yildiz, F. H. and Schoolnik, G. K. (1998) 'Role of rpoS in stress survival and virulence of *Vibrio cholerae*', *Journal of Bacteriology*.

Yokota, N. *et al.* (1999) 'Characterization of the LolA-LolB System as the General Lipoprotein Localization Mechanism of *Escherichia coli*', *Journal of Biological Chemistry*, 274(43), pp. 30995–30999. doi: 10.1074/jbc.274.43.30995.

Young, K. D. (2010) 'Bacterial Shape: Two-Dimensional Questions and Possibilities', *Annual Review of Microbiology*, 64(1), pp. 223–240. doi: 10.1146/annurev.micro.112408.134102.

Yousif, S. Y., Broome-Smith, J. K. and Spratt, B. G. (1985) 'Lysis of *Escherichia coli* by beta-lactam antibiotics: deletion analysis of the role of penicillin-binding proteins 1A and 1B.', *Journal of general microbiology*, 131(10), pp. 2839–2845. doi: 10.1099/00221287-131-10-2839.

Zarei, M. *et al.* (2012) 'Seasonal prevalence of *Vibrio* species in retail shrimps with an emphasis on *Vibrio parahaemolyticus*', *Food Control*, 25(1), pp. 107–109. doi: 10.1016/j.foodcont.2011.10.024.

Zastrow, M. L. and Pecoraro, V. L. (2014) 'Designing Hydrolytic Zinc Metalloenzymes', *Biochemistry*, 53(6), pp. 957–978. doi: 10.1021/bi4016617.

Zhu, J. *et al.* (2002) 'Quorum-sensing regulators control virulence gene expression in *Vibrio cholerae*', *Proceedings of the National Academy of Sciences*, 99(5), pp. 3129–3134. doi: 10.1073/pnas.052694299.

Zimmer, J., Nam, Y. and Rapoport, T. A. (2008) 'Structure of a complex of the ATPase SecA and the protein-translocation channel', *Nature*, 455(7215), pp. 936–943. doi: 10.1038/nature07335.

Acknowledgments

First of all, I would like to express my sincere gratitude to my mentor and supervisor, Dr. Simon Ringgaard for giving me the opportunity to work on this and other projects over the years ever since I started as a Masters student. Furthermore, I would like to thank my IMPRS committee and thesis committee, specifically Prof. Dr. Martin Thanbichler, Prof. Dr. Michael Bölker, Prof. Dr. Lars-Oliver Essen, Prof. Dr. Lotte Søgaard-Andersen and Prof. Dr. Victor Sourjik. I want to thank Dr. Dorota Skotnicka for proof-reading this PhD thesis. I also thank our collaborators Dr. Oihane Irazoqui and Dr. Susanne Brenzinger as well as their supervisors for help, support and fruitful discussions.

I want to thank the entire Ringgaard lab, both former and present members: Samada, Ale, Shankar, Carolina, Erick, Marco, Barbara, Karo, Stephan (all in no particular order, and sorry to anyone I forgot). Thank you guys so much for a great atmosphere in the lab, and lots of fun outside the lab as well. I will never forget the great time we had as the “Ringgaardians of the Galaxy”, “Photo-Activatables” or “Demogorgonzolas”. Especially a big thank you to Petra! Without you, nothing would work and we would all be lost.

Thanks to everyone from A1 floor, with a big thank you to Steffi, for never giving me permanent “Laborverbot”. Also thank you to the rest of the A2 floor, for a nice atmosphere and some fun times in- and outside the lab.

A big thank you goes to my entire family and friends, especially my mum and dad for always supporting me along the way and shaping me to be the person who I am today, I love you.

Dorota, thank you so much for your support both in- and outside the lab, your help, and your delicious food: I am thankful, for every cup and plate full. Thanks for pushing me forward, when I needed it. Thank you for sometimes being my conscious and making me a better person. You are awesome! I love you

List of publications

Heering, J., Alvarado, A., Ringgaard, S.

Induction of Cellular Differentiation and Single Cell Imaging of *Vibrio parahaemolyticus* Swimmer and Swarmer Cells. *J. Vis. Exp.* 2017*; e55842,* doi:10.3791/55842

Heering, J., Ringgaard, S.

Differential localization of chemotactic signaling arrays during the lifecycle of *Vibrio parahaemolyticus*. *Front. Microbiol. 2016; 7:1767,* doi:10.3389/fmicb.2016.01767

Skotnicka, D., Petters, T., **Heering, J**., Hoppert, M., Kaever, V., Søgaard-Andersen, L.

Cyclic Di-GMP Regulates Type IV Pilus-Dependent Motility in *Myxococcus xanthus*

J. Bacteriol. Dec 2015, 198 (1) 77-90; doi: 10.1128/JB.00281-15

Erklärung

Hermit versichere ich, dass ich die vorliegende Dissertation mit dem Titel „Identification and characterization of M23 peptidase VcsP involved in cell separation of *Vibrio parahaemolyticus*“ selbstständing verfasst, keine anderen als die Text angegebenen Hilfsmittel verwendet und sämttliche Stellen, die im Wortlaut oder dem Sinn nach anderen Werken entnommen sind, mit Quellenangaben kenntlich gemacht habe.

Die Dissertation wurde in der jetzigen oder einer ähnlichen From noch bei keiner anderen Hochschule eingereicht und hat noch keinen sonstigen Prüfungswegen gedient.

_____ _____

Ort, Datum Jan Heering

Einverständniserklärung

Ich erkläre mich dam einverstanden, dass die vorliegende Dissertation

„Identification and characterization of M23 peptidase VcsP involved in cell separation of *Vibrio parahaemolyticus*“

in Bibliotheken allgemein zugänglich gemacht wird. Dazu gehört, dass sie

- von der Bibliothek der Einrichtung, in der ich meine Arbeit anfertig habe, zur Benutzung in ihren Räumen bereitgehalten wird;
- in konventionellen und maschinenlesbaren Katalogen, Verzeichnissen und Datenbanken verzeichnet wird;
- im Rahmen der urheberrechtichen Bestimmungen für Kopierzwecke genutzt werden kann.

Marburg, den __.__.2019

_____

Jan Heering

_____

Dr. Simon Ringgaard